OPTICAL DETERMINATION OF THE PROPERTIES OF EXCITONS BOUND TO IMPURITIES IN SEMICONDUCTORS

Thesis by

Kenneth Robert Elliott

In Partial Fulfillment of the Requirements

for the Degree of

Doctor of Philosophy

California Institute of Technology

Pasadena, California

1980

(Submitted August 21, 1979)

ACKNOWLEDGMENTS

I would like to thank Dr. T. C. McGill and Dr. D. L. Smith for their assistance with this work.

I have had numerous helpful discussions through the course of this work with M. Chen, S. A. Lyon, J. Schulman, D. S. Pan, A. Hunter, G. Mitchard, G. Osbourn, R. Feenstra, Y. C. Chang and U. Rehbein. I owe special thanks to Steve Lyon for his work on problems similar to those discussed in this thesis, to D. S. Pan and Y. C. Chang for their calculations of the electronic properties of bound excitons, and to G. Osbourn and D. L. Smith for their calculation of bound exciton oscillator strengths and bound exciton Auger rates. I am also indebted to Dr. J. W. Mayer, Dr. M. Haas, and Dr. G. Picus for their assistance and suggestions with regard to my work at Cal Tech.

I would like to thank the Extrinsic Silicon group at Hughes Research Labs for supplying the silicon samples I have used. I would like to thank R. Dawson for some of the GaP crystals used in the course of this work. I would like to thank V. Snell for her helpful manner and for typing this thesis.

For financial support I owe thanks to the California Institute of Technology, the Office of Naval Research and the Advanced Research Projects Agency.

This thesis is dedicated to my family.

ABSTRACT

This thesis deals with the electronic and optical properties of excitons bound to impurities in semiconductors. The first three chapters are concerned with the electronic structure of bound exciton states. The fundamental process in which a bound exciton is formed on a neutral acceptor in silicon is studied. Three lines are observed in the absorption spectra of the acceptors Al, Ga, and In in silicon. Of the various schemes used to explain these lines, it is determined from the relative oscillator strengths that the correct scheme is one in which two j=3/2 holes are coupled to form states with total angular momentum J=0 and J=2. The cubic environment of the crystal in the neighborhood of the impurity leads to a splitting of the J=2 state. In the bound exciton spectra of Si:Tl, four lines are observed in contrast to the three lines observed for the acceptors Al, Ga, and In. The oscillator strength of the thallium bound exciton is measured and continues the trend towards large oscillator strengths for the deep impurities. The excited state structure of the donor bound excitons in GaP is also presented. It is established that excitons bound at these impurities should have a structure which consists of a D^- core to which a hole is loosely bound. Two different types of excited states have been identified for the donor bound excitons. Some of these states are excitations of the hole about the

D^- core of the bound exciton. Other states have been identified which are due to excitations of the D^- electron core. These excitations have different symmetry than the ground state.

The observation of a low lying excited state of the neutral indium acceptor is reported. This state is interesting because current theories of the electronic states of the acceptor do not predict it. The state may exist as the result of the Jahn-Teller effect.

The systematics of the spectroscopy of multiple exciton complexes bound to donors in silicon are reported. It is found that the spectroscopy of these complexes changes very little between different impurities. This suggests that carrier-carrier interactions are more important than the impurity potential in determining the binding of excitons to the complexes. Any model of the structure of the complexes must take this into account.

Measurements of the capture cross-section of a free exciton on a neutral In acceptor in silicon are reported. In lightly doped silicon the decay of the luminescence associated with In bound excitons is determined by the rate at which excitons are captured on the indium site. By measuring the decay time of the luminescence as a function of indium concentration and temperature, it is possible to obtain the capture cross-section of a free exciton on a site. The capture cross-section is strongly temperature dependent changing by two orders of magnitude between 10^oK and 30^oK.

Parts of this thesis have been published under following titles:

Chapter 2: Bound Exciton Absorption in Si:Al, Si:Ga, and Si:In. K. R. Elliott, G. C. Osbourn, D. L. Smith, and T. C. McGill, Phys. Rev. B17, 1808 (1978).

Chapter 3: Absorption and Luminescence of the Bound Exciton in Thallium Doped Silicon. K. R. Elliott, D. L. Smith, and T. C. McGill, Solid State Commun. 27, 317 (1978).

Chapter 4: Excited States of Donor Bound Excitons in GaP. K. R. Elliott and T. C. McGill, submitted to Physical Review.

Chapter 5: Evidence for an Excited Level of the Neutral Indium Acceptor in Silicon. K. R. Elliott, S. A. Lyon, D. L. Smith and T. C. McGill, Phys. Lett. 70A, 52 (1979).

Chapter 6: Systematics of Bound Excitons and Bound Multiple Exciton Complexes for Shallow Donors in Silicon. K. R. Elliott and T. C. McGill, Solid State Commun. 28, 491 (1978).

Chapter 7: Capture Cross Section of Excitons on Neutral Indium Impurities in Silicon. K. R. Elliott, D. L. Smith, and T. C. McGill, Solid State Commun. 24, 461 (1978).

Publications not included in this thesis are;

Time and Spatially Resolved Absorption at 3.4 μm in Highly Excited Germanium. K. R. Elliott and T. C. McGill, Phys. Rev. B18, 963 (1978).

Transients of the Photoluminescence from Electron Hole Droplets in Doped and Undoped Germanium. M. Chan, S. A. Lyon, K. R. Elliott, D. L. Smith, and T. C. McGill, Il Nuovo Cimento 39, 622 (1977).

Observation of Long Lifetime Lines in Photoluminescence from Si:In. G. S. Mitchard, S. A. Lyon, K. R. Elliott, and T. C. McGill, Solid State Commun. 29, 425 (1979).

Auger and Radiative Recombination of Acceptor Bound Excitons in Semiconductors. G. C. Osbourn, S. A. Lyon, K. R. Elliott, D. L. Smith, and T. C. McGill, Solid State Electronics 21, 1339 (1978).

Photoluminescence Studies of Acceptors in Silicon. S. A. Lyon, K. R. Elliott, G. Mitchard, D. L. Smith, T. C. McGill, J. P. Baukus, R. Baron, M. H. Young, and O. J. Marsh, presented at the 1978 IRIS Conference at Annapolis, Md.

TABLE OF CONTENTS

ACKNOWLEDGMENT	ii
ABSTRACT	iii
TABLE OF CONTENTS	vii
CHAPTER 1.	1
INTRODUCTION	2
I. Background	2
II. Neutral Impurities	11
III. Bound Excitons	16
IV. Outline of Thesis	19
References	21
CHAPTER 2. BOUND EXCITON ABSORPTION IN Si:Al, Si:Ga AND Si:In	23
I. Introduction	24
II. Experimental Results	27
III. Theoretical Analysis of the No Phonon Oscillator Strengths	37
IV. Summary and Conclusions	47
References	50
CHAPTER 3. ABSORPTION AND LUMINESCENCE OF THE Si:Tl BOUND EXCITON	53
I. Introduction	54
II. Experiment	56

III. Results 56
IV. Discussion 61
V. Conclusions 66
References 70
CHAPTER 4. LUMINESCENCE EXCITATION SPECTROSCOPY OF BOUND EXCITONS IN GaP 71
I. Introduction 72
II. Experiment 75
III. Results 78
IV. Discussion 89
V. Conclusions 99
References 101
CHAPTER 5. EVIDENCE FOR AN ADDITIONAL EXCITED STATE OF THE NEUTRAL INDIUM ACCEPTOR IN SILICON 102
I. Introduction 103
II. Experiment 105
III. Results 108
IV. Discussion 109
V. Conclusions 119
References 120
CHAPTER 6. SYSTEMATICS OF BOUND EXCITONS AND BOUND MULTIPLE EXCITON COMPLEXES FOR SHALLOW DONORS IN SILICON 121
I. Introduction 122

II. Experiment 130
III. Results 133
IV. Discussion 141
V. Conclusions 146
References 150
CHAPTER 7. CAPTURE CROSS-SECTION OF EXCITONS ON NEUTRAL INDIUM IMPURITIES IN SILICON 152
I. Introduction 153
II. Experiment 154
III. Results and Discussion 155
IV. Conclusions 165
References 167

Chapter 1

INTRODUCTION

I. Background

Impurities and defects in semiconductors have an important effect on the electrical properties of such materials. The presence of impurities in a semiconductor crystal can change carrier concentrations by many orders of magnitude. In addition impurities and defects can act as recombination centers, scattering centers, and traps which can significantly affect the transport properties of carriers. Thus, it is important to understand the properties of states associated with these centers. It is also important to develop methods with which one can measure the presence of impurities and defects in order to evaluate semiconductor materials.

The optical properties of semiconductors are very sensitive to the presence of impurities and defects and can be used to study the states associated with these centers and to measure their presence. The optical spectrum associated with many impurities is highly detailed, and it is possible to discriminate between centers with different optical properties. This thesis is primarily concerned with characterizing the optical properties of known centers and understanding the physics involved in the optical processes. Such information is important if one plans to use optical techniques to study and detect these centers.

To characterize such centers it is necessary to consider the

different processes which can occur in a semiconductor (Fig. 1.1 shows schematically some of the states involved in such processes.). Absorption of a photon with sufficient energy in a semiconductor will excite an electron from the valence band to the conduction band. Such a process produces an electron hole pair in the semiconductor. In the absence of interactions between the electron and hole, both particles are free to propagate throughout the crystal as free carriers. The inverse process is also possible. A free hole and free electron can recombine to form a photon. (1)

In the presence of interactions between the electrons and holes it is possible to form new states. The coulomb attraction between an electron and hole makes it possible to form a state in which the two particles are bound to each other. Such a state is known as a free exciton.

In the presence of impurities, interactions between the electron hole pair and the impurity can also lead to the formation of new states. A neutral donor consists of an electron bound to a positively charged point defect in the semiconductor. The neutral donor will form a state with an electron-hole pair which consists of two electrons and a hole bound at the defect. Similarly a neutral acceptor, which consists of a hole bound to a negatively charged point defect, will form a state with an electron-hole pair which consists of one electron and two holes bound to the defect. Such states are shown schematically in Figure 1.1 and are called bound exciton states. More

Figure 1.1. Schematic diagram of some of the states involved in semiconductor recombination. These include free carriers such as an electron or hole and free excitons which consist of a bound electron-hole pair. Neutral donors and acceptors consist of an electron or hole bound to a charged impurity center. Bound excitons are formed when free excitons bind to neutral impurities. Bound multiple exciton complexes are formed when more than one exciton binds to an impurity.

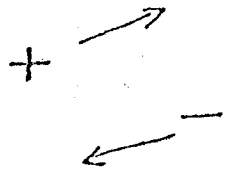

free carriers

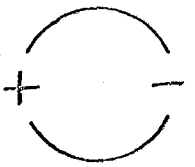

free exciton

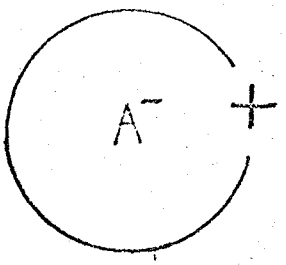

neutral acceptor

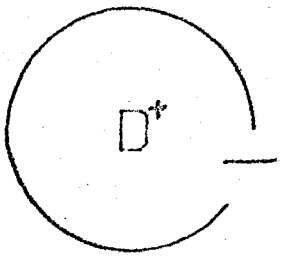

neutral donor

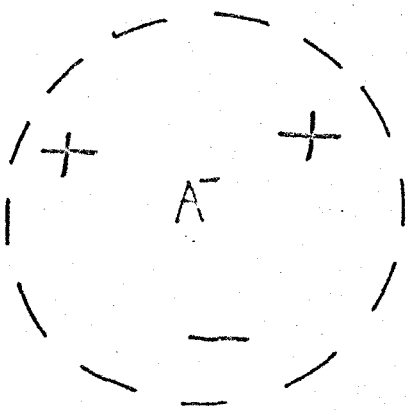

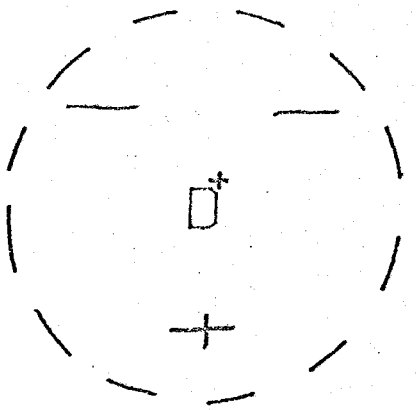

bound excitons

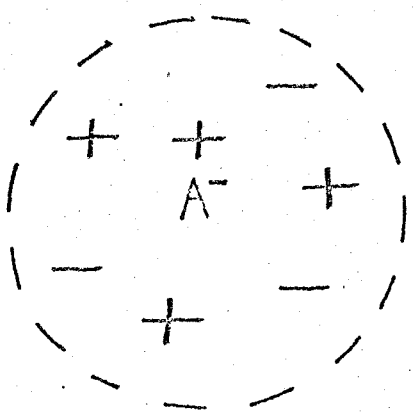

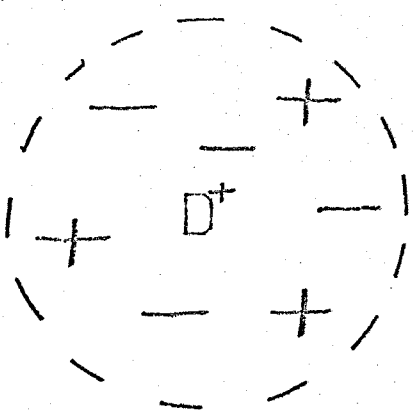

bound multiple exciton complexes

than one exciton can become bound to a neutral donor or neutral acceptor. These states are known as bound multiple exciton complexes.

When an electron-hole pair in any one of these states recombines, the energy of the luminescence which is produced is characteristic of the semiconductor and the impurity states involved in the recombination. In addition one of these states can be formed when a photon produces an electron-hole pair. Therefore, photoluminescence and optical absorption can be used to study free excitons, bound excitons and bound multiple exciton complexes. Bound exciton transitions have been observed in most common semiconductors including the direct semiconductors CdS [2], InP [3], and GaAs [4] and the indirect semiconductors Ge [5], GaP [6], and SiC [7]. Bound multiple exciton complexes have been reported in Si [8], GaP [9], Ge [10] and SiC [11].

To understand the spectra obtained from exciton transitions, it is necessary to understand the structure associated with these states. If the hole is taken to be a positively charged particle with effective mass m_h and the electron to be a negatively charged particle with mass m_e then the energy associated with a free exciton state is

$$E = E_{gap} - \frac{e^4\mu}{2\hbar^2\varepsilon^2 n^2} + \frac{(\hbar K)^2}{2(m_e+m_h)} \quad .$$

E_{gap} is the energy associated with a free electron-hole pair, e is the electronic charge, ε is the static dielectric constant, μ is the reduced mass of the electron and hole, $\hbar K$ is the momentum associated

with the propagation of the free exciton through the crystal, and n is the principal quantum number associated with the state [1].

There has been considerable theoretical interest in understanding the basic structure of the bound exciton in recent years [12-18]. The structure of the bound exciton is more complex than the free exciton since there are three particles involved in the binding. In general, the binding energy depends on the ratio of the electron to hole mass. The most recent calculations indicate that the exciton will bind to the neutral impurity for all ratios of electron to hole mass. When the electron to hole mass ratio approaches zero, the two electrons are much lighter than the hole and the structure of the bound exciton resembles that of a simple diatomic molecule. When the electron to hole mass ratio approaches infinity, the two electrons are expected to bind to the neutral impurity with a structure analogous to that of the atomic H^- ion. Such a state is referred to as D^- state for donors or an A^+ state for acceptors. The coulombic attraction between the hole and the D^- state leads to the binding of the hole in the bound exciton [18]. The structure of bound multiple exciton complexes is not understood in detail at the present time. The many body nature of the problem has made a theoretical treatment difficult.

The simple view of free excitons and bound excitons must be modified to account for the observed optical properties in semiconductors. Details observed in the photoluminescence of GaAs [19],

InP [20], Si [21] and GaP [22] cannot be explained in the simple model. To explain these details it is necessary to examine the band structure. The simple model treats the electrons and holes as particles with effective masses m_e and m_h. In reality the band structure is more complicated.

This thesis reports on studies in two common semiconductors, silicon and gallium phosphide. Figure 1.2 shows the band structure for silicon [23]. The band structure for gallium phosphide is not shown but is similar in many respects to the band structure for silicon. Silicon is an indirect semiconductor with conduction band minima at points about .85 k_o between the Γ point at the center of the Brillouin zone and the X point at the edge of the Brillouin zone. k_o is the distance in k-space between these two points. The top of the valence band occurs at the center of the Brillouin zone, the Γ point. Gallium phosphide is similar to silicon in that the conduction band minima occur near the X point. However, in GaP, these minima occur much closer to the X point and for many purposes can be taken to occur at the X point. As in silicon, the top of the valence band occurs at the Γ point at the center of the Brillouin zone.

Figure 1.2. Band structure of silicon. The X point lies at the edge of the Brillouin zone along the 100 direction. The Γ point is at the center of the Brillouin zone. The bottom of the conduction band occurs at .85 k_o where k_o is the wavevector from the Γ point to the X point. The top of the valence band occurs at the Γ point. This figure does not include the spin-orbit splitting of the valence band. The spin-orbit interaction produces a splitting of the valence band which leaves the top of the valence band fourfold degenerate with a twofold degenerate split-off band lying 40 meV below the top of the valence band. (From D. J. Chadi, Phys. Rev. B16, 3572 (1977).)

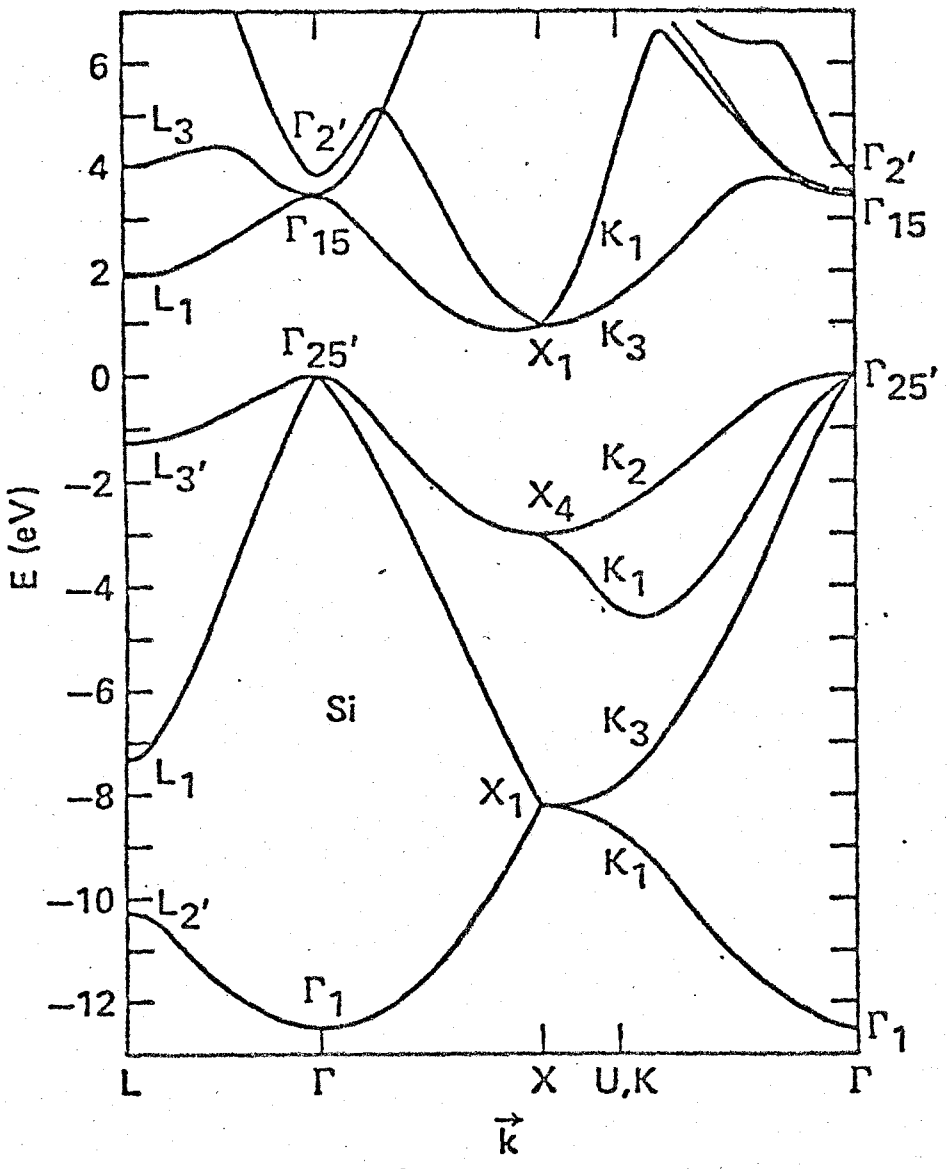
6
4
2
0
−2
−4
−6
−8
−10
−12
E (eV)
L
Γ
X
U,K
Γ
$\vec{k}$
L_3
$\Gamma_{2'}$
Γ_{15}
L_1
$\Gamma_{25'}$
$L_{3'}$
L_1
$L_{2'}$
Γ_1
X_1
X_4
K_1
K_3
K_2
K_1
K_3
K_1
$\Gamma_{2'}$
Γ_{15}
$\Gamma_{25'}$
Γ_1
Si

II. Neutral Impurities

It is possible to demonstrate the effects of the band structure by considering the cases of the neutral donor and acceptor in these semiconductors. In the simple model the energy levels for a neutral donor or acceptor are given by [1]

$$E^n_{donor} = \frac{e^4 m_e}{2\hbar^2 \varepsilon^2 n^2} \qquad E^n_{acceptor} = \frac{e^4 m_h}{2\hbar^2 \varepsilon^2 n^2}$$

where the symbols describe the same quantities as given previously for the free exciton. Qualitatively this picture works well for many impurity states. To describe donor and acceptor estates in Si and GaP several modifications are necessary.

Several features in the band structure of silicon make it necessary to modify the simple model for the neutral donors. As stated previously, the conduction band minima do not occur at the zone center in either Si or GaP. As a result, there are multiple conduction band minima in both of these materials. It is necessary to modify the simple model to include the effects of the multiple conduction band minima. Because the ground state of the impurity is localized near the impurity site, the amplitude function of the electron is spread over the full conduction band. Thus the electron can be in more than one minima at any given time. In silicon there are six minima and the effect of the short range impurity potential splits the six states associated with the minima into three types of states which are determined from symmetry considerations. In GaP there are

effectively three minima and two types of states. The energy splitting between these states is referred to as the valley-orbit splitting. Since the short range impurity potential depends to some extent on the chemical nature of the impurity, the valley-orbit splitting depends to some extent on the specific impurity [24].

Figure 1.3 shows schematically the experimentally determined ordering and classification of states associated with substitutional phosphorus in silicon [25]. These states are labeled 1s, 2s, 2p, etc. in analogy to the hydrogenic states which would be associated with these levels in the absence of other effects. Higher angular momentum states are split by the anisotropy of the conduction band into states which can be labeled by the z component of the angular momentum. Because states associated with different conduction band minima are mixed by the short range impurity potential, the 1s state is split into three levels labeled $1s(\Gamma_1)$, $1s(\Gamma_5)$, and $1s(\Gamma_3)$. The labels Γ_1, Γ_3, and Γ_5 describe the symmetry associated with each of these states. Of these states only the $1s(\Gamma_1)$ state has an amplitude on the impurity site and thus "feels" the strongest effects from the short range impurity potential. Normally the short range impurity potential is attractive and the Γ_1 state has the lowest energy. In GaP the 1s state is split into two levels which can be labeled $1s(\Gamma_1)$ and $1s(\Gamma_3)$.

In the case of the neutral acceptor the simple model must be modified for different reasons than for the neutral donor. The top of

Figure 1.3. Schematic diagram of neutral donor and neutral acceptor states in a semiconductor. The ordering for the neutral donor states is that of substitutional phosphorus in silicon. The ordering of states of the neutral acceptor was determined by a calculation for GaP.

Figure 1.3

neutral donor		neutral acceptor	
$3p_1^{\pm}$	-3.1 meV		
3s	-4.7 meV	$2p_{1/2}$	-4.2 meV
$3p_o$	-5.46 meV		
$2p_1^{\pm}$	-6.4 meV		
2s	-8.8 meV	$2p_{5/2}$	-11.7 meV
$2p_o$	-11.45 meV		
		$2s_{3/2}$	-13.7 meV
		$2p_{3/2}$	-19.1 meV
$1s(\Gamma_3)$	-32.6 meV	$1s_{3/2}$	-47.5 meV
$1s(\Gamma_5)$	-33.9 meV		
$1s(\Gamma_1)$	-45.5 meV		

the valence band of Si and GaP is fourfold degenerate. If one tries to use the simple model, it is not apparent what effective mass to use in describing the energies of the acceptor states. Thus it is necessary to treat the problem in more detail. Recently Baldereschi and Lipari have performed such a detailed calculation [26]. They have shown that the states of the acceptor can be classified by considering the form of the Hamiltonian associated with the top of the valence band. This Hamiltonian has the cubic symmetry of the crystal. Baldereschi and Lipari have shown that this Hamiltonian can be decomposed into two parts, one with spherical symmetry and one with the cubic symmetry. The free particle eigenfunctions of the spherical Hamiltonian have the symmetry of a particle with angular momentum J=3/2. They found that the states of the neutral acceptor could be classified in terms of a total angular momentum $\vec{F}=\vec{J}+\vec{L}$. In this case $\vec{J}=3/2$ and $\vec{L}$ is the angular momentum associated with a particular envelope function. The cubic term in the Hamiltonian may be treated in perturbation theory. Figure 1.3 shows the expected ordering of such states in GaP as determined by Baldereschi and Lipari [26].

III. Bound Excitons

A large part of this thesis is dedicated to understanding the properties of bound excitons. The ordering of states in the neutral impurity is often a good starting point for understanding the observed structure of states associated with bound excitons. A simple example shows that a great deal of structure can be associated with the bound exciton.

Consider the acceptor bound exciton in silicon. Schematically the Hamiltonian for the bound exciton can be expressed as

$$H = T_{h_1} + T_{h_2} + T_e + V_{imp\text{-}h_1} + V_{imp\text{-}h_2} + V_{imp\text{-}e}$$

$$+ V_{e\text{-}h_1} + V_{e\text{-}h_2} + V_{h_1\text{-}h_2}$$

where T represents a kinetic energy term, V represents a potential energy term, h_1 and h_2 are subscripts describing the two holes, e is a subscript describing the electron, and imp is a subscript describing the negatively charged impurity. The degeneracy associated with the bound exciton can be very large if all the interactions in this Hamiltonian are not active. For instance the top of the valence band in silicon is fourfold degenerate. In addition there are twelve possible states associated with the electron. The holes can be coupled together in six different ways which obey the Pauli principle. As a result the bound exciton can have a degeneracy as high as 72. This degeneracy can be broken if some of the terms in

the Hamiltonian are large enough. For instance the hole-hole, electron-hole exchange, and valley-orbit interactions can lower this degeneracy. It is important to understand how these interactions can play a role in determining the structure of the bound exciton.

Hole-hole coupling can split the degeneracy associated with the valence band when the two holes are coupled together. In a spherical model the hole can be treated as a particle with angular momentum $j=3/2$ [26]. For a system with two holes the total angular momentum is a constant. In the absence of interactions between the two holes in the bound exciton this results in degenerate states with total angular momentum $J=0$ and $J=2$. The coulomb repulsion of the two holes splits these states. In addition the kinetic energy terms in the Hamiltonian do not have absolutely spherical symmetry. This leads to a term in the Hamiltonian which can further split the $J=2$ state into two states leading to a total of three different states.

The electron-hole exchange interaction can also split states in the bound exciton. Such an interaction becomes important when the electron and hole occupy the same cell of the crystal lattice. The exchange interaction occurs because the total wavefunction of the system must be antisymmetric with respect to interchange of two electrons. In the absence of the hole there is an exchange energy associated with the electron in the conduction band and the electrons in the valence band. This energy is included in the band structure of the semiconductor in a single particle picture of the solid. When a hole

is present, the exchange energy is changed and must be taken into account. Such a term in the Hamiltonian couples an electron with spin 1/2 with a J=3/2 hole in a spherical model. As a result in the bound exciton, a state with total angular momentum J=2 can be split into states with J=3/2 and J=5/2 [24].

The valley-orbit splitting occurs for the electron in the bound exciton in the same way as in the neutral donor. Such an effect arises from the multivalleyed conduction band of an indirect semiconductor. Since there are six equivalent valleys in the conduction band, the electron has a degeneracy of six in the absence of the valley-orbit interaction. The potential associated with the bound exciton can split this degeneracy into three levels.

In general some of these interactions are more important than others. Experimental studies can be used to determine which interactions are active and need to be accounted for to explain the observed bound exciton spectra. In this thesis it has been possible to explain many of the features of bound exciton spectra. As a result it has been possible to determine which interactions are important and need to be considered in explaining the binding of these states.

IV. Outline of Thesis

In this thesis I present the results of experimental studies of various semiconductor systems which have been undertaken to gain more knowledge about the properties of the excitonic states and the impurities to which excitons bind. Chapter 2 deals with the fundamental absorption process in which a bound exciton is formed on a neutral acceptor in Si. Three lines are observed in the absorption spectra of Si:Al, Si:Ga, and Si:In. Several different schemes had been previously proposed to explain these lines. By comparing the oscillator strengths of these lines, it is established that the correct scheme is one in which two j=3/2 holes are coupled to form states with total angular momentum J=0 and J=2. The cubic environment of the crystal in the neighborhood of the impurity leads to a splitting of the J=2 state. Chapter 3 deals with measurements of the luminescence and absorption spectra due to the bound exciton in Si:Tl. Although Tl occurs in the same row of the periodic table as Al, Ga, and In the bound exciton spectra is qualitatively different. The results for Si:Tl are compared with those of Si:Al, Si:Ga, and Si:In.

In Chapter 4 the results of a study of the excited states of bound excitons in GaP:S and GaP:Se are presented. It is established that excitons bound at these impurities should have a structure which consists of a D^- core to which a hole is loosely bound. We have identified two different types of excited states. Some of these states have been identified as excitations of the hole about the donor bound

exciton. Other states have been identified which are due to excitations of the electron into D^- states with different symmetry.

Chapter 5 discusses the observation of an excited state in Si:In. This state is close in energy to the ground state of the In acceptor and is interesting because such a state has not been predicted. The possible explanations for the origin of this state are discussed. Chapter 6 reports the systematics of the spectroscopy of multiple exciton complexes bound to donors in silicon. At the present time, little is known about the structure of these complexes. By studying the luminescence associated with these states we have determined that the observed structure in the spectra does not change appreciably with the chemical nature of the impurity to which the complexes are bound. Thus any model for the structure of the complexes must be able to explain this behavior.

Chapter 7 presents measurements of the capture cross-section of a free exciton on a neutral In acceptor in silicon. In lightly doped silicon the decay of the luminescence associated with In bound excitons is determined by the rate at which excitons are captured on the In site. By measuring the decay time of the luminescence as a function of In concentration and temperature, we can obtain the cross-section for capture of a free exciton. The capture cross-section shows a strong temperature dependence changing by two orders of magnitude between 10^oK and 30^oK. This measurement is the only known measurement of the free exciton capture cross-section on a neutral impurity in any semiconductor.

REFERENCES

1. J. I. Pankove, Optical Properties in Semiconductors, (Dover Publications, Inc., New York, 1971).
2. D. G. Thomas and J. J. Hopfield, J. Appl. Phys. 33, 3243 (1962).
3. W. J. Turner and G. D. Pettit, Appl. Phys. Lett. 3, 102 (1963).
4. M. A. Gilleo, P. T. Bailey, and D. E. Hill, Phys. Rev. 174, 898 (1968).
5. C. Benoit a la Guillaume and O. Parodi, Int. Conf. on Physics of Semiconductors, Prague (1961), p. 426.
6. D. G. Thomas, M. Gershenzon, and J. J. Hopfield, Phys. Rev. 131, 2397 (1963).
7. W. J. Choyke and L. Patrick, Phys. Rev. 127, 1868 (1962).
8. A. S. Kaminskii, Y. E. Pokrovskii, and N. V. Alkeev, Zh. Eksp. Teor. Fiz. 59, 1937 (1970) Sov. Phys. JETP. 32, 1048 (1971).
9. R. Sauer, W. Schmid, J. Weber, and U. Rehbein, to be published in Phys. Rev. B, June 15, 1979.
10. R. W. Martin, Sol. St. Commun. 14, 369 (1974).
11. P. J. Dean, D. C. Herbert, D. Bimberg, and W. J. Choyke, Phys. Rev. Lett. 37, 1635 (1976).
12. J. J. Hopfield in Proceedings of the 7th International Conference of Physics of Semiconductors (Edited by Hulin M.), p. 725 ff, Dunod, Paris (1964).
13. R. R. Sharma and S. Rodriguez, Phys. Rev. 159, 649 (1967).

14. G. Munschy and C. Carabatos, Phys. Stat. Sol.(b) 57, 523 (1973).

15. B. Stebe and G. Munschy, Phys. Stat. Sol.(b) 88, 713 (1978).

16. D. S. Pan, D. L. Smith, and T. C. McGill, Sol. State Comm. 18, 1557 (1976).

17. D. C. Herbert, J. Phys. C10, 3327 (1977).

18. Y. C. Chang and T. C. McGill, Sol. St. Commun., in publication.

19. A. M. White, P. J. Dean and B. Day, J. Phys. C7, 1400 (1974).

20. M. Schmidt, T. N. Morgan, and W. Schairer, Phys. Rev. B11, 5002 (1975).

21. P. J. Dean, W. F. Flood and G. Kaminsky, Phys. Rev. 163, 721 (1967).

22. P. J. Dean, R. A. Faulkner, S. Kimura and M. Ilegems, Phys. Rev. B14, 1926 (1971).

23. D. J. Chadi, Phys. Rev. B16, 3572 (1977).

24. F. Bassani, and G. Pastori Parravincini, Electronic States and Optical Transitions in Solids, (Pergamon Press, Oxford, 1975).

25. R. L. Aggarwal and A. K. Ramdas, Phys. Rev. 137, A602 (1965).

26. A. Baldereschi and N. O. Lipari, Phys. Rev. B8, 2697.

Chapter 2

BOUND EXCITON ABSORPTION IN Si:Al, Si:Ga AND Si:In

I. Introduction

The bound exciton (BE) spectra for acceptors in Si has been previously studied using both luminescence [1-4] and absorption [5]. Three emission lines associated with the BE have been observed in Si:Al [3,4] and Si:Ga [2,4]; in Si:In [1,4] two emission lines and in Si:B [1,4] one emission line associated with the BE have been seen. The multiplet structure seen for all acceptors except B is due to low lying excited states of the BE [6]. In Si:Al and Si:Ga, the energy separation between the two excited states is much less than the energy separation between the ground state and the first excited state [2-4]. In previous absorption experiments, the two excited states in Si:Al and Si:Ga had not been resolved.

Because of the degenerate valence band and multiple valley conduction band in Si, there are numerous possible ways to construct low lying excited states of the acceptor BE. The first explanation proposed to explain the observed excited states was based on a j-j coupling scheme for the two holes [5]. As stated in Chapter 1 the holes transform under rotation like particles with angular momentum j=3/2 in a model where the valence band has spherical symmetry. In the acceptor bound exciton there are two such holes which are coupled together by their coulombic repulsion. This produces states with total angular momentum J=0 and J=2. In the cubic environment of the crystal the J=2 state can be further split into two states. In addition the J=2 state can be split by the electron-hole exchange

interaction [7-9].

The exchange interaction occurs because the bound exciton wavefunction must be antisymmetric with respect to the exchange of the electron states associated with the electron in the conduction band with those associated with the hole in the valence band [9]. This gives rise to an additional term in the Hamiltonian with the form [25]

$$H_{exchange} = \langle \psi_{ck_{\hat{e}}}(r)\psi_{vk'_{\hat{n}}}(r')|\frac{e^2}{|r-r'|}|\psi_{vk_{\hat{n}}}(r)\psi_{ck'_{\hat{e}}}(r')\rangle \quad .$$

where $\psi_{ck_e}(r)$ is the wavefunction of an electron with wavevector k_e in the conduction band, ψ_{vk_h} is the wavefunction of a hole in the valence band and $e^2/|r-r'|$ is the coulomb potential. When this term is included, the electron with spin 1/2 angular momentum is coupled to the J=2 and J=0 hole states. States with total angular momentum J=1/2 are formed from the J=0 hole state. States with total angular momentum J=3/2, 5/2 are formed from the J=2 state.

If both the cubic crystal field and the electron hole exchange are active splitting mechanisms, four emission lines would be observed. An alternative splitting mechanism which produces three states is the valley-orbit splitting of the single electron in the acceptor bound exciton [7]. Such a splitting occurs because the electron can be in any one of six valleys and the effective potential of the two holes and the impurity center can lead to a splitting in the levels associated with these valleys.

When this work was completed, there was no evidence to determine which of these three splitting schemes was the correct one for the acceptor in silicon. The purpose of this work was to determine the splitting scheme for the acceptor BE in Si by analyzing the relative no-phonon oscillator strengths for the same three BE lines. In the first part of this chapter high resolution absorption data are presented for Si:Al, Si:Ga and Si:In in the no-phonon region. These data is used to determine the oscillator strengths for the three BE absorption lines. It is preferable to determine the relative oscillator strengths from an absorption experiment rather than a luminescence experiment because it is not necessary to divide out temperature dependent Boltzmann factors in the absorption experiment. (Sample heating by the excitation source can be a serious problem in the analogous luminescence experiment.) The results of theoretical calculations are presented for the oscillator strengths of the three BE lines assuming each of the three coupling schemes described above. For the j-j coupling scheme with the J=2 state further split by the crystal field, experiment agrees with theory for Si:Al and Si:Ga. For the other two schemes the experiments do not agree with theory. It is concluded that electron-hole exchange and valley orbit splitting for the acceptor BE in Si are small. The data for the sharp J=0 BE line in Si:Al (the lowest energy line of the main triplet) show that this line is further split into two components (by 0.07 meV), the ratio of the line inten-

sities for these components are such that they can be interpreted as due to the valley orbit splitting effect. In Si:In, both components of the J=2 BE line are observed which had not been seen previously. Two higher lying absorption lines which appear to be highly excited states of the BE have also been observed.

II. Experimental Results

The transmission was measured as a function of frequency in the no-phonon region of Si doped with Al, Ga and In. The impurity concentration in each sample was determined by a Hall measurement made at Hughes Research Laboratories. The doping levels ranged from $10^{16}cm^{-3}$ to $10^{17}cm^{-3}$. The sample lengths were between 2 and 3 cm.

Light from a tungsten source was focused on the end of the sample which was immersed in superfluid helium at $2^{o}K$. The transmitted light was collected and focused onto the entrance slit of a Spex 1400-II spectrometer. A cooled RCA 7102 photomultiplier was used to detect the signal at the spectrometer output. The obtainable spectral resolution was about 0.05 meV.

In Fig. 2.1, the transmission spectrum of Si:Ga in the no-phonon region is shown. Absorption lines at 1.1490 eV, 1.1504 eV and 1.1508 eV are observed. These lines have been seen previously in emission by Thewalt [2] and by Lyon et al [4]. In earlier absorption measurements, the two higher energy lines were not resolved. The relative

oscillator strengths for the three lines are listed in Table 2.1. In Table 2.2 the total oscillator strength for the sum of the three lines is given. The low energy line in Fig. 2.1 is considerably narrower than the two higher lying lines. Thus, to determine the relative oscillator strengths of the three lines, it is necessary to integrate the area under the absorption peaks. If one uses peak heights, the relative oscillator strength of the lowest energy line will be considerably overestimated. From the theoretical analysis of the relative oscillator strengths outlined later in the chapter, it is concluded that the three lines are produced by hole-hole coupling, the lowest energy state is the J=0 (Γ_1 [10] in the point group notation of Ref. (11)) and the higher lying lines are the J=2 state split by the cubic crystal field. These states are labeled Γ_3 and Γ_5 in accordance with their symmetry properties [11]. The assignment of the Γ_5 and Γ_3 states is made by their relative oscillator strengths.

In Fig. 2.2 I show the transmission spectrum of Si:Al in the no-phonon region. The spectrum is very similar to that for Si:Ga. Three main lines are observed at 1.1494 eV, 1.1506 eV and 1.1509 eV. These lines have been seen previously in emission by Lightowlers and Henry [3] and by Lyon et al [4]. The lowest lying line(labeled Γ_1) is split into two components. The splitting is 0.07 meV. This small splitting has not been previously observed. This splitting has also been observed in luminescence and in several samples with different

doping levels. In Table 2.1 the relative oscillator strengths of the four absorption lines in Si:Al are listed and in Table 2.2 the absolute oscillator strength for the sum of the four lines is listed. Based on the relative oscillator strengths, symmetry labels have been assigned for the three main lines in the same way as for Si:Ga (same splitting scheme). The small additional splitting of the Γ_1 line can be interpreted as due to valley orbit splitting. Based on relative oscillator strengths for the two components, the lowest lying component would be the electron Γ_3 valley state and the higher lying component the Γ_1 valley state. (The Γ_5 valley state has a forbidden optical transition.)

In Fig. 2.3, the transmission spectrum of Si:In in the no-phonon region is shown. Although the binding energy for the In acceptor in Si is much greater than that for Al or Ga, features are observed in the Si:In spectrum which are qualitatively similar to those for Si:Al and Si:Ga. In addition to lines which have been observed previously at 1.1409 eV and 1.1440 eV [1,4,5], a broad peak centered at 1.1472 eV was detected. These three are labeled peaks in analogy with the labeling for Si:Ga and Si:Al. In Table 2.1 the relative oscillator strengths are listed for the labeled lines in Fig. (3) and in Table 2.2 the absolute oscillator strength for the sum of these lines. The comparison of the relative oscillator strengths with the theoretical result is less favorable for Si:In than for Si:Ga and Si:Al.

Figure 2.1 Transmission vs photon energy in the no-phonon region of Si:Ga. Three absorption lines due to the bound exciton are observed. Absorption to the ground state is labeled Γ_1 and to the two excited states Γ_5 and Γ_3.

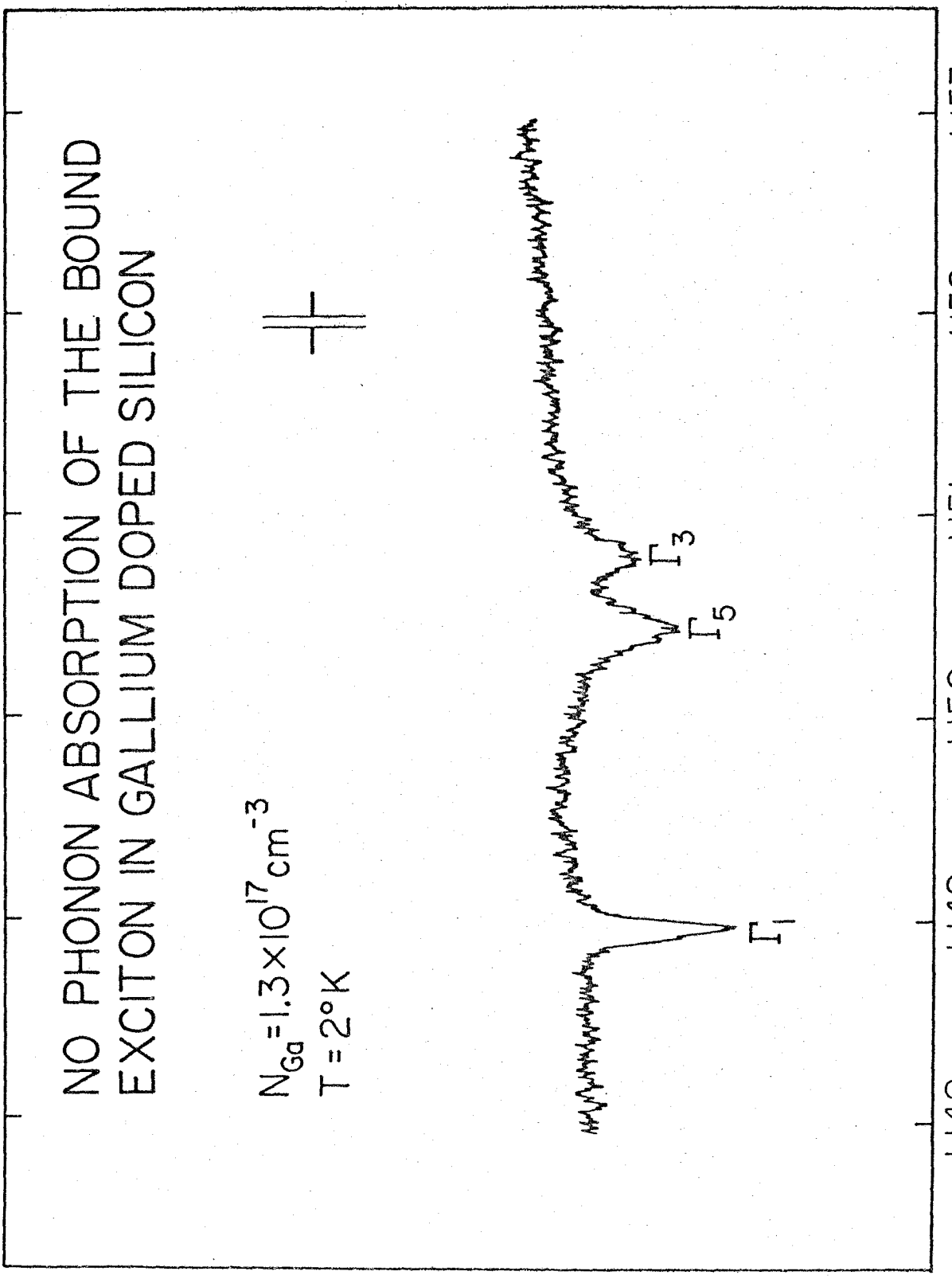
NO PHONON ABSORPTION OF THE BOUND EXCITON IN GALLIUM DOPED SILICON
$N_{Ga}=1.3\times10^{17}cm^{-3}$
T = 2°K
Γ_1
Γ_5
Γ_3
1.148
1.149
1.150
1.151
1.152
1.153
PHOTON ENERGY (eV)

Figure 2.2 Transmission vs photon energy in the no-phonon region of Si:Al. Three main absorption lines due to the bound exciton are observed; the lowest energy line is further split into a doublet.

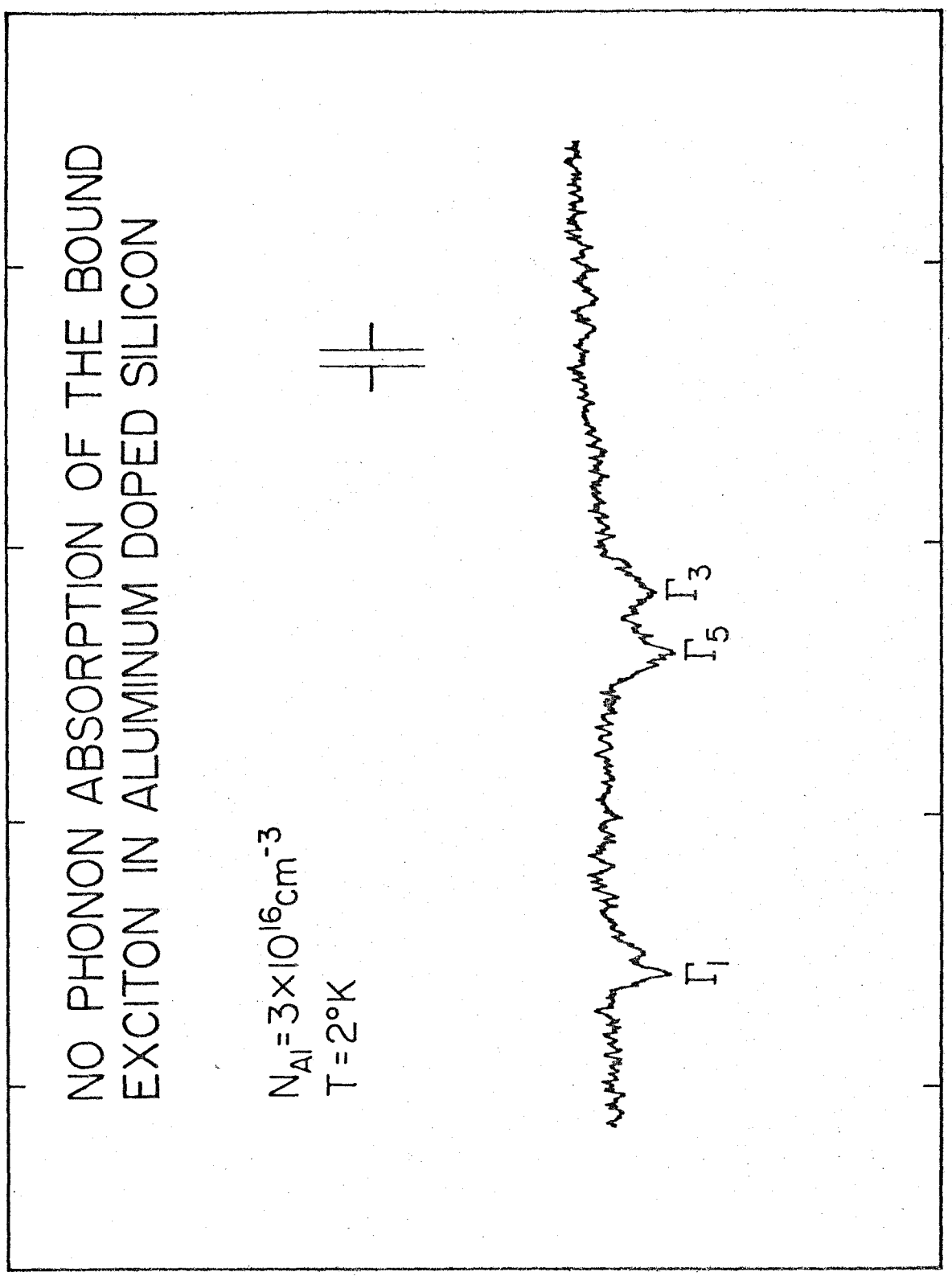
NO PHONON ABSORPTION OF THE BOUND EXCITON IN ALUMINUM DOPED SILICON
$N_{Al}=3\times10^{16}cm^{-3}$
T=2°K
Γ_1
Γ_5
Γ_3
1.149
1.150
1.151
1.152
PHOTON ENERGY (eV)

Figure 2.3 Transmission vs photon energy in the no-photon region of Si:In. Three absorption lines, similar to those observed in Si:Al and Si:Ga are seen. The line labeled Γ_3 is very broad, its position is marked with an arrow. Fine structure on the Γ_1 line is shown in the insert. We also see two lines at higher energy (not labeled) which correspond to absorption into a highly excited state of the bound exciton.

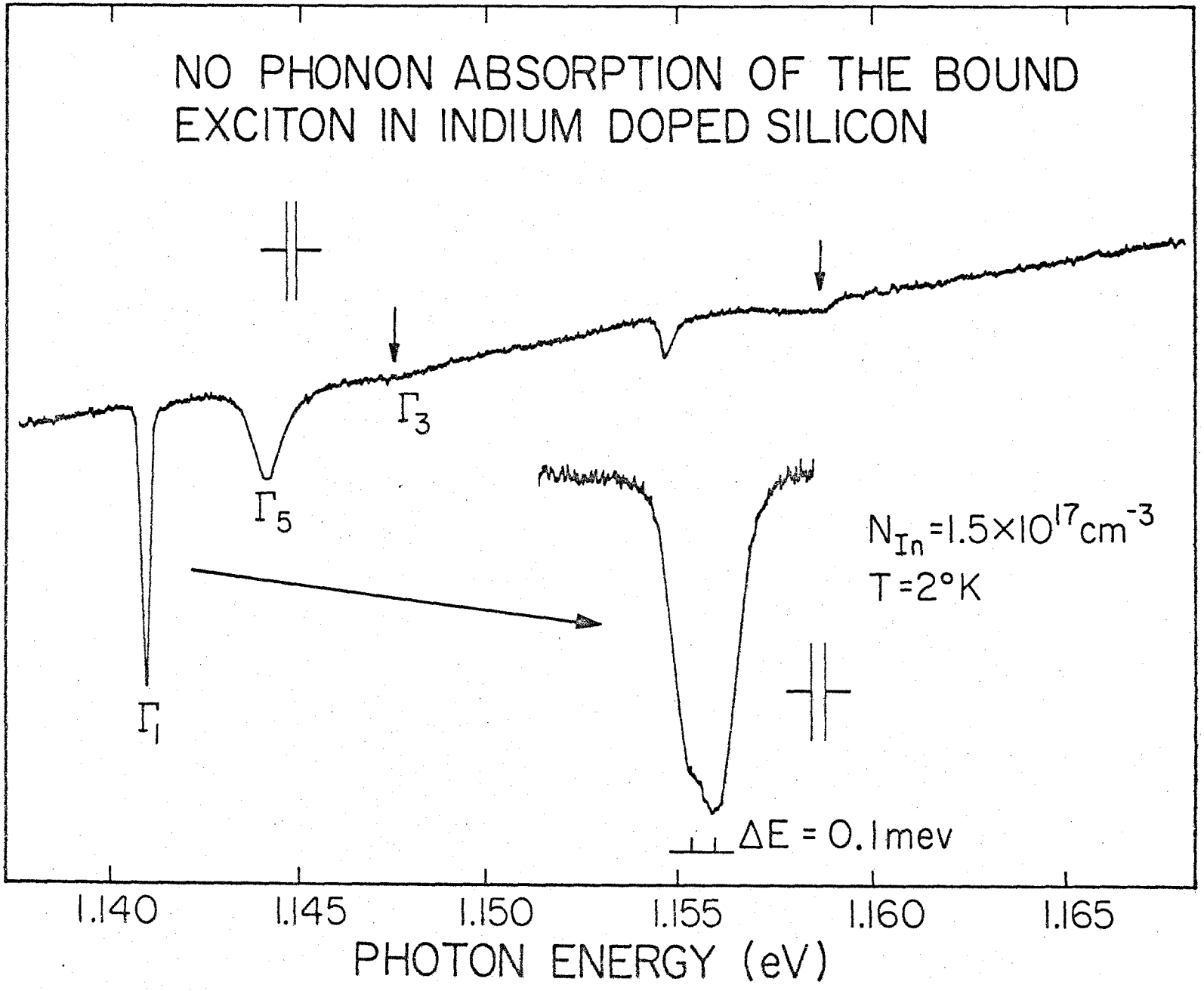
NO PHONON ABSORPTION OF THE BOUND EXCITON IN INDIUM DOPED SILICON
Γ_3
Γ_5
Γ_1
$N_{In}=1.5\times10^{17}cm^{-3}$
T=2°K
ΔE = 0.1mev
1.140
1.145
1.150
1.155
1.160
1.165
PHOTON ENERGY (eV)

Thus, the labeling of the lines in Si:In must be considered tentative. The insert in Fig. 2.3 shows a high resolution spectrum of the Γ_1 line. This spectrum indicates that there is additional structure on the line. This splitting was also observed in a second sample of Si:In. Because of the reproducibility of the structure, we believe that it is due to the In BE and not an external perturbation such as stress.

I have also observed in the spectrum of Si:In a narrow line at 1.1544 eV and a broad feature at 1.1584 eV. These lines do not have the correct energy for a phonon assisted transition and thus, it is concluded that they are due to the no-phonon creation of a BE in a highly excited state. Since In is a relatively deep acceptor in Si, it is possible that these lines can be described by a "pseudo-donor" model in which the electron experiences the effective potential of a net positive charge from the two holes which are tightly bound to the negative In ion. Such a model has been used to describe excited states of BE in other materials [13]. The 1.1544 eV line is only bound with respect to the free exciton by 0.4 meV; whereas, the higher energy line is not bound in this respect and, therefore, must be interpreted as a resonant state. Finally, a smoothly varying background is observed in the absorption of Si:In which is not observed for Si:Al and Si:Ga. This absorption background is probably due to photoionization of neutral In acceptors.

Comparing our experimental results for the relative oscillator

strengths for lines labeled Γ_1, Γ_5 and Γ_3 in Fig. 2.1 to 2.3 with previous estimates from luminescence data, there is some discrepancy. The absorption measurements should be more accurate for this purpose than luminescence measurements because it is not necessary to divide out temperature dependent Boltzmann factors. Small uncertainties in line separations or temperature in the sample under external excitation could account for the discrepancy. Also, it is necessary to use integrated intensities rather than peak heights because the lines have different widths. The absolute no-phonon oscillator strength measurements in this study are rather close to those previously measured by Dean and co-workers [5].

III. Theoretical Analysis of the No-Phonon Oscillator Strengths

Smith has used a model for the acceptor which allowed him to calculate the relative line ratios obtained in the bound exciton absorption for a variety of schemes which produce splittings [24]. Of all the possible splitting mechanisms it is clear that some are not important. If one counts states, there are 72 possible states of the bound exciton which could be low in energy. This is because there are six electron valleys and the valence band is fourfold degenerate. From symmetry considerations there are 24 levels which could have different energies. Since only three lines are observed

the effects of many of the possible mechanisms must be small. In this section we will outline Smith's calculation of the no phonon oscillator strengths.

The three coupling schemes which are considered were those mentioned in the introduction to the chapter. First two holes with angular momentum J=3/2 are coupled together by their mutual interaction in a spherical model to form states with total angular momentum J=0 and J=2. The J=2 level is then split by the electron-hole exchange interaction into two states. In the second scheme the J=2 state is split by the cubic environment of the crystal instead of the electron-hole exchange. In the third scheme the splitting is due to the valley-orbit splitting of the electron.

In the direct band gap semiconductors, InP [8] and GaAs [9], three emission lines for acceptor BE are also seen. In Ref. (8), it is argued that the first splitting scheme applies in InP:Zn. In Ref. (9), it is argued that in GaAs;Si (Si acceptors) the crystal field splitting of the J=2 hole state (second scheme) is more important than the electron-hole exchange effect. One might expect that electron-hole exchange splitting is less important in indirect gap materials like Si than in direct gap materials because in the indirect gap materials it requires Coulomb exchange scattering between a hole state near the zone center and an electron state near the zone edge. The Coulomb matrix element is inversely proportional to the square of the wavevector transfer.

The wavevector transfer in such a scattering event is large so that the Coulomb matrix element is small. In the indirect gap material GaP, the number of emission lines observed for acceptor BE depends on the acceptor type [7]. It appears that both hole-hole coupling and valley-orbit splitting play a role in the acceptor BE in GaP [7].

To determine the splitting mechanism in silicon the experimental results are compared with the calculated no phonon oscillator strengths of the three absorption lines for the three different coupling schemes. The no phonon oscillator strength is defined by

$$f_N = \frac{2}{\hbar\omega_N m_o} |\langle\psi_o|P_y|\psi_N\rangle|^2 \qquad (1)$$

where the squared matrix element is to be averaged over the initial acceptor states and summed over final BE states that are degenerate. Here, $\hbar\omega_N$ is the energy of the photon involved in the transition, $|\psi_o\rangle$ is the acceptor wavefunction, $|\psi_N\rangle$ is the BE wavefunction, P_y is the y component of the momentum operator and m_o is the free electron mass. The wavefunctions have the form

$$|\psi_o\rangle = \sum_{K_h m} a_m^M(K_h)\, C_{K_h m}\, |G\rangle \qquad (2a)$$

and

$$|\psi_N\rangle = \sum_{m_1 m_2 v} \sum_{k_e k_h k_h'} A^N_{m_1 m_2 \sigma v}(k_e, k_h, k_h') C_{k_h m_1} C'_{k_h m_2} C^+_{k_e v\sigma} |G\rangle \qquad (2b)$$

where N and M label the BE and acceptor quantum numbers, respectively. Here $C^{+}_{k_e v\sigma}$ creates an electron of wavevector k_e in valley v with spin σ, $C_{k_h m_1}$ creates a hole with wavevector k_h and spin projection m_1, $|G\rangle$ is the state with all conduction band states empty and all valence band states occupied and a and A are amplitude functions for the acceptor and BE, respectively. The transition matrix element becomes

$$\langle\psi_o|P_y|\psi_N\rangle = \sum_{m_1 m_2 v\sigma} \sum_{k_e k_h} \langle\phi_{k_e m_1}|P_y|U_{k_e v\sigma}\rangle\, a^{M}_{m_2}(k_h) \left[A^{N}_{m_1 m_2 \sigma v}(k_e,k_e,k_h) - A^{N}_{m_2 m_1 \sigma v}(k_e,k_h,k_e)\right] \qquad (3)$$

where $U_{k_e v\sigma}$ is the periodic part of the electron Bloch function and $\phi k_e m_1$ is the periodic part of the hole pseudo-Bloch function.

To proceed, it is necessary to specify a model for the amplitude functions A and a. Smith has used a simple model which allows him to determine the relative oscillator strengths of the three absorption lines from symmetry considerations; he takes

$$a^{M}_{m_2}(k_h) = F(k_h)\,\delta_{M,m_2} \qquad (4a)$$

and

$$A^{D_\alpha \nu_\beta}_{m_1 m_2 \sigma v}(k_e,k_h,k_h') = C^{D_\alpha}_{m_1 m_2 \sigma}\, B_v^{\nu_\beta} f_h(k_h)\, f_h(k_h'(\, f_{ev}(k_e) \qquad (4b)$$

Here, M labels the acceptor quantum number (column of the Γ_8 representation), D_α labels the hole and electron spin quantum numbers in the BE (D gives the representation and α gives the column of the representation, the nature of D_α dependson the coupling scheme) and ν_β labels the electron valley states in the BE (ν gives the representation and β gives the column of the representation). The function $F(k_h)$ is the Fourier transform of an s-like spatial envelope function for the acceptor, $f_h(k_h)$ is the Fourier transform of an s-like spatial envelope function for a hole in the BE and $f_{ev}(k_e)$ is the Fourier transform of the spatial envelope function for the BE electron in conduction band valley v. The coefficients $B_v^{\nu_\beta}$ are the same as those for the valley orbit states of the donor in Si; they can be found in the article by Kohn [16]. The coefficients $C^{D_\alpha}_{m_1 m_2 \sigma}$ depend on the coupling scheme.

In the simple model for the amplitude functions defined by Eq. (6), the following have been neglected: mixing of D like and higher angular momentum functions in the spatial envelope functions for the holes in the acceptor and BE, mixing of the spin orbit split Γ_7 valence band and the possibility that the envelope functions f_h and f_{ev} in the BE could depend on the quantum numbers D and ν. These approximations are expected to be better for the shallower impurities Al and Ga than they will be for In and estimates of the relative oscillator strengths of closely spaced lines are expected to be better than for lines with greater energy separation. The no-phonon oscillator strengths are quite sensitive to the envelope

function f_h [17]. For closely spaced lines, the envelope functions f_h for the states are expected to be similar; but for farther spaced lines there may be corrections to this approximation.

In the acceptor BE, the holes are more strongly localized near the acceptor than the electron. As a result, the hole envelope function $f_h(k)$ is more spread out in k-space than the electron envelope function $f_e(k)$. In the acceptor BE in Si, the hole function, f_h, is largest at the zone center and the electron function, f_e, is strongly peaked at the conduction band minimum. (Variational calculations for these functions, in a simple model for the four common acceptors in Si, are given in Ref. (17)). As a result of the sharp peaking of the function $f_e(k)$, the one electron matrix elements involved in the optical transition are evaluated at the conduction band minimum.

With the model for the amplitude functions given by Eq. (4), the no-phonon oscillator strengths for the BE lines labeled by D and ν become

$$f_{D\nu} = Q\frac{1}{r}\sum_{M}\sum_{\alpha,\beta}\left|\sum_{\nu,m_l,\sigma} B_\nu^\beta \langle \phi_{k_{ev}m_l}|P_y|U_{k_{ev}\sigma}\rangle \left(C^{D_\alpha}_{m_l,M,\sigma} - C^{D_\alpha}_{M,m_l,\sigma}\right)\right|^2 \qquad (5a)$$

where

$$Q = \frac{2}{h\omega_{D\nu} m_o} \left| \sum_{k_h} F(k_h)\, f_h(k_h) \right|^2 \left| \sum_{k_e} f_h(k_e)\, f_{ev}(k_e) \right|^2 \qquad (5b)$$

In deriving Eq. (5), Smith used the fact that $|\sum_{k_e} f_h(k_e)\, f_{ev}(k_e)|$ does not depend on v and that $f_{ev}(k_e)$ is sharply peaked at the conduction band minimum for the v valley, k_{ev}. Performing the sums indicated in Eq. (5) gives the result,

$$f_{D_\nu} = Q|\langle\Delta_5|P_y|\Delta_1\rangle|^2 \frac{2}{9}\{1\delta_{D,\Gamma_1} + 2\delta_{D,\Gamma_3} + 3\delta_{D,\Gamma_5}\}\{1\delta_{\nu,\Gamma_1} + 2\delta_{\nu,\Gamma_3} + 0\delta_{\nu,\Gamma_5}\} \qquad (6)$$

when electron-hole exchange is assumed to be negligible. An important result in Eq. (6) is that the valley orbit splitting only produces two absorption (or emission) lines because transitions to the Γ_5 valley orbit state are forbidden. (Transitions to these states are forbidden because transitions to valleys on the opposite side of the zone come in with opposite phase and cancel.) If valley orbit splitting is the only important splitting mechanism, there should be two absorption lines with intensity ratios $(\Gamma_1;1) : (\Gamma_3;2)$. If the hole-hole splitting mechanism is dominant, there should be three absorption lines with intensity rations $(\Gamma_1;1) : (\Gamma_3;2) : (\Gamma_5;3)$.

Next consider the case in which electron-hole exchange scat-

tering is assumed important, but the cubic crystal field is not important. In this case, the two holes are first coupled in a spherical model to produce J=0 and J=2 states. When electron spin is included, the J=0 state becomes a state of total spin S = 1/2 and the J=2 state splits to form states of total spin S = 3/2 and S = 5/2. Performing the sums indicated in Eq. (6) gives the result

$$f_{D_\nu} = Q|\langle\Delta_5|P_y|\Delta_1\rangle|^2 \frac{2}{9}\{1\delta_{D,1/2} + 4\delta_{D,3/2} + 1\delta_{D,5/2}\}$$

$$\{1\delta_{\nu,\Gamma_1} + 2\delta_{\nu,\Gamma_3} + 0\delta_{\nu,\Gamma_5}\} \qquad (7)$$

The ratios for the valley orbit split states are the same as before. If the spherical hole-hole coupling followed by electron-hole exchange coupling is the dominant splitting mechanism, we expect three absorption lines with intensity ratios (S = 1/2;1) : (S = 3/2;4) : (S = 5/2;1). This is the same result as for direct band gap materials [19,20].

Comparing the calculated intensity ratios for the three coupling schemes with the measured results, there is fairly good agreement with the measured results in Si:Ga and Si:Al for hole-hole coupling in the cubic crystal field (see Table 2.1). For the valley orbit splitting scheme and the hole-hole coupling (spherical model) with electron-hole exchange scattering scheme, there is no agreement with

experiment. It is concluded that electron-hole exchange scattering and valley orbit splitting for the acceptor BE in Si are small. By comparing the measured intensity ratios with the calculated ones, one can assign the symmetry labels to the absorption lines as shown in the figures. As expected, the agreement with experiment is best for the ratio of the closely spaced Γ_5 and Γ_3 lines. The measured oscillator strength of the Γ_1 line is somewhat larger than expected. This is attributed to a change in the envelope function $f_h(k_h)$ in going to the more tightly bound Γ_1 state. Also, as expected the agreement with experiment is better in Si:Ga and Si:Al than in Si:In.

In Si:Al, the Γ_1 hole-hole coupling state is observed to be split into two states separated by about 0.07 meV. This splitting can be attributed to valley orbit splitting. If this is the case, the lowest lying state must be the Γ_3 valley orbit state and the higher lying one the Γ_1 valley orbit state because of their intensity ratios. (The quantitative agreement between the measured ratios and the 2:1 ratio expected for this assignment is quite good.) This ordering is the opposite for that observed for the substitutional donors in Si[14]. This change in ordering of the valley orbit states in the donors and acceptor BE is to be expected. In the donor case, the interaction between the positively charged impurity and the electron is everywhere attractive and is strongest near the impurity. For the BE, however, the electron experiences a repulsive interaction near the negatively charged impurity. Of the valley orbit states, only the Γ_1 state has

TABLE 2.1. Relative oscillator strengths. The Γ_5 value is taken to be three for normalization. The theory is for the hole-hole coupling scheme. For Si:Al, we give the ratios for the split Γ_1 level (lowest level normalized to two); theory is for valley orbit splitting.

	Γ_1	Γ_5	Γ_3
Theory	1	3	2
	(Γ_3;2) : (Γ_1;1) (valley orbit)		
Si:Al	$1.8\pm.1$	3	$2.0\pm.1$
	(Γ_3;2) : (Γ_1;$1.1\pm.1$)(valley orbit)		
	2[a]	3[a]	2.3[a]
	1.6[c]	$5(\Gamma_3+\Gamma_5)$[c]	
Si:Ga	$1.6\pm.1$	3	$2.0\pm.1$
	2.1[b]	3[b]	3.0[b]
	2.0[c]	$5(\Gamma_3+\Gamma_5)$[c]	
Si:In	$2.7\pm.1$	3	$1.9\pm.3$
	3.0[c]	3[c]	-

(a) Ref. (3) (b) Ref. (2) (c) Ref. (1)

an amplitude at the impurity site. Thus, for the substitutional donor, the Γ_1 state is the lowest energy state, but for the acceptor BE, it should be the highest energy state. We expect that the valley orbit splitting in the acceptor BE is much less than that for the substitutional donor because the electron is much more tightly bound to the donor than to the acceptor BE. We have not observed valley orbit splitting in Si:Ga; in Si:In there appears to be some fine structure on the Γ_1 line, but it is not clearly resolved. The Si:Al Γ_1 line is sharper than the Γ_1 lines in Si:Ga and Si:In (perhaps because the doping in this sample is lower) and this may account for the fact that this splitting was only observed in Si:Al.

The absolute no-phonon oscillator strengths can be calculated if a model for the envelope functions is specified. Such a model has been developed, by Osbourn and Smith, in a recent paper which dealt with Auger transition rates [17]. The results of this calculation are given in Table 2.2 along with the experimental values obtained in this work.

IV. Summary and Conclusions

High resolution measurements of BE absorption in the no-phonon region have been presented for Si:Al, Si:Ga and Si:In. In each case at least three absorption lines associated with the acceptor BE have been observed. By comparing the measurements of the relative no-phonon oscillator strengths with calculations for these ratios based on different coupling schemes, it has been shown that the three lines

TABLE 2.2. Absolute no-phonon oscillator strengths for the sum of the main triplet lines.

	Si:Al	Si:Ga	Si:In
Theory	$3.5 \cdot 10^{-6}$	$9.0 \cdot 10^{-6}$	$9.3 \cdot 10^{-5}$
This Work	$5 \cdot 10^{-6}$	$7 \cdot 10^{-6}$	$8 \cdot 10^{-5}$
Ref. (5)	$7 \cdot 10^{-6}$	$1 \cdot 10^{-5}$	$9 \cdot 10^{-5}$

result from coupling the two holes in a cubic crystal field. By comparing observed and calculated relative oscillator strengths, symmetry labels have been assigned to the three lines. The Γ_1 state is the ground state, the Γ_5 excited state is slightly lower in energy than the Γ_3 excited state.

The ordering of the J=0 (Γ_1) and J=2 (Γ_3 and Γ_5) is the opposite of that predicted by atomic theory. However, this inverted ordering has been observed for acceptor BE in other materials such as GaSb [21] and GaAs;Sn [22]. Possible reasons for the inverted ordering have been discussed by Morgan [23].

In SiAl, the lowest lying line of the main triplet is further split into two components. This splitting has been interpreted as being due to valley orbit splitting of the electron in the acceptor BE. The lowest of these two components is the Γ_3 valley orbit state and the Γ_1 valley orbit state is slightly higher in energy. (The Γ_5 valley orbit state has a forbidden optical transition but is probably close in energy to the Γ_3 valley orbit state.) In Si:In, two states have been found which are higher in energy than the main triplet. These are probably highly excited states of the In BE in which the electron has been excited about the two holes and the impurity center. Such states can be referred to as "pseudodonor" states of the bound exciton.

REFERENCES

1. M. A. Vouk and E. C. Lightowlers in Proceedings of the 13th International Conference on the Physics of Semiconductors, Rome, 1976, edited by F. G. Fumi, (Tipografia Marves, Rome, 1977) p. 1098.
2. M. L. W. Thewalt, Phys. Rev. Lett. 38, 521 (1977).
3. E. C. Lightowlers and M. O. Henry, J. Phys. C10, 1247 (1977).
4. S. A. Lyon, D. L. Smith, and T. C. McGill (to be published).
5. P. J. Dean, W. F. Flood and G. Kaminsky, Phys. Rev. 163, 721 (1967).
6. This is easily established by the temperature dependence of the relative intensities of the three emission lines, Refs. (1-4).
7. P. J. Dean, R. A. Faulkner, S. Kimura and M. Ilegems, Phys. Rev. B14, 1926 (1971).
8. A. M. White, P. J. Dean and B. Day, J. Phys. C7, 1400 (1974).
9. M. Schmidt, T. N. Morgan, and W. Schairer, Phys. Rev. B11, 5002 (1975).
10. We use the notation of Ref. (11) when referring to irreducible representations of the double point groups and the notation of Ref. (12) for the single point groups.
11. R. J. Elliott, Phys. Rev. 96, 280 (1954).
12. L. P. Bouchaert, R. Smoluchowski, and E. Wigner, Phys. Rev. 50, 58 (1936).
13. See for example, Y. Nisida and M. von Ortenberg, Solid State

Commun. 22, 581 (1977) and references therein.

14. If these additional splitting mechanisms were important, they would produce more than the three observed absorption (or emission) lines. It is possible, in principle, for electron valley anisotropy-hole splitting to produce three groups of states if both valley orbit splitting and hole-hole splitting are negligibly small. Since hole-hole splitting has been found to be important in other materials, it seems unlikely that it should be negligibly small in Si. If this valley-hole splitting were responsible for the three acceptor BE absorption lines observed in Si, we find that the intensity ratios for the lines should be 3:8:1. This does not agree with experiment.
15. C. Kittel and A. Mitchell, Phys. Rev. 96, 1488 (1954).
16. W. Kohn, Solid State Physics, 5, 257 (1958).
17. G. C. Osbourn and D. L. Smith (to be published).
18. G. F. Koster, J. O. Dimmock, R. G. Wheeler, and H. Statz, Properties of the Thirty-two Point Groups, (MIT, Cambridge, Mass., 1963).
19. A. M. White, J. Phys. C6, 1971 (1973).
20. T. N. Morgan, J. Phys. C10, L131 (1977).
21. W. Rhule and D. Bimberg, Phys. Rev. B12, 2382 (1975).
22. W. Schairer, D. Bimberg, W. Kottler, K. Cho, and M. Schmidt, Phys. Rev. B13, 3452 (1976).

23. T. M. Morgan in Proceedings of the Twelfth International Conference on the Physics of Semiconductors, edited by M. H. Pilkuhn (B. G. Teubner, Stuttgart, 1974) p. 391.

24. K. R. Elliott, G. C. Osbourn, D. L. Smith, and T. C. McGill, Phys. Rev. B17, 1808 (1978).

25. The electron-hole exchange is discussed in detail by F. Bassani and G. Pastori Parravincini, Electronic States and Optical Transitions in Solids, (Pergamon Press, Oxford, 1975).

Chapter 3

ABSORPTION AND LUMINESCENCE OF THE Si:Tl BOUND EXCITON

1. Introduction

In Chapter 2 the bound exciton spectra associated with Al, Ga, and In acceptors were reported. In each case at least three low lying states of the bound exciton were observed. It was found the data could be adequately explained by considering the effects of the hole-hole coupling in the crystal field. In such a model the holes are treated first in a spherical model such as that described in the first chapter. In such a model the holes transform as particles with angular momentum j=3/2. The holes are coupled together by their mutual coulombic repulsion. This coupling produces states with total angular momentum J=0 and J=2 [1]. When cubic terms in the Hamiltonian due to the crystal field are included, the J=2 state splits into two states [2].

The question naturally arises about whether this model is applicable when one considers acceptors and bound excitons with larger binding energies. For Si:In the binding energy of a neutral acceptor is 155 meV [3]. The binding energy of a free exciton to the indium acceptor is 14.0 meV [1]. The next acceptor in the Group III column of the periodic table after aluminum, gallium, and indium is the element thallium. Vouk and Lightowlers [4,5] observed a triplet structure for the bound exciton luminescence in Si:Tl which was qualitatively different from that observed in the luminescence of Si:Al, Si:Ga, and Si:In. They observed a pair of lines at lower energies with a single line at higher energies. As discussed in

Chapter 2, the bound exciton spectra for the acceptors Al and Ga show one line at lower energies and two lines at higher energy. Such spectra were interpreted in terms of the simple model in which hole-hole coupling was the dominant splitting mechanism. This model for the shallow acceptors predicted line ratios of 1:3:2. Vouk and Lightowlers observed line ratios of 1:1:1 from the luminescence of Si:Tl [4]. Thus the simple model does not enable one to readily understand the spectra of Si:Tl. Since the splitting mechanism which is important for Si:Tl is likely to be important for other deep impurities, it is important to try to understand the nature of this splitting.

In this chapter the results of high resolution absorption and luminescence measurements of the bound exciton spectra in Si:Tl are presented. Four lines are observed in the spectra of the bound exciton. This is one more line than was observed by Vouk and Lightowlers. The existence of this extra line indicates that the splitting scheme is different than for the other type III acceptors.

In addition I report the relative oscillator strengths for each of the four observed transitions and the absolute oscillator strengths for the sum of the four lines. This measurement indicates that the total no-phonon oscillator strength follows the trend observed for the shallower impurities that the oscillator strength varies as the cube of the acceptor binding energy. The Auger decay rate for the bound exciton has also been estimated from the observed radiative effi-

ciency. This measurement indicates that the Auger rate also follows the trend observed for the shallower impurities. In this case the Auger rate varies roughly as the sixth power of the acceptor binding energy. As a result the luminescence efficiency decreases roughly as the cube of the acceptor binding energy.

II. Experiment

Both the luminescence and absorption spectra of Si:Tl were measured. The apparatus used in this experiment was identical to that described in Chapter 2 for the transmission measurements in Si:Al, Si:Ga, and Si:Al. The transmission measurements were performed with the sample immersed in superfluid helium at $2^{o}K$. The luminescence measurements were performed at a number of different temperatures between $2^{o}K$ and $30^{o}K$. An argon ion laser was used as an excitation source for the luminescence measurements. In addition it was necessary to flush the spectrometer with dry nitrogen gas since the Si:Tl bound exciton absorption is masked by atmospheric absorption lines. The sample used in this experiment was grown at Hughes Research Laboratories. The impurity content was determined by a Hall measurement to be $3x10^{16}cm^{-3}$.

III. Results

The transmission spectra of Si:Tl in the no-phonon region is shown in Figure 3.1. Four lines are observed in this spectrum.

Figure 3.1. The transmission spectrum of Si:Tl. The arrows indicate lines identified with the absorption process where an electron-hole pair is produced in a bound state at a neutral Tl.

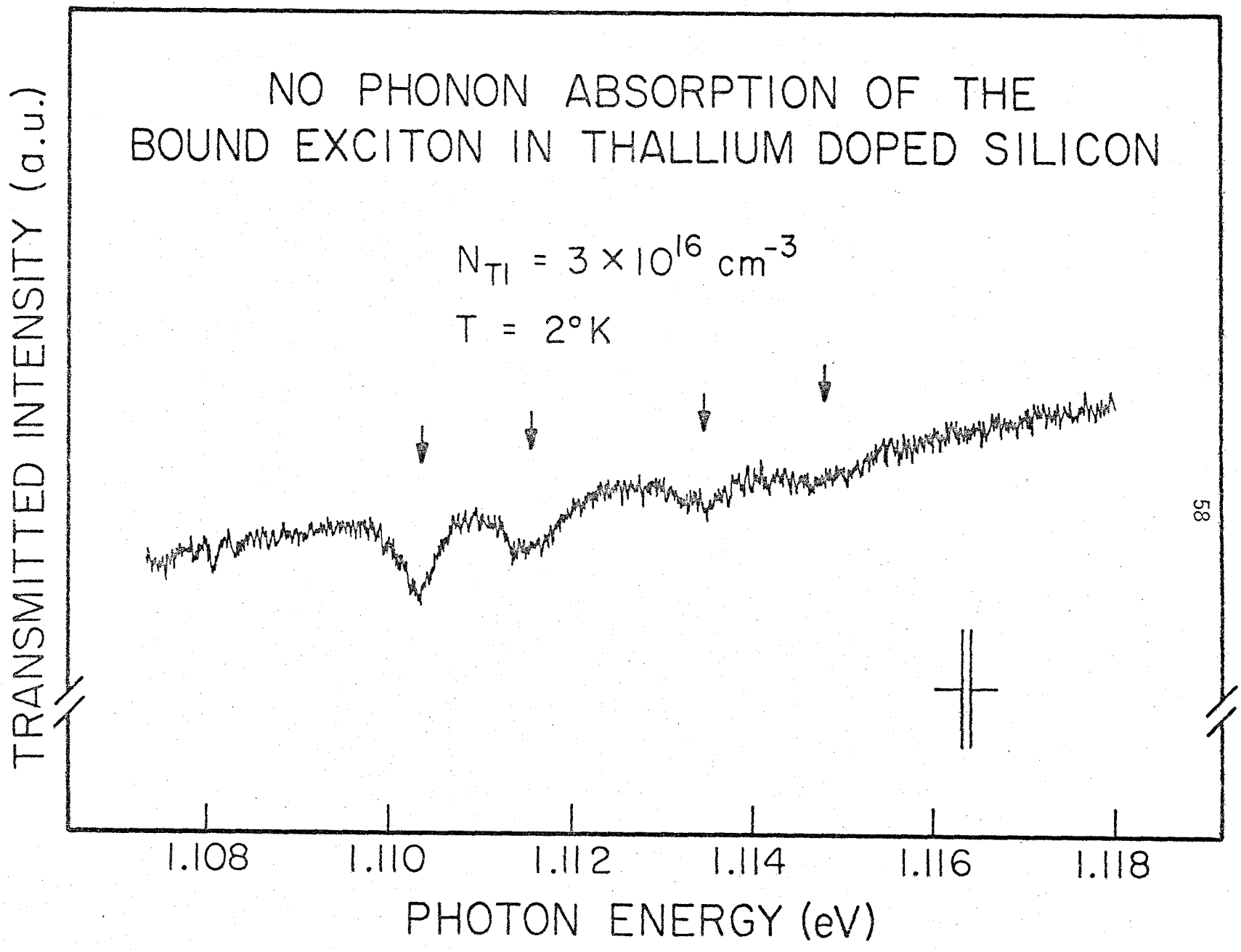
NO PHONON ABSORPTION OF THE
BOUND EXCITON IN THALLIUM DOPED SILICON
$N_{Tl} = 3 \times 10^{16}$ cm^{-3}
T = 2°K
TRANSMITTED INTENSITY (a.u.)
1.108
1.110
1.112
1.114
1.116
1.118
PHOTON ENERGY (eV)

Figure 3.2. The luminescence spectrum of Si:Tl. The four lines observed are identified with the decay of an electron-hole pair bound to a neutral Tl.

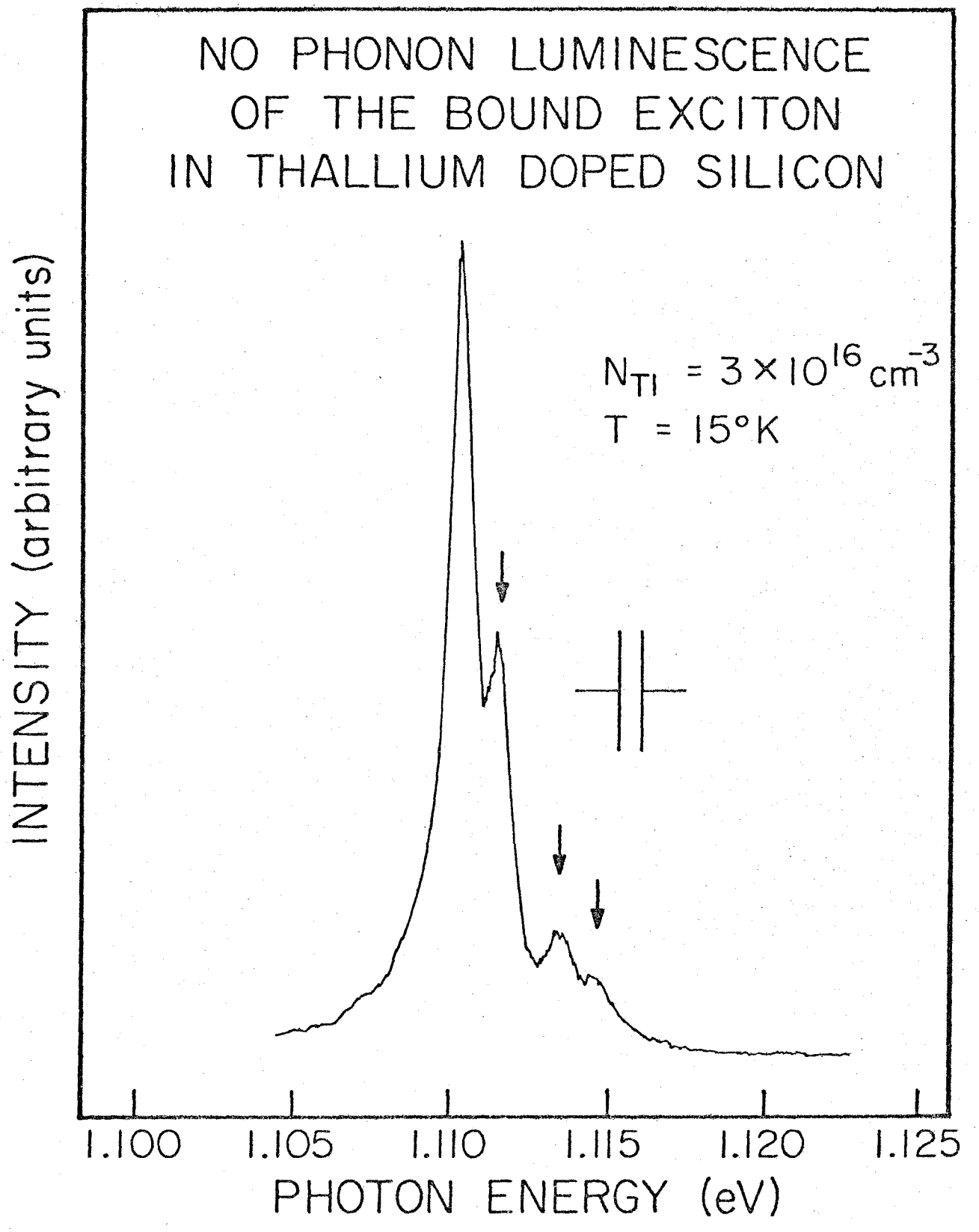
NO PHONON LUMINESCENCE
OF THE BOUND EXCITON
IN THALLIUM DOPED SILICON
$N_{Tl} = 3 \times 10^{16} cm^{-3}$
T = 15°K
INTENSITY (arbitrary units)
1.100
1.105
1.110
1.115
1.120
1.125
PHOTON ENERGY (eV)

These lines occur at 1.1104 eV, 1.1115 eV, 1.1134 eV, and 1.1148 eV. The 1.1148 eV line has not been previously observed. The integrated ratios of the four lines were found to be 1.6±.2, 1.6±.2, 1.0±.1, and 1.2±.1, respectively. The absolute oscillator strength for the sum of all four lines is approximately 4×10^{-4}. The oscillator strength was obtained in the same manner as that described in the previous chapter for Si:Al, Si:Ga, and Si:In.

In Figure 3.2 the no-phonon replicas of the same four lines are shown in luminescence. All of the lines which are observed in luminescence occur at the same energy as the lines observed in absorption within experimental error. Measurements of the temperature dependence of the luminescence were made to determine whether the observed lines were due to excited states of the bound exciton. These measurements showed that all the lines thermalize with energies given by their splittings. These data clearly indicate that the line at 1.1104 eV is the ground state of the bound exciton and that the other lines are associated with low lying excited states of the bound exciton for Si:Tl.

IV. Discussion

The observed spectra for Si:Tl are considerably different from that observed for the shallower acceptors Al, Ga, and In. For these three impurities only three lines are observed. In addition the line ratios disagree with those obtained from the model which works for Si:Al, Si:Ga, and Si:In. Si:Tl is different from the shallower

acceptors in that it is a much deeper level and consequently binds holes much more tightly. Since the hole binding energy to the neutral acceptor (E_A = 255 meV) [3] and the exciton binding energy which we observe ($E_{\text{bound exciton}}$ = 44.2 meV) are not small in comparison to the spin orbit splitting ($E_{\text{spin-orbit}}$ = 44 meV), it may not be a good approximation to neglect effects of the split-off band.

In addition, electron-hole exchange scattering may be important for the deep levels. The effects of the electron-hole exchange interaction were discussed in Chapter 2. Such an interaction is not important for the shallow acceptors because the electron and hole wavefunctions are not strongly localized. In order for the electron-hole exchange to be important, the exchange matrix elements must be large enough to be significant. However the exchange matrix elements are inversely proportional to the square of the wavevector difference between the electron and hole states. Since the electron and hole are localized in two different parts of K-space, the wavevector difference is large and the exchange matrix elements are small. However, the hole states will have an appreciable amplitude throughout the Brillouin zone when the hole wavefunction is localized near the central cell of the impurity. Such localization occurs in the deeper acceptors and a large wavevector transfer between the electron states and the hole states is no longer necessary. In this case the effects of the electron hole exchange may be substantial.

In Chapter 2 the effects of the electron hole exchange on the

spectroscopy of acceptor bound excitons was considered. It was found that such an interaction taken together with terms in the Hamiltonian resulting from the cubic crystal field would split the J=2 states into three states with different energy. When the J=0 state is taken into account this results in four emission lines. There may be other splitting mechanisms which play a role. As seen in Fig. 3.1 the 1.1115 eV and 1.1148 eV lines have asymmetric line shapes which suggest that these lines have unresolved fine structure. Such structure may arise from the electron valley-orbit splitting. Such a splitting occurs because the six degenerate electron valley states can have different energy in the environment of the two holes and the impurity.

The dominant mechanism by which bound excitons decay in silicon is an Auger process in which an electron-hole pair decays nonradiatively by exciting the third particle in the bound exciton [7,8]. Both the optical cross-section and the Auger rate are expected theoretically and have been found experimentally to increase with the binding energy for the shallower acceptors [7,8]. In Fig. 3.3 the measured oscillator strength for bound exciton formation in Si:Tl as compared to the shallower impurities B, Al, Ga, and In is shown. A continued increase in the oscillator strength is observed for the deep acceptor Tl. The oscillator strength f increases rapidly with the binding energy of the acceptor varying $f \sim E_b^3$ where E_b is the acceptor binding energy.

Figure 3.3. The total absolute oscillator strength for the lowest known transitions of an electron-hole pair bound to acceptor. For Si:B the value is for a single unresolved line. For Si:Al, Si:Ga, and Si:In all the lines observed in Ref. 2 were included. For Si:Tl all the lines shown in Fig. 1 were included. The data indicated by ■ were taken from Ref. 1. The data ● were taken from Ref. 2.

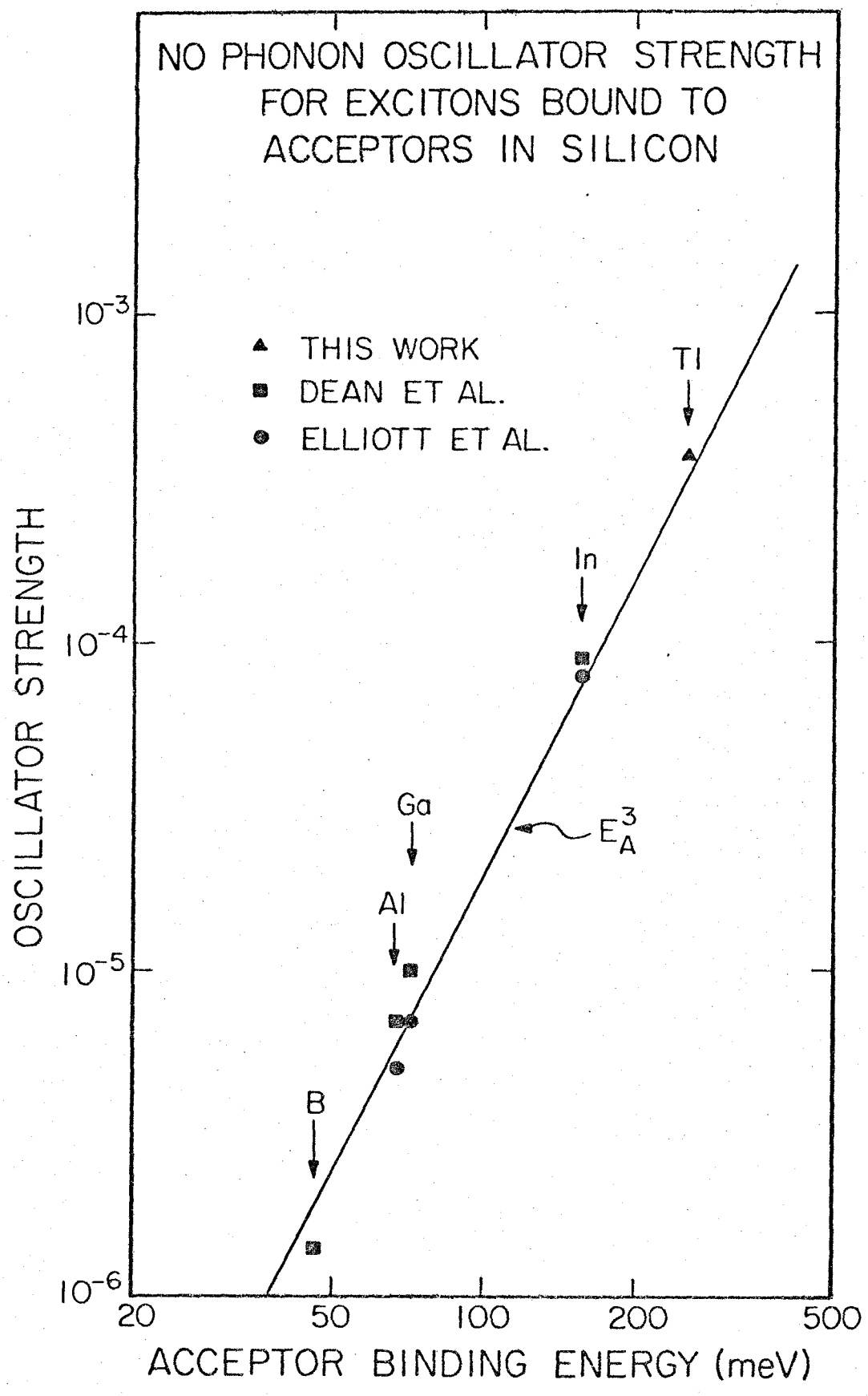
NO PHONON OSCILLATOR STRENGTH
FOR EXCITONS BOUND TO
ACCEPTORS IN SILICON
THIS WORK
DEAN ET AL.
ELLIOTT ET AL.
OSCILLATOR STRENGTH
10^{-3}
10^{-4}
10^{-5}
10^{-6}
B
Al
Ga
In
Tl
E_A^3
20
50
100
200
500
ACCEPTOR BINDING ENERGY (meV)

The luminescence efficiency η associated with the Tl bound exciton is quite small. Comparison of the bound exciton intensity with that from a sample doped with Al indicates that $\eta_{Tl} \sim (.05\text{-}.2)\eta_{Al}$. Since $\eta = \tau_{total}/\tau_{Radiative}$ and $\tau_{total} \simeq \tau_{Auger}$ where $1/\tau$ represents the decay rate, the decay rate due to the Auger process can be estimated. On the basis of this comparison we can estimate τ_{Auger} to be between 75 and 300 picoseconds for an exciton bound to a Tl acceptor. This observation is consistent with an extrapolation of the recent calculation by Osbourn and Smith [7]. Fig. 3.4 shows a plot of the Auger lifetime associated with type III acceptors as a function of binding energy. The calculation of Osbourn and Smith matches the data for B, Al, Ga, and In. The empirical relation $1/\eta_{Auger} \sim E_B^6$ fits these data well. It is apparent from the figure that this relation works well for Si:Tl also. Therefore, if this trend towards large optical cross-sections continues bound exciton transitions should be observable in absorption for other deep impurities, even though the luminescence may be weak and unobservable.

V. Conclusions

The bound exciton spectra associated with Si:Tl consist of four lines. This behavior is different from that observed for the shallower group III impurities Al, Ga, and In. One possible explanation for this behavior is that the electron hole exchange interaction is important for the deep impurities. The oscillator strength has been

Figure 3.4. The measured Auger decay rate for acceptors in silicon. The rate varies as $1/\tau_{Auger} \sim E_B^6$ where E_B is the acceptor binding energy. As a result luminescence associated with bound excitons in silicon is very inefficient. (Ref. 8)

BOUND EXCITON LIFEIMES

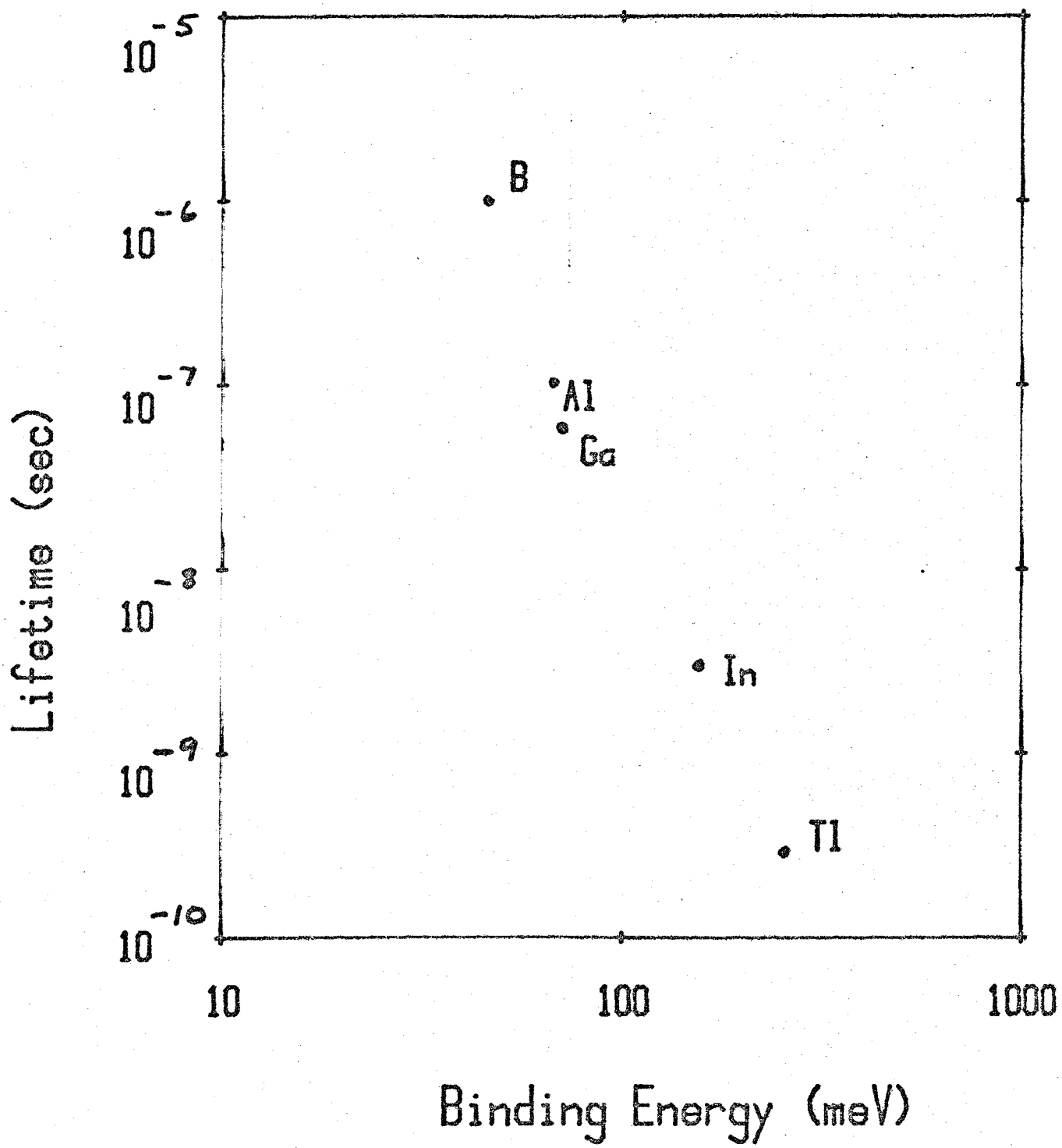

measured. In addition the Auger rate associated with the decay of the bound exciton has been estimated from the luminescence efficiency. These measurements indicate that the decay of the bound exciton and oscillator strength of the bound exciton follow an extrapolation of results obtained for the shallower acceptors B, Al, Ga, and In.

REFERENCES

1. P. J. Dean, W. F. Flood, and G. Kaminsky, Phys. Rev. 163, 721 (1967).
2. K. R. Elliott, G. C. Osbourn, D. L. Smith, and T. C. McGill, Phys. Rev. B17, 1808 (1978).
3. H. J. Hrostowski, Semiconductors, ch. 10, N. B. Hannay, Ed. New York: Reinhold, 1959.
4. M. A. Vouk and E. C. Lightowlers, in Proceedings of the Thirteenth International Conference on the Physics of Semiconductors, Rome (Edited by F. G. Fumi), p. 1098,Tipografia Marver, Rome (1976).
5. M. A. Vouk and E. C. Lightowlers, Luminescence 15, 357 (1977).
6. The oscillator strengths were calculated from the absorption spectra using the relationship $Nf = .97 \times 10^{16}\ n\ \alpha_{max} \Delta E$, where $N(cm^{-3})$ is the concentration of impurity centers, f is the oscillator strength, n is the refractive index, $\alpha_{max}(cm^{-1})$ is the peak absorption coefficient, and ΔE (eV) is the half height bandwidth. This relation is identical to Equation (1) in Ref. (7).
7. G. C. Osbourn and D. L. Smith, Phys. Rev. B16, 5426 (1977).
8. S. A. Lyon, G. C. Osbourn, D. L. Smith, and T. C. McGill, Solid State Commun. 23, 425 (1977).

Chapter 4

LUMINESCENCE EXCITATION SPECTROSCOPY OF BOUND EXCITONS IN GaP

I. Introduction

In the previous two chapters the results of studies on the electronic structure of acceptor bound excitons in silicon have been reported. In order to get a better understanding of bound exciton structure it is necessary to study also donor bound excitons. In silicon donor bound excitons have a very small oscillator strength and thus are difficult to study in absorption. However donor bound excitons in GaP have a much larger oscillator strength and can be studied much more easily. Since GaP and Si both have multiple conduction band minima and because the valence band in both materials have the same symmetry, the bound exciton spectra can be expected to have similar properties in both systems. In this chapter I present the results of studies of the excited state structure of donor bound excitons in GaP.

Luminescence from excitons bound to donors in GaP has been investigated by Dean [1]. This study primarily dealt with ground state of the bound exciton for S, Se and Te doped GaP. However Dean also observed in absorption several excited states of the bound exciton. These included two states labeled by Dean as S_0' and S_0'' which had a large oscillator strength compared to several other transitions which were observed and labeled S_A, S_B, S_C, and S_D. The nature of these states as well as the observed S_A, S_B, S_C, and S_D transitions has not been explained [1].

Recently several authors have attempted to calculate the excited

state spectrum of bound excitons. Chang and McGill[2] have calculated the energies of excited states of bound excitons in a spherical model as a function of the mass ratio of the electron and hole. Herbert has developed a detailed theory for which he presents results for the observed spectra in GaAs [3]. Ruhle and Klingenstein have applied a non-rigid rotational model to describe states observed in InP and GaAs [4]. Of these models only that of Chang can be directly applied to the case of GaP. However the model used by Chang does not take into account the details of the specific band structure expected for GaP. It is thus important to understand what effects the band structure have on the excited state structure of the bound exciton and also to test Chang's model for GaP.

To do this I have measured the excited state structure of donor bound excitons in GaP. By noting the systematic differences between transitions observed in GaP:Se and GaP:S it is possible to distinguish between phonon assisted and no-phonon transitions of the lines previously observed by Dean in absorption. Dean was not able to identify the transitions that he observed. By considering the form of the optical transition matrix elements it has been possible to identify the nature of most of the transitions observed by Dean as well as other transitions observed in this study. Dean labeled the lines he saw as S_0', S_0'', S_A, S_B, S_C, and S_D. The S_0' line observed by Dean is identified to be an excitation of the hole in the bound exciton to a higher lying state about a bound exciton core consisting

of two electrons bound in a D^- configuration. (The D^- state is analogous to the atomic H^- ion. It consists of two electrons bound to a positively charged center.) The S_0" line is observed to be the sum of two lines, one of which is observed to be the TA phonon assisted complement of the S_A transition observed by Dean while the other line is also identified as being due to an excitation of the hole about a D^- exciton core. These excitations of the hole are expected to occur from Chang's theory.

The other lines observed by Dean are apparently associated with states which have an electron core with different symmetry than the ground state. As discussed later in this chapter, it is expected that such states will have weak transitions in the no-phonon region while having comparatively large transition rates in the phonon assisted regions. The S_A and S_C transitions are apparently TA phonon assisted components of weak no-phonon transitions. The S_D line is apparently the LA phonon replica of the S_A transition. These transitions are probably associated with states of this type.

It has thus been found that the excited states of donor bound excitons in GaP can be classified into two different types. The first of these are excitations of the hole in the bound exciton and have been predicted by the theory of Chang. The second type of state involves excitations of the D^- electron core and arises from the many valleyed nature of the conduction band.

II. Experiment

The method used in this experiment is virtually identical to that used by Cohen and Sturge to study the excited states of excitons bound to nitrogen pairs in GaP [5]. Fig. 4.1 shows a schematic diagram of the experimental apparatus. A sample is optically pumped with a tunable source and the luminescence from a particular transition is monitored as the source is tuned. In this experiment the tunable source is a continuous dye laser with constant output power operating with the dye sodium fluorescein pumped with an Ar^+ laser.

The output of the laser was focused on the sample which was placed in a variable temperature dewar. Luminescence from the sample was collected and passed through a grating monochromator and monitored with a C31034 photomultiplier. This method has several advantages over normal methods of studying the absorption. First, the laser has a very narrow linewidth with high brightness compared to a thermal source filtered with a spectrometer. Secondly, the luminescence is proportional to the light absorbed and is relatively insensitive to small fluctuations in the laser intensity. This feature makes it possible to observe weak features in the absorption spectrum. Finally, the laser spot can be focused to a very small size and thus samples a very small region within the material. Thus, small regions in bulk material which have less internal strain and yield better overall spectra can be studied.

In this study results are presented from samples doped with S and Se. The spectrum of the GaP:Se indicated that there was a

Figure 4.1. A schematic diagram of the experimental apparatus. A tunable dye laser excites a GaP sample which has been cooled to liquid helium temperatures. The resulting luminescence is monitored as the dye laser is scanned in wavelength. The resulting spectra show peaks where absorption into bound exciton states occur.

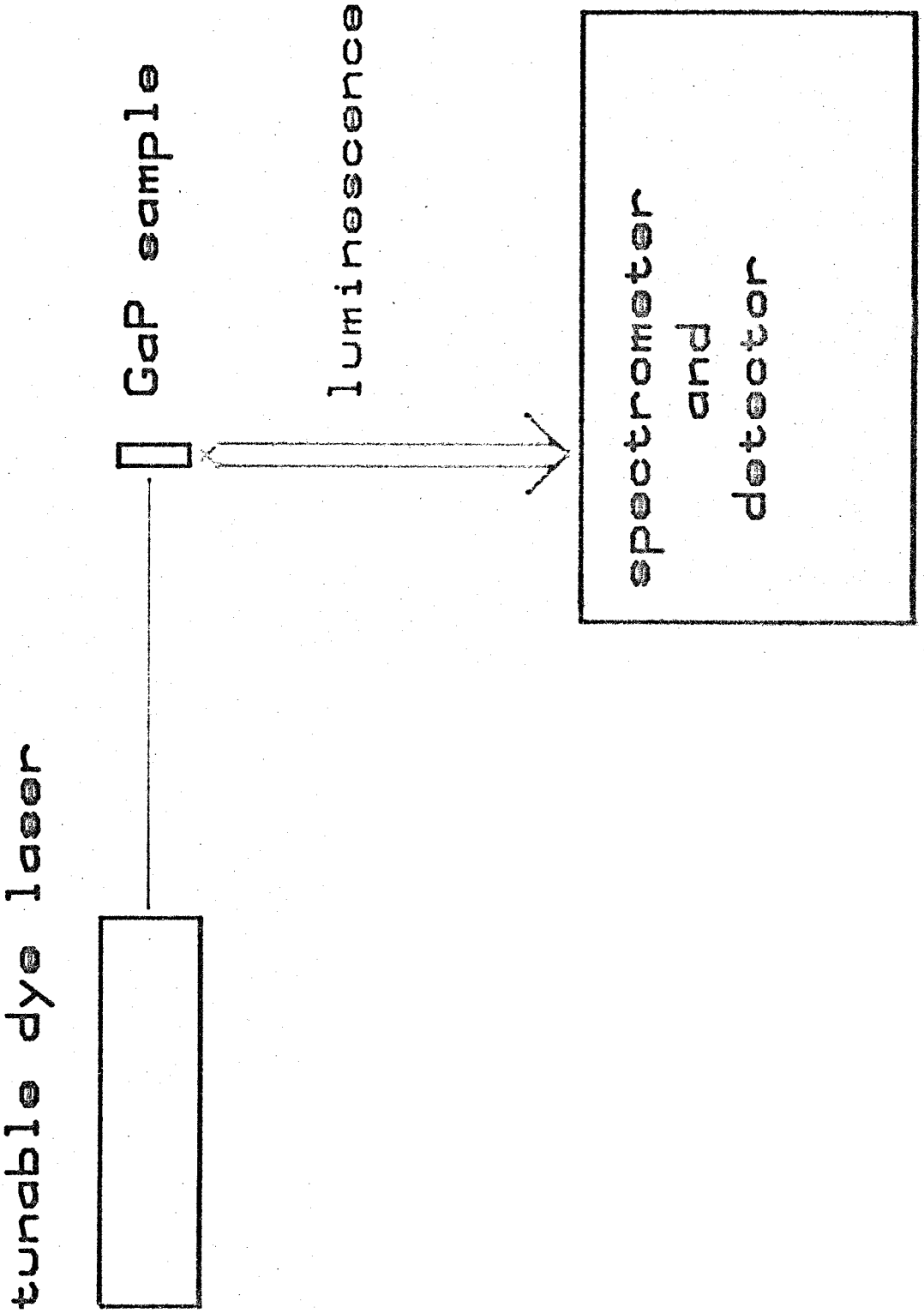
tunable dye laser
GaP sample
luminescence
spectrometer
and
detector

negligible contribution from sulfur in this sample. Because additional structure was observed in samples contaminated with nitrogen which made the results uninterpretable, only samples with low nitrogen content were used. The doping level was estimated to be approximately $3x10^{17}$ for the GaP:Se sample and $5x10^{16}$ for the GaP:S sample by the suppliers.

III. Results

Figures 4.2 and 4.3 show the luminescence excitation spectra obtained from GaP doped with S and Se. The luminescence was monitored from two spectral regions. In the top panel of each figure the luminescence which is monitored as the dye laser is scanned appears at 1.77 eV. This luminescence occurs in a broad emission band peaked at approximately 7000 Å which was observed in both the case of GaP:S and GaP:Se. Such an emission band is probably associated with recombination from a deep center [6]. Presumably excitations, which are created by light absorbed in the sample, decay rapidly into states producing the broad band in the spectrum. If such excitation transfer occurs with uniform efficiency for all excitations created in the crystal then the observed luminescence spectrum accurately portrays the absorption spectrum. If such excitation transfer does not occur with uniform efficiency then the observed spectrum will be influenced by the details of the transport process of the excitation to the luminescent center. To evaluate the effects of such transport, the optical absorption spectra were measured directly in the GaP:Se sample. Although the quality of the absorption spectra was not as

good as that obtained by using the tunable laser, the details of the spectra were basically the same in both cases. In addition the observed spectra are relatively independent of temperature. It is thus assumed that the details of the spectra are not influenced by the transport process but rather reflect changes in the optical absorption.

The luminescence of the ground state no-phonon bound exciton transition was also measured as a function of pump wavelength from the dye laser. For GaP:S this peak occurs at 2.3095 eV and for GaP:Se it occurs at 2.3079 eV. In the bottom panels of Figs. 4.2 and 4.3 these spectra are shown. Such luminescence is also affected by excitation transfer especially from highly excited states. Excitation into a state which is not bound has a large probability of decaying to a deeper level; whereas, a state which is tightly bound has a much lower probability of such a transfer. States which are loosely bound have a higher probability of thermalizing to the free exciton continuum than deeper lying states. By comparing these spectra with those obtained from the previous method where the luminescence from deeper levels was monitored, valuable information on the nature of the states can be obtained.

Figure 4.2 shows the spectra for GaP:S. In addition to features previously observed by Dean, these spectra contain additional lines which make it possible to interpret much of the structure. These lines have been labeled in accordance with the interpretation which is given later in the chapter. In the top panel of Fig. 4.2 spectra are shown for GaP:S where luminescence at 1.77 eV was monitored. At

energies 13.1 ± .2 meV and 14.3 meV ± .2 meV above the ground state two weak lines labeled S_o^{TA} and S_c^o are seen. The energy of the first line matches that of the TA phonon assisted ground state transition. In addition, at higher energies there are two strong lines labeled $S_{o''}^o + S_{FE}^o$, a weaker line labeled S_B^o and a broad feature labeled $S_{o''}^o + S_A^{TA}$. There is a structure at 31 meV above the ground state which is apparently associated with the LA phonon assisted bound exciton transition. The line labeled $S_{o'}^o$ is apparently the same as the $S_{o'}$ transition observed by Dean [1].

In the bottom panel of Fig. 4.2 spectra for GaP:S are shown where luminescence at 2.3095 eV was monitored. This spectrum is more detailed than the first and in addition the strong continuum above 2.33 eV is much weaker. This continuum is interpreted as being primarily due to the no-phonon creation of free excitons scattering off the neutral donor. Such states will have a high probability of decaying to deeper levels and only give rise to weak luminescence at 2.3095 eV. In addition to lines observed in the top panel, lines are observed at 7.7 meV ± .2 meV, 9.4 meV ± .2 meV, and 27.6 meV above the ground state. The latter two lines are most likely the S_A and S_C lines observed by Dean [1]. The 7.7 meV line is most likely associated with the nitrogen N_A^o line which occurs at the same energy. This line is weak in the top spectra and is in general stronger in all samples when donor bound exciton luminescence is monitored than when the deeper luminescence is monitored. This may indicate that nitrogen

Figure 4.2. The luminescence excitation spectra for GaP:S. In the top panel luminescence is monitored at 1.77 eV. In the bottom panel, luminescence is monitored at 2.3095 eV, the energy of the ground state transition. The two small arrows in the top panel point out weak features in the spectra which are discussed in the text. The ground state transition is not shown in this figure but is approximately 4 times stronger than the S_0^0, transition.

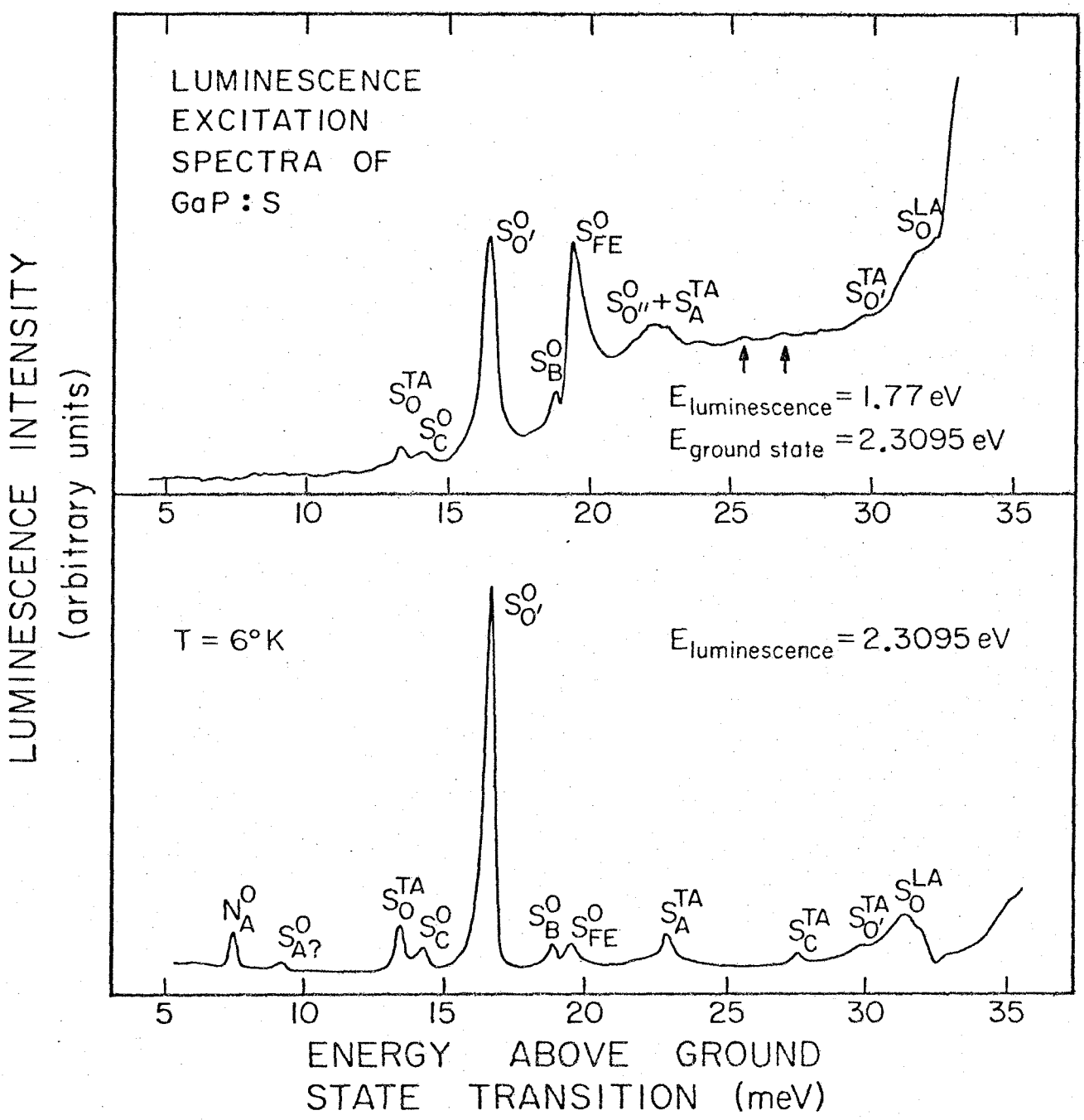
LUMINESCENCE
EXCITATION
SPECTRA OF
GaP : S
$S_{O'}^{O}$
S_{FE}^{O}
S_{O}^{LA}
$S_{O''}^{O} + S_{A}^{TA}$
$S_{O'}^{TA}$
S_{O}^{TA}
S_{C}^{O}
S_{B}^{O}
$E_{luminescence} = 1.77$ eV
$E_{ground\ state} = 2.3095$ eV
5
10
15
20
25
30
35
T = 6° K
$S_{O'}^{O}$
$E_{luminescence} = 2.3095$ eV
N_{A}^{O}
$S_{A?}^{O}$
S_{O}^{TA}
S_{C}^{O}
S_{B}^{O}
S_{FE}^{O}
S_{A}^{TA}
S_{C}^{TA}
$S_{O'}^{TA}$
S_{O}^{LA}
LUMINESCENCE INTENSITY
(arbitrary units)
ENERGY ABOVE GROUND
STATE TRANSITION (meV)

preferentially transfers to the deeper donor bound exciton levels. Considerable structure has been observed in the excitation spectra at the energy of the N_A line in samples with a higher nitrogen content.

A line in the region of the $S^o_{0''}$ line occurs at 22.9 meV ± .2 meV above the ground state. This energy is slightly higher than the $S^o_{0''}$ and S^{TA}_A of which the $S^o_{0''}$ is relatively broad and at slightly lower energies than the S^{TA}_A which is the line observed at 22.9 meV. In addition the line labeled S^o_{FE} at 19.6 meV is much weaker in this spectrum This behavior suggests that these peaks are associated with states which decay into free excitons with high probability since they are weak in the lower spectra. The higher lying transitions which are observed at 22.9 and 27.6 meV and labeled S^{TA}_A and S^{TA}_C are not particularly weak and thus are more likely due to TA phonon assisted transitions. The separation in energy between these lines and those at 9.4 meV and 14.3 meV suggest that the lower energy lines are possibly the corresponding no-phonon transitions. In addition the S_A line matches the energy of the LA phonon replica expected for the S_A transition and, as mentioned by Dean, appears to track the phonon assisted components in intensity [1]. As shown later in this section the interpretation of the higher states as being phonon assisted is strongly supported by similar data observed for GaP:Se. In Fig. 4.2 these transitions have been labeled in accordance with this interpretation and the corresponding lines and their positions have been

listed in Table 4.1.

Figure 4.3 shows the luminescence excitation spectra for GaP:Se. As in the spectra for GaP:S the top panel shows the spectra for luminescence monitored at 1.77; the bottom panel shows the spectra for luminescence monitored at 2.3079 eV, the energy of the ground state no phonon bound exciton transition. Close inspection shows that much of the structure in these spectra matches that of the GaP:S spectra if the energy scale is shifted by 1.6 meV, the difference in energy between the GaP:S and GaP:Se bound exciton ground states. A one to one correspondence between the S_A^{TA}, S_C^{TA}, and $S_{0'}^{o}$, and S_C^{o} transitions and corresponding transitions for GaP:Se is thus noted. A simple observation confirms that the S_A^{TA} and S_C^{TA} transitions are phonon assisted. In the Se doped samples the phonon assisted transitions are much stronger than the no-phonon components. However, the ratios between the S_A^{TA} and S_C^{TA} line strengths and the S_0^{TA} ground state transition line strength are nearly the same as for the ratios between the corresponding lines observed in GaP:Se even though the ratio between no-phonon and TA components has changed by a factor of 5. This suggests very strongly that these transitions are phonon assisted and explains why such states can appear above the FE threshold in the spectra shown in the lower panels of Figs. 4.2 and 4.3.

The peak which is labeled Se_{FE}^{o} appears in the spectra for GaP:Se at 21.1 meV above the ground state and occurs at the same position in

TABLE 4.1

Energies measured for features in the luminescence excitation spectra of GaP:S. The maximum possible error in the measurements is .2 meV. The separation between the weak feature labeled S_A^0 and S_A^{TA} is slightly larger than the observed TA phonon energy and therefore the S_A^0 transition is labeled with a question mark.

	ENERGY (eV)	ENERGY RELATIVE TO S_0^0(meV)
S_0^0	2.3095	0
$S_{B'}^0$	2.3261	16.6
$S_{0''}^0$	2.3319	22.4
S_{FE}^0	2.3290	19.5
S_A^0	2.3187	9.2
S_B^0	2.3283	18.8
S_C^0	2.3237	14.2
S_0^{TA}	2.3229	13.4
$S_{0'}^{TA}$	2.3394	29.9
S_A^{TA}	2.3324	22.9
S_C^{TA}	2.3370	27.5
S_0^{LA}	2.3409	31.4

Figure 4.3. The luminescence excitation spectra for GaP:Se. In the top panel luminescence is monitored at 1.77 eV. In the bottom panel, luminescence is monitored at 2.3079 eV, the energy of the ground state transition. The ground state transition for GaP:Se is about 1.6 meV lower in energy than the corresponding transition in GaP:S. The ground state transition is not shown in this figure but is approximately 4 times stronger than the Se^{0}_{0}, transition.

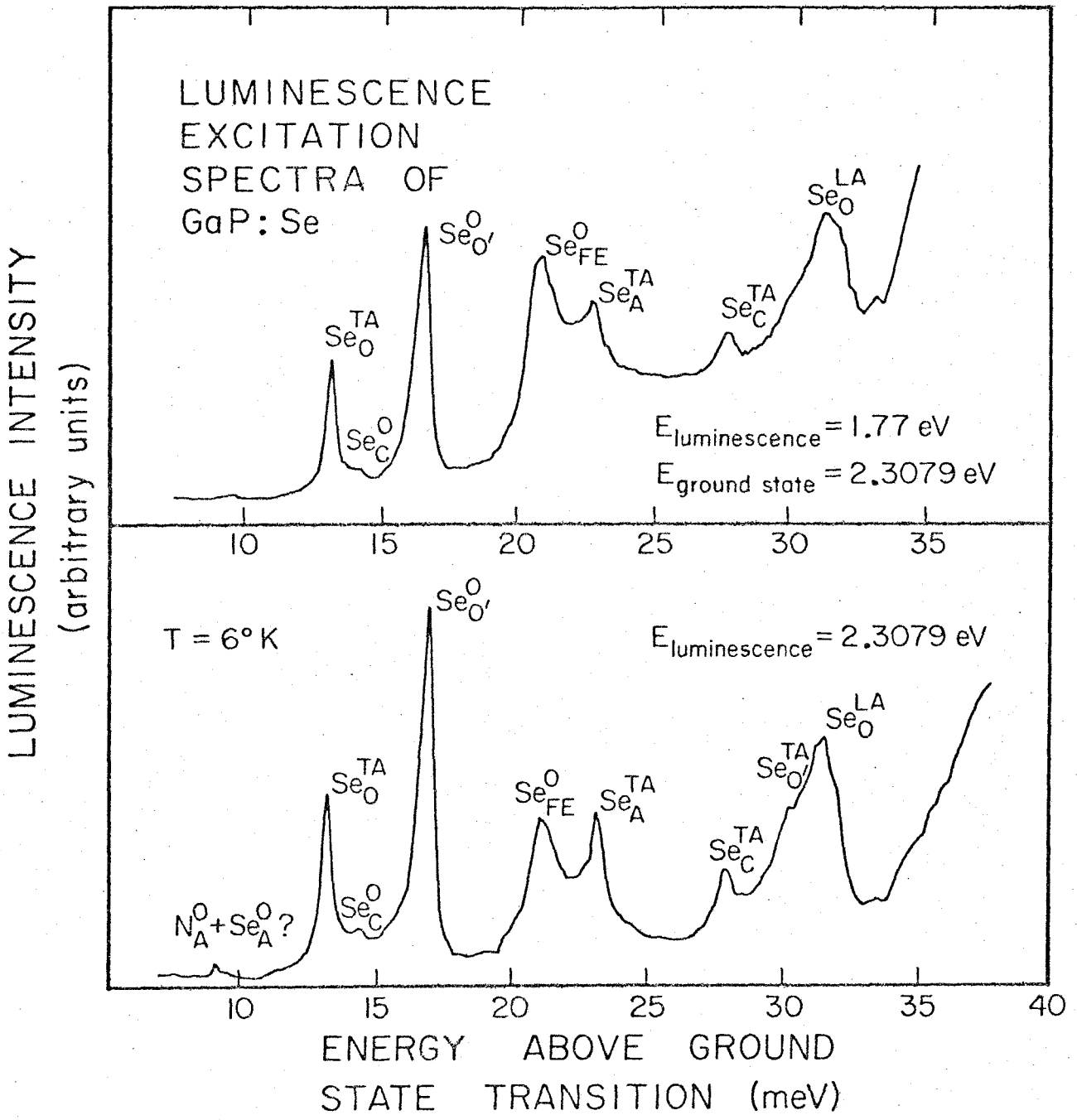
LUMINESCENCE
EXCITATION
SPECTRA OF
GaP:Se
Se_O^{LA}
$Se_{O'}^{O}$
Se_{FE}^{O}
Se_A^{TA}
Se_C^{TA}
Se_O^{TA}
Se_C^{O}
$E_{luminescence} = 1.77$ eV
$E_{ground\ state} = 2.3079$ eV
10
15
20
25
30
35
T = 6° K
$Se_{O'}^{O}$
$E_{luminescence} = 2.3079$ eV
Se_O^{LA}
$Se_{O'}^{TA}$
Se_{FE}^{O}
Se_A^{TA}
Se_C^{TA}
Se_O^{TA}
Se_C^{O}
$N_A^{O}+Se_A^{O}$?
10
15
20
25
30
35
40
LUMINESCENCE INTENSITY
(arbitrary units)
ENERGY ABOVE GROUND
STATE TRANSITION (meV)

TABLE 4.2

Energies measured for features in the luminescence excitation spectra of GaP:Se. The maximum possible error in the measurements is .2 meV. The feature Se_A^0 is very weak and occurs near the N_A^0 nitrogen no-phonon bound exciton transition. Therefore the assignment of this feature as being due to Se must be considered speculative.

	ENERGY (eV)	ENERGY RELATIVE TO Se_0^0 (meV)
Se_0^0	2.3079	0
$Se_{0'}^0$	2.3248	16.9
Se_{FE}^0	2.3289	21.0
Se_A^0	2.3175	9.6 ?
Se_C^0	2.3224	14.5
Se_0^{TA}	2.3211	13.2
$Se_{0'}^{TA}$	2.3380	30.1
Se_A^{TA}	2.3309	23.0
Se_C^{TA}	2.3357	27.8
Se_0^{LA}	2.3393	31.4

energy as the peak in GaP:S which is labeled S^o_{FE} which occurs 19.6 meV above the ground state. Both of these peaks occur very close to the free exciton threshold. It is likely that these peaks are associated with the creation of free excitons in the vicinity of the donor impurity. The fact that both of these are weaker than the S^o_0, peak in the spectra shown in the lower panels of Figs. 4.2 and 4.3 than in the top panels supports this conclusion. The lines which have been observed for the GaP:Se and their positions have been listed in Table 4.2.

IV. Discussion

Of the available calculations for the excited state structure of bound excitons, Chang's calculation [2] is the only one carried out for the approximate mass ratio. Figure 4.4 shows the results of his calculation. Chang assumed in his calculation that the electrons and holes were oppositely charged particles with masses m_e and m_h. His results show that for donor bound excitons, the resulting complex resembles a molecule if the electrons are much lighter than the hole. If the electrons are much heavier than the hole, the binding is not of the same nature. Rather, the two electrons are expected to bind to the impurity in a D^- configuration. As stated earlier the D^- state is analogous to the atomic H^- ion ground state. The hole is bound by the coulombic attraction of the net negative charge of the two electrons and the impurity in this case.

The nature of the excited states is different in the two cases. In the first case, where the ratio of the electron mass to the hole mass is close to zero, the excited state spectrum is expected to resemble the vibrational-rotational spectrum characteristic of a molecular system. In the second case, where the electron to hole mass ratio approaches infinity, the excited state spectrum is expected to resemble the spectrum of the neutral acceptor.

Chang's theory predicts the excited state spectrum of bound excitons for all mass ratios [2]. In Fig. 4.4 the energies of the excited states are plotted as a function of mass ratio. In addition the ionization energy for the hole is also plotted. The dotted lines are plots in which the energy units are in terms of the acceptor Rydberg. This is just the energy which binds a hole in the acceptor. At large mass ratios the excited state spectrum matches that of the neutral acceptor. At lower mass ratios the spacing between the ground state and the excited states changes but the spacing between the excited states and the ionization threshold does not change appreciably until the mass ratio is less than one. The behavior at low mass ratios becomes more apparent if one plots the excited state energies in terms of the donor Rydberg. The donor Rydberg is the energy with which an electron is bound in a neutral donor. The solid lines show these plots. It is apparent that at mass ratios below .5 from these plots that the nature of the excited states changes a great deal.

Figure 4.4. Energies of s-like excited states of the bound exciton as a function of the mass ratio $\sigma = m_e/m_h$. The solid curves are plots of the energy in terms of the donor Rydberg. The dotted-dashed lines represent a plot of the energy in terms of the acceptor Rydberg. At very small mass ratios the excited state structure shows molecular behavior. At large mass ratios the excited state spectrum is simply that of the neutral acceptor. The dotted line represents the bound exciton dissociation energy. (Ref. 2)

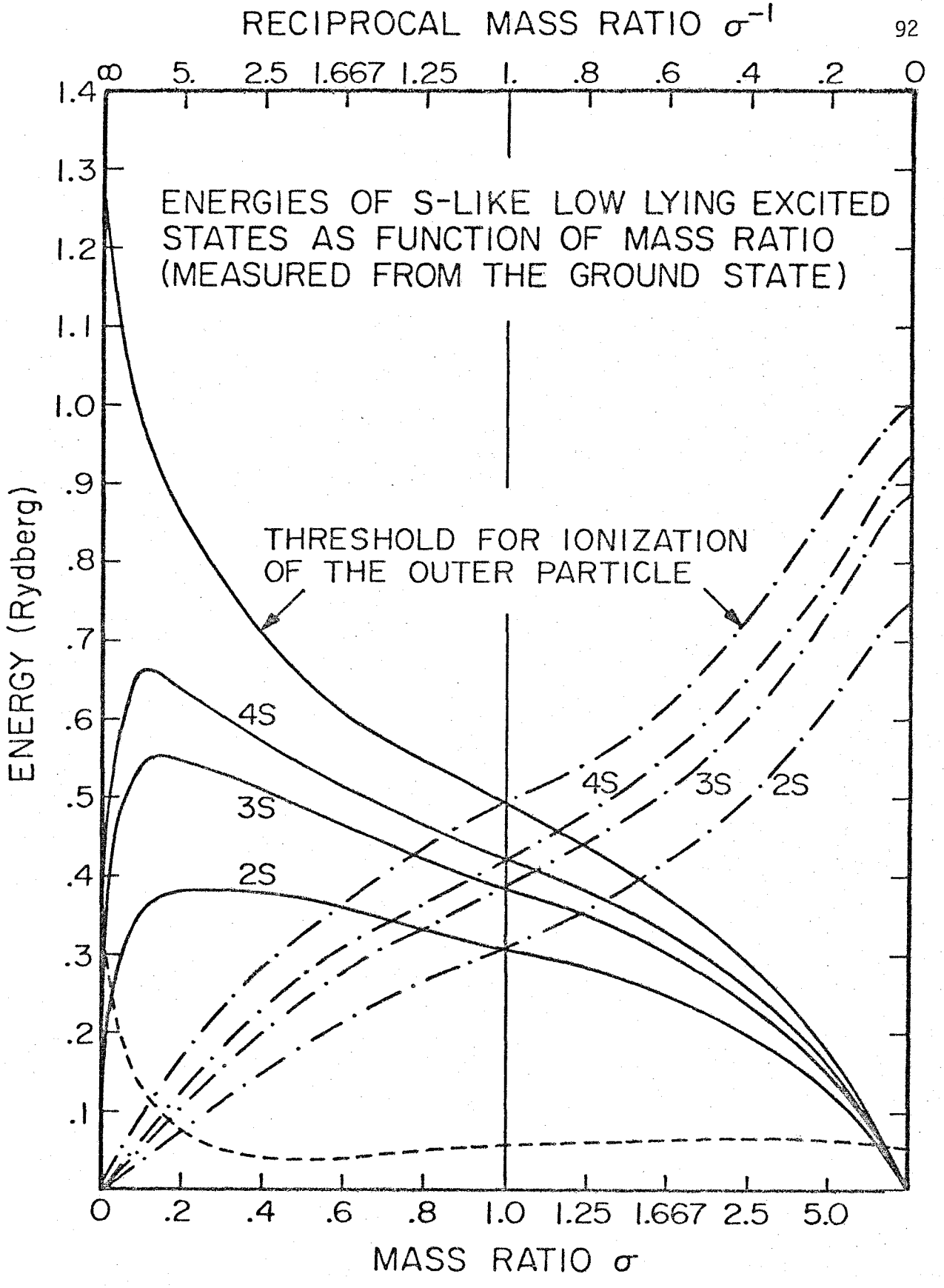
RECIPROCAL MASS RATIO σ^{-1}
∞ 5. 2.5 1.667 1.25 1. .8 .6 .4 .2 0
ENERGIES OF S-LIKE LOW LYING EXCITED STATES AS FUNCTION OF MASS RATIO (MEASURED FROM THE GROUND STATE)
THRESHOLD FOR IONIZATION OF THE OUTER PARTICLE
4S
3S
2S
4S
3S
2S
ENERGY (Rydberg)
1.4 1.3 1.2 1.1 1.0 .9 .8 .7 .6 .5 .4 .3 .2 .1
0 .2 .4 .6 .8 1.0 1.25 1.667 2.5 5.0
MASS RATIO σ

The ionization energy for a free hole increases rapidly; whereas, the excited state energies approach zero. Such behavior suggests that the excited state structure is molecular in nature at these mass ratios; whereas, at higher mass ratios the structure is acceptor-like. In GaP it is possible to make an estimate of the appropriate mass ratio to use in the calculation of Chang by considering the ratio of the donor binding energy to the acceptor binding for simple impurities. If 100 meV is taken as a typical donor binding energy and 50 meV as the simple acceptor binding energy a mass ratio of 2 is obtained which is considerably greater than .5. Thus it seems most likely that the data can be explained in a model which has the features of the excited states described by Chang.

Since the band structure is considerably more complicated than the spherical nondegenerate bands used by Chang in his calculation, it is necessary to consider what effect the details of the band structure will have on the excited state spectrum of the bound exciton. Since the conduction band in GaP has several equivalent minima, it is possible to construct several D^- states of different symmetry. In addition the excitations of the neutral acceptor are not simply described by a hydrogenic spectrum but have a more complicated form. From Chang's calculation it is expected that the nature of the excited states in the bound exciton will be similar to the excited states of the neutral acceptor and can therefore be classified according to the scheme developed by Baldereschi and Lipari [7]. This scheme was

briefly discussed in Chapter 1.

If the form of the optical transition matrix element is considered, it is seen that some of these states are expected to have relatively large oscillator strengths in no-phonon transitions; whereas, others are expected to have relatively weak transitions in the no-phonon region. The neutral donor and the donor bound exciton wave functions have the form

$$|\psi_o\rangle = \sum_{k_e^o v_o \sigma_o} a^o_{v\sigma}(\vec{k}_e^o)\, C^+_{k_e^o v\sigma}\, |G\rangle \qquad (1)$$

and

$$|\psi^j_{BE}\rangle = \sum_{\substack{m \\ v_1\sigma_1 \\ v_2\sigma_2}} \sum_{\vec{k}_e^1, \vec{k}_e^2, \vec{k}_h} A^j_{\substack{m \\ v_1\sigma_1 \\ v_2\sigma_2}}(\vec{k}_e^1, \vec{k}_e^2, \vec{k}_h) \times C_{\vec{k}_h m}\, C^+_{\vec{k}_e^1 v_1\sigma_1}\, C^+_{\vec{k}_e^2 v_2\sigma_2}\, |G\rangle \qquad (2)$$

$C_{k_h m}$ creates a hole with wavevector k_h and spin projection m, $C_{k_e^1 v_1\sigma_1}$ creates an electron with wavevector k_e^1 in a valley combination v_1 with spin σ_1, and $|G\rangle$ is the state with all conduction band states empty and all valence band states occupied. a^o is the amplitude function for the ground state of the neutral donor and A^j is the

amplitude function for the jth excited state of the donor bound exciton. The transition matrix element becomes

$$\langle\psi_o|P_y|\psi^j_{BE}\rangle = \sum_{\substack{m\\ v_1\sigma_1\\ v_2\ 2}} \sum_{\vec{k}_e,\vec{k}_h} \langle\phi_m(\vec{k}_h)|P_y|\phi_{\sigma_2 v_2}(\vec{k}_h)\rangle$$

$$\times\ a^{o*}_{v_1\sigma_1}(\vec{k}_e)\left[A^j_{\substack{m\\ v_1\sigma_1\\ v_2\sigma_2}}(\vec{k}_e,\vec{k}_h,\vec{k}_h) - A^j_{\substack{m\\ v_1\sigma_1\\ v_2\sigma_2}}(\vec{k}_h,\vec{k}_e,\vec{k}_h)\right] \qquad (3)$$

where $|\phi_m(k_h)\rangle$ and $|\phi_{\sigma_2 v_2}(k_h)\rangle$ are the periodic parts of respectively the pseudo-Bloch function of the hole and the Bloch function of the electron and P_y is the y component of the momentum operator. The functions $A^j_{\substack{m\\ v_1\sigma_1\\ v_2\sigma_2}}$ can be expanded in terms of the amplitude functions of the neutral b(k) donor $a^p(k)$ (where p labels the state of the neutral donor) and for the single particle amplitude function the hole $b^r(k)$ (where r labels the basic states).

To illustrate the important features of this equation, most of the indices can be suppressed and the matrix element appears in the form

$$\langle\psi_o|P_y|\psi_{BE}\rangle = \sum_{pqr}\left\{D(p,q,r)\ [(\sum_{ke} a^{o*}(\vec{k}_e)\ a^p(\vec{k}_e)]\right.$$

$$\left.[\sum_{kr} M(\vec{k}_h)\ a^q(\vec{k}_h)\ b^r(\vec{k}_h)]\right\}\ . \qquad (4)$$

where $M(k_h)$ is the momentum matrix element, and D is the set of

expression coefficients for the bound exciton wavefunction. This equation shows that the matrix element is the product of two terms in brackets: the overlap in k space between the initial state of electron in the bound exciton and the electronic state of the neutral donor, and the overlap in k space of the electron and hole amplitude functions weighted by the momentum matrix elements. The first term in the product is zero unless the two single electron states involved are the same. The second term can be approximated by noting that the hole wavefunctions are relatively localized in k space at $k_h=0$ and that the momentum matrix element is not a rapidly varying function of k_h [8]. Then this term is approximately $M(k_h=0) \sum_{k_h} a^p(\vec{k}_h)\, b^r(\vec{k}_h)$. Hence, the size of this term depends on the k-space overlap of the electron and hole wavefunctions near the zone center. In addition, if the amplitude functions $a^p(\vec{k}_h)$ and $b^r(\vec{k}_h)$ have opposite parity this sum will be zero.

For GaP, these considerations lead one to expect that only certain bound exciton states will be involved in the no-phonon absorption process. These states are those with a substantial projection on the single particle configuration consisting of two electrons in $1s(\Gamma_1)$ states and the hole in an even parity state. One of the electrons must be in a $1s(\Gamma_1)$ state because the initial state in absorption is the $1s(\Gamma_1)$ ground state of the neutral donor. In addition the $1s(\Gamma_1)$

electron state is the only state which is sufficiently spread out in k space to have a large overlap with the hole. Thus, the second electron must also be in the $1s(\Gamma_1)$ state for the second term in Eq. 4 to be appreciable. The hole must have the same parity as the electron and therefore has even parity. Thus transitions to hole levels with p-like rotational symmetry are not expected.

There are three features in the excited state spectrum which have fairly large oscillator strengths in the no-phonon region for GaP:S and two such features for GaP:Se. These are the lines $S^o_{o'}$, S^o_{FE}, and $S^o_{o''}$ for GaP:S and the lines $Se^o_{o'}$ and Se^o_{FE} for GaP:S. On the basis of the preceding arguments, the $S^o_{o'}$ and the $Se^o_{o'}$ lines are expected to be due to creation of a bound exciton with a D^- (Γ_1) core and the hole excited in a $2S_{3/2}$ state. The $S_{o''}$ line, as pointed out earlier in this paper, appears to be the sum of two lines which we have relabeled S^{TA}_A and $S^o_{o''}$. This transition is possibly due to the creation of a bound exciton with a hole excited in a $3S_{3/2}$ state.

Cohen and Sturge [5] have observed acceptor-like excited states of excitons bound to nitrogen pairs in GaP. Since the highly excited hole states of both the N and S bound excitons are expected to have the same relative energy positions, the data can be compared. Cohen and Sturge observed a 3s state which was consistently between 6 and 7 meV above the 2s state. Such a separation agrees with our assignment of the $S^o_{o'}$ and $S^o_{o''}$ transitions.

In Figure 4.2 two features have been marked with small arrows in

the luminescence excitation spectra for GaP;S which match the same relative positions as the 4s and 5s states reported by Cohen and Sturge and must tentatively be considered as candidates for such transitions for the case of GaP:S [5]. Such states are technically resonant states since they lie above the threshold for free exciton formation. If the relative energies of the excited state spectrum for GaP:S are assumed to match those of the acceptor-like spectrum observed by Cohen and Sturge, a hole ionization energy of 30 meV ± 1 meV is obtained. Assuming a free exciton binding energy of 22 meV ± 2 meV and a bound exciton binding energy of 20 meV ± 1 meV, we obtain a value of approximately 12 meV for the binding energy of an electron in the D^- (Γ_1) state.

The bound exciton excited states associated with the S_A^{TA}, S_C^{TA}, Se_A^{TA} and Se_C^{TA} transitions are most likely states with an electron core with overall symmetry different from Γ_1. Such states have been previously reported for excitons bound to donors in silicon [9,10]. Preliminary calculations by Chang indicate that D^- states with Γ_3 symmetry and a strong projection on the single particle product $1s(\Gamma_1)\ 1s(\Gamma_3)$ have the correct energy to be responsible for these transitions [11]. Such states are expected to have weak no-phonon components since the $1s(\Gamma_3)$ state is not sufficiently localized to have significant overlap with the hole in momentum space. If a transition is phonon assisted such an overlap is no longer necessary and the oscillator strength should be comparable to the phonon

assisted ground state transition. Two such states occur for the $D^-(\Gamma_3)$, one being an electron spin singlet, the other being a spin triplet. When coupled to a Γ_8 hole these states split in energy into a multitude of possible final states for the bound exciton transitions. It is also possible that these states are associated with p-like rotational states associated with the hole. However, there is no compelling reason to believe that such rotational states should have a large oscillator strength in phonon assisted transitions.

V. Conclusions

The excited state structure for excitons bound to neutral donors in GaP:S and GaP:Se has been observed using luminescence excitation spectroscopy. By comparing different spectra it has been possible to distinguish between phonon assisted and no-phonon transitions of lines which had been previously observed. In addition several new lines have been observed. It has been possible to identify the nature of most of these lines by considering the form of the transition matrix element. There are basically three different types of features in the observed spectra. First, peaks have been observed which appear to be due to the no-phonon creation of free excitons in the vicinity of the impurity. Second, there are transitions which have a large oscillator strength in the no-phonon region. Third, there are transitions which have relatively strong phonon assisted components. These data indicates that there are two different types of excited states

in the bound exciton. The first of these results from excitations of the hole about a $D^-(\Gamma_1)$ electron core. The second type of state involves excitations of the electron core with different overall symmetry. Such states result from the many-valleyed nature of the conduction band. Thus as a result it will be necessary for future calculations to include the many valleyed nature of the conduction band to describe all the states which are observed.

REFERENCES

1. P. J. Dean, Phys. Rev. 157, 655 (1967).
2. Y. C. Chang and T. C. McGill, Solid State Commun. 32, 319 (1978).
3. D. C. Herbert, J. Phys. C. Solid State Physics 10, 3327 (1977).
4. W. Ruhle and W. Klingenstein, Phys. Rev. B18, 7011 (1978).
5. E. Cohen and M. D. Sturge, Phys. Rev. B15, 1039 (1977).
6. J. M. Dishman, D. F. Daly, and W. P. Knox, J. Appl. Phys. 43, 4693 (1972).
7. A. Baldereschi and N. O. Lipari, Phys. Rev. B8, 2697 (1973).
8. Since the charge on impurity is the same as that for the hole, the hole is spatially delocalized, and hence it is localized in k-space near k_h=0. See, for example, D. S. Pan, D. L. Smith, and T. C. McGill, Solid State Commun. 18, 1557 (1976) and Ref. 2.
9. M. L. W. Thewalt, Solid State Commun. 22, 671 (1977).
10. E. C. Lightowlers, M. O. Henry, and M. A. Vouk, J. Phys. C. Solid State Physics 10, 2713 (1977).
11. Y. C. Chang and T. C. McGill (unpublished).

Chapter 5

EVIDENCE FOR AN ADDITIONAL EXCITED STATE OF THE NEUTRAL INDIUM ACCEPTOR IN SILICON

I. Introduction

The luminescence associated with bound excitons can be used to observe the electronic properties of neutral impurities in semiconductors. The most commonly observed luminescence from bound excitons is that from the ground state to ground state transition. In such a transition the initial state is the ground state of the bound exciton. Upon recombination of an electron hole pair in the bound exciton the impurity is left in the ground state. Transitions also occur which leave the neutral impurity in an excited electronic state. Such transitions are referred to as "two electron transitions". The transition was initially visualized as being due to the excitation of the second electron or hole in the bound exciton to an excited state of the neutral impurity following recombination of the electron hole pair in the bound exciton [1].

The energy of the excited state relative to the ground state can be determined from the energy of the "two electron" luminescence. Since both the ground state to ground state transitions and the "two electron" transitions have the same initial state, any difference in energy occurs in the final state. Hence the energy difference between the ground state to ground state transition and the "two electron" transitions yields energies for the excited states of the neutral impurity.

The study of these processes is important because they can provide valuable information about states which are not observed in infra-

red absorption spectra. States with s-like symmetry, for instance, are not observed in infrared absorption experiments. These states can show up in the "two electron" spectra associated with bound exciton luminescence [2].

Recently Lyon et al [3] and Vouk et al [4] reported studies of the luminescence associated with bound excitons in Si:In. In addition to previously observed transitions such as the bound exciton ground state to ground state transition these studies reported several new transitions, one of which is approximately 4 meV lower in energy than the principal bound exciton transition. Following Vouk et al [4] this line will be referred to as U1. Neither Lyon et al [3] or Vouk et al [4] suggested an origin for this line. Vouk et al did mention that the feature appeared to increase in intensity relative to the bound exciton with increasing temperature. Fig. 5.1 shows a spectrum with these lines.

Data presented in this chapter indicate that this line is most likely due to a "two electron" (actually a "two hole" transition in this case) transition which leaves the indium acceptor in an excited state. Data from pump power, doping level and temperature measurements are presented. These measurements indicate that U1 and the bound exciton transition have the same initial state. This fact indicates that the splitting is in the final state, in this case a state of the neutral acceptor.

This state is a low lying state of the indium. The binding energy of the neutral indium acceptor is 155 meV while the excited state is only 4 meV above the ground state. The most recent calculations of the excited state spectrum of the neutral acceptor do not show any indication that such a state should exist. Therefore the origin of this excited state is of considerable interest.

II. Experiment

Spectra were obtained from four different samples doped with Si:In. The impurity concentration was determined in each of these samples with a Hall measurement performed at Hughes Research Laboratories. The impurity concentrations were found to be $2x10^{14}cm^{-3}$, $3.2x10^{15}cm^{-3}$, $1.7x10^{16}cm^{-3}$, and $2x10^{17}cm^{-3}$. Optical excitation was provided by a Rhodamine 6G dye laser at 600 nm. The sample was placed in a variable temperature dewar and the temperature was monitored with a silicon diode sensor mounted directly on the sample. The photoluminescence was passed through a grating monochromator and detected with a cooled photomultiplier with S-1 response and a photon counting system. A multichannel analyzer was used to obtain reliable estimates of line ratios.

Figure 5.1. A spectrum of the no-phonon region in Si:In. The J=0 and J=2 transitions are transitions which leave the impurity in the ground state. The J=2 transition is from an excited state of the bound exciton to the ground state of the neutral impurity. The J=0 line is the ground state to ground state transition. The line labeled U1 is studied in this chapter. It appears to have the same initial state as the J=0 line.

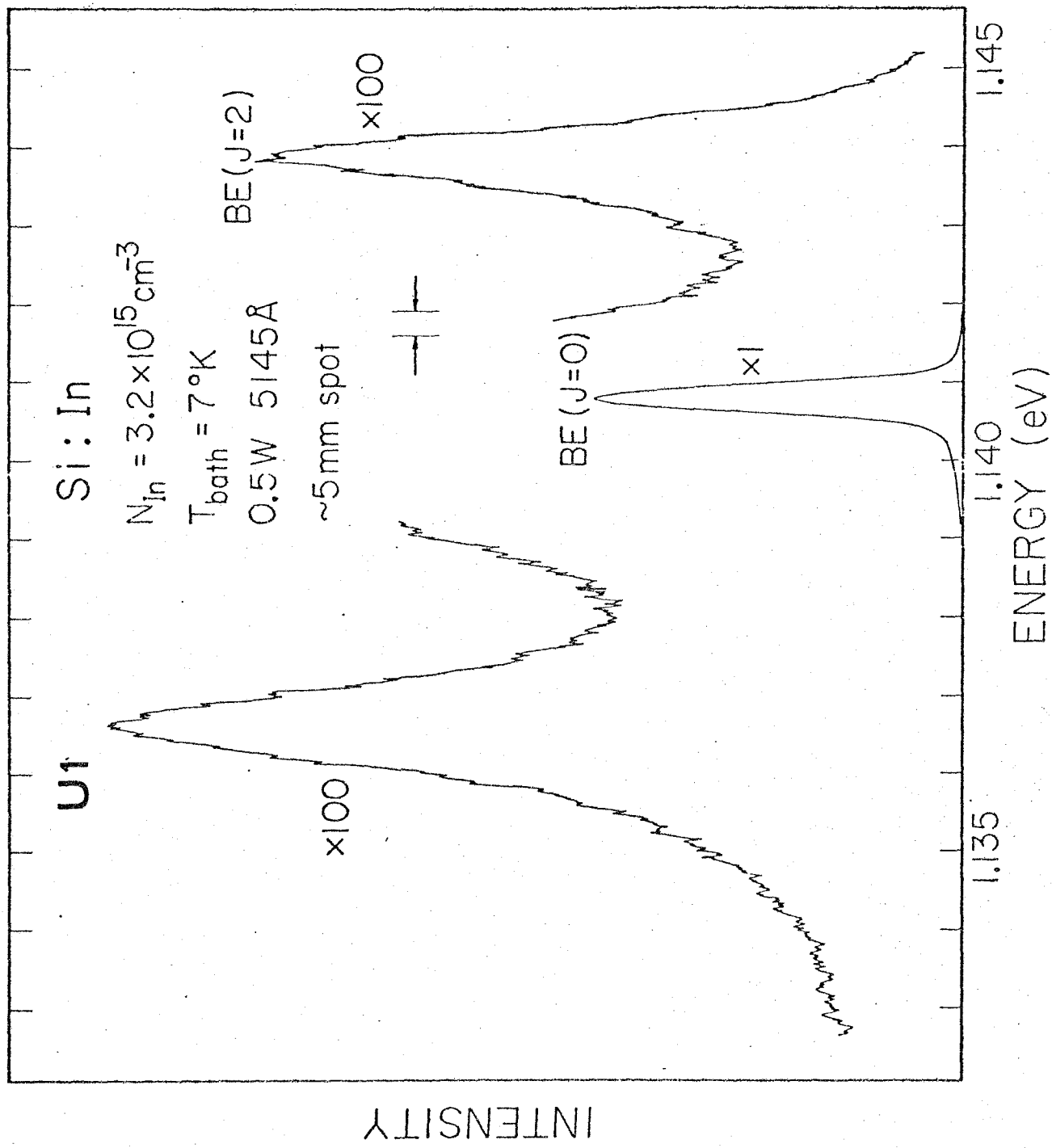
U1
Si : In
$N_{In} = 3.2 \times 10^{15} cm^{-3}$
$T_{bath} = 7°K$
0.5W 5145Å
~5mm spot
BE (J=2)
BE (J=0)
×100
×100
×1
1.135
1.140
1.145
ENERGY (eV)
INTENSITY

III. Results

Figures 5.2, 5.3 and 5.4 show the ratio of the line U1 to the bound exciton line in the no-phonon region as a function of pump power, doping level, and temperature, respectively. The ratio is observed to be independent of these three parameters. The fact that the ratio is independent of pump power and doping level establishes that the line is not due to a multiple exciton complex. Such lines are observed to increase in intensity with pump power and decrease in intensity at higher doping levels with respect to the bound exciton. Fig. 5.4 shows that the ratio of U1 to the bound exciton is independent of temperature up to 15^{o}K. These data indicate that the splitting does not occur in the initial state. In order to obtain these data it is necessary to subtract out the background to obtain a reliable estimate of the ratio. This background is always present on the low energy tail of the bound exciton and it increases at higher temperatures and higher doping levels. Above 15^{o}K it is not possible to obtain a reliable estimate of the ratio. It is also necessary that one uses the integrated intensity of the bound exciton since the bound exciton line broadens appreciably as a function of temperature.

In view of the temperature and concentration dependence of the data it is unlikely that U1 is due to the recombination of a bound exciton on a site other than a substitutional indium. In such a case one would expect some temperature dependence to the ratio since the capture cross-section of an exciton on an isolated indium site is

relatively sensitive to temperature [6]. In addition the samples used in this study had different past histories. Some were grown using a float zone technique; others were grown by the Czochralski method. In all cases the same ratio was obtained for the intensity of U1 to the bound exciton. Thus on the basis of these data it has been concluded that the transition U1 has the same initial state as the bound exciton transition.

IV. Discussion

The origin of the splitting between the U1 line and the bound exciton line has been determined to occur in the final state of the transition. It is possible that this splitting is due to the creation of a resonant phonon mode upon recombination. Such a phonon mode is similar to a local phonon mode in that it is associated with the defect. Due to the large mass of the indium center, modes of this type are degenerate with the continuum of lattice modes associated with the crystal and are referred to as resonant modes. The masses of the indium center and a silicon atom differ by a factor of four. Since the energy difference between the lattice optical modes and the local modes can be expected to scale as the square root of the ratio of the masses, it is possible to estimate the energy of the resonant mode. Assuming an optical mode energy of 60 meV this would correspond to a resonant mode energy of about 30 meV. Thus, the U1

Figure 5.2. Ratio of the intensity of the intensity of U1 to the bound exciton versus pump. The absolute pump power ranged approximately from 100 mwatts/cm^2 to 3000 mwatts/cm^2.

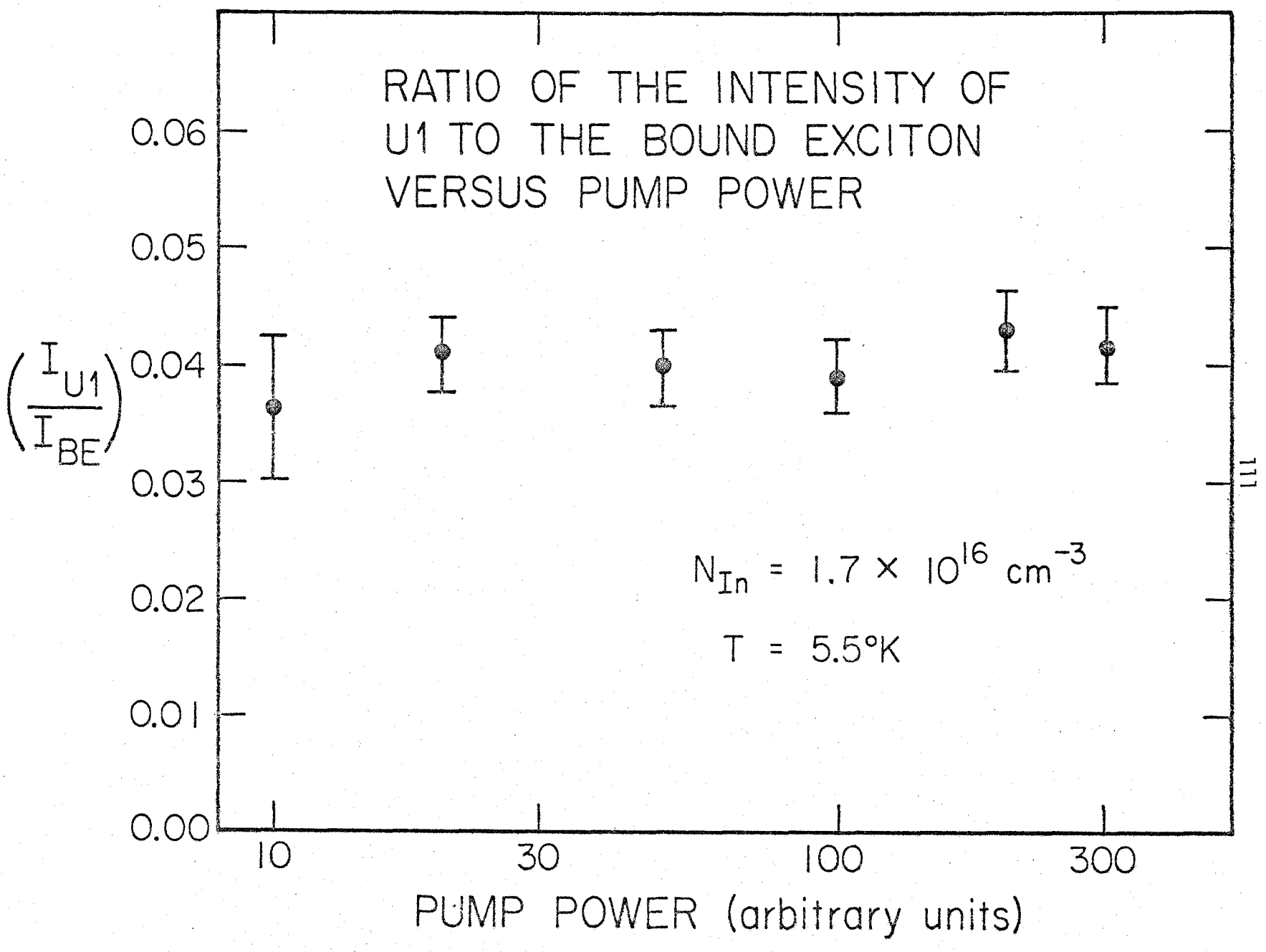
RATIO OF THE INTENSITY OF
U1 TO THE BOUND EXCITON
VERSUS PUMP POWER
$\left(\frac{I_{U1}}{I_{BE}}\right)$
0.06
0.05
0.04
0.03
0.02
0.01
0.00
N_{In} = 1.7 × 10^{16} cm^{-3}
T = 5.5°K
10
30
100
300
PUMP POWER (arbitrary units)

Figure 5.3. Ratio of the intensity of U1 to the bound exciton as a function of indium concentration.

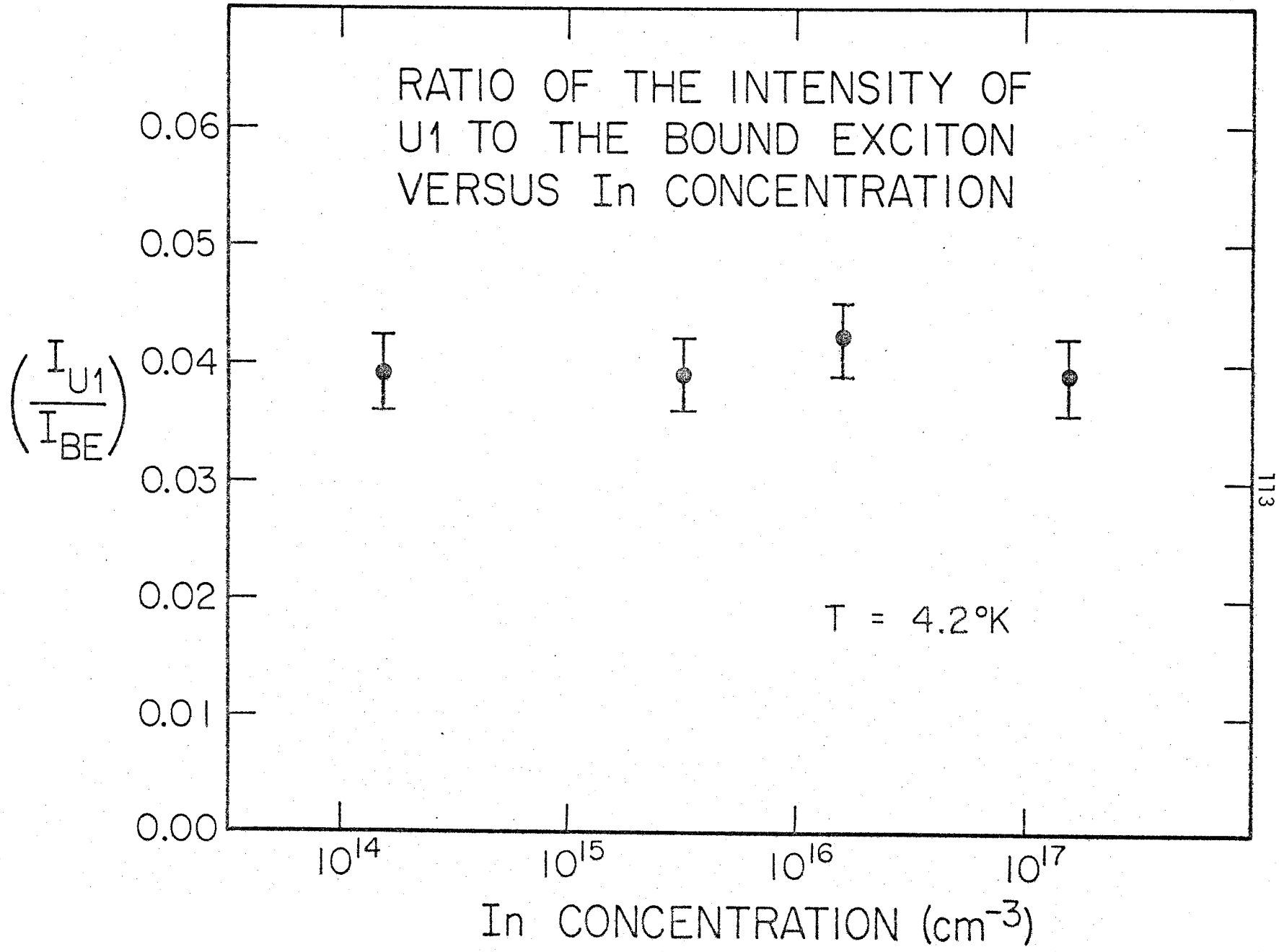
RATIO OF THE INTENSITY OF
U1 TO THE BOUND EXCITON
VERSUS In CONCENTRATION
$\left(\frac{I_{U1}}{I_{BE}}\right)$
0.06
0.05
0.04
0.03
0.02
0.01
0.00
T = 4.2°K
10^{14}
10^{15}
10^{16}
10^{17}
In CONCENTRATION (cm^{-3})

Figure 5.4. Ratio of the intensity of U1 to the bound exciton as a function of temperature. The excitation intensity was approximately 1000 mwatts/cm^2.

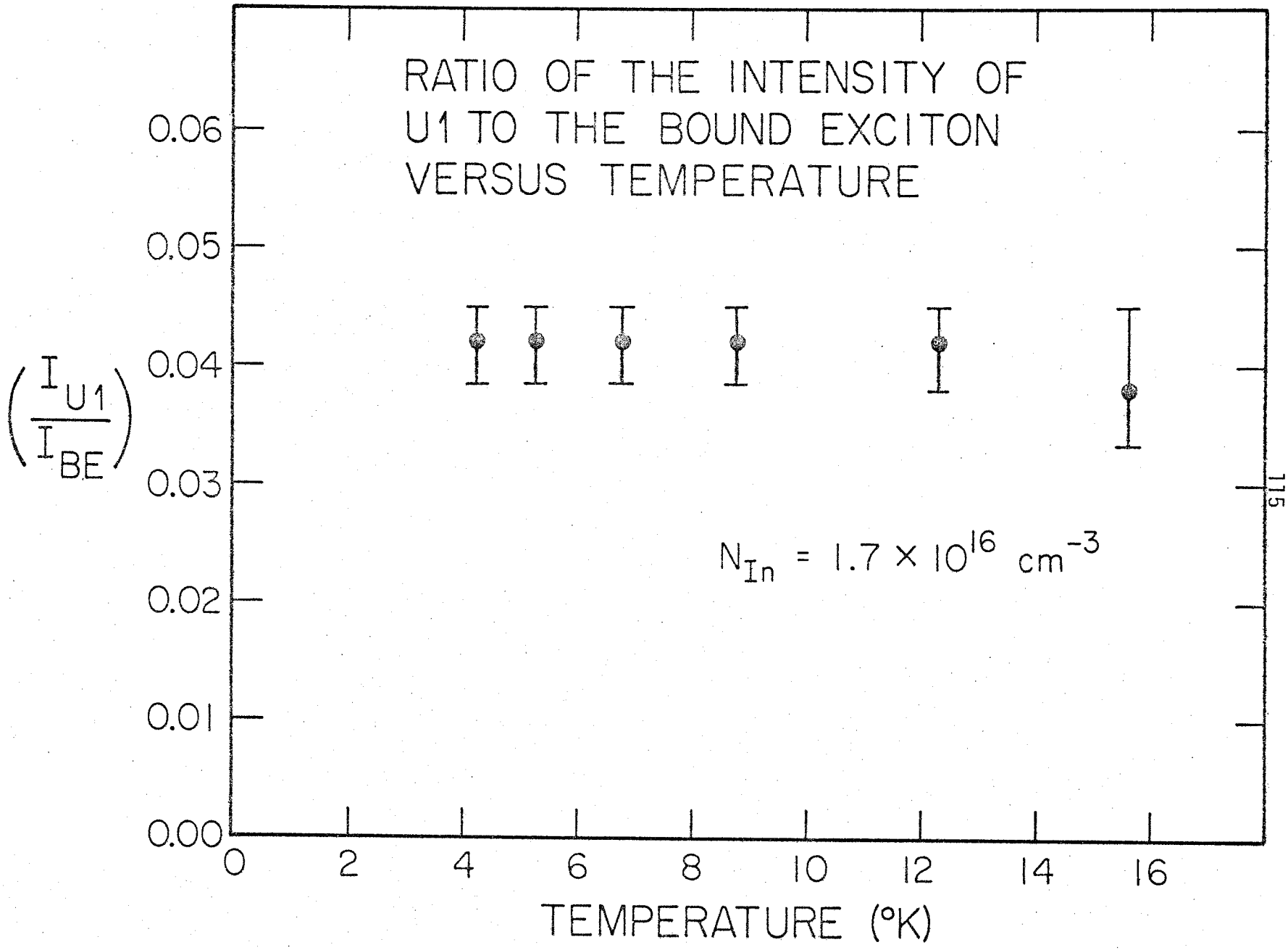
RATIO OF THE INTENSITY OF
U1 TO THE BOUND EXCITON
VERSUS TEMPERATURE
$\left(\frac{I_{U1}}{I_{BE}}\right)$
0.06
0.05
0.04
0.03
0.02
0.01
0.00
$N_{In} = 1.7 \times 10^{16}$ cm^{-3}
0
2
4
6
8
10
12
14
16
TEMPERATURE (°K)

line does not appear to be due to a resonant phonon mode of the indium.

A more likely explanation for the U1 line is that the final state of the U1 transition is due to an excited level of the indium acceptor. An excited level of the indium acceptor has been recently measured indirectly in ultrasonic absorption measurements in silicon at an energy 4.2 meV above the ground state [5]. This agrees with the value of 4.1 ± .1 meV measured here and provides convincing evidence that the level is not due to a resonant phonon mode.

The existence of this level is significant in that current theories of the electronic structure of the neutral acceptor do not predict a level at this energy. It has been predicted though that the dynamic Jahn-Teller effect should play a role in the acceptor system for silicon [5,7]. Morgan has pointed out that systems with Γ_8 symmetry such as acceptors in silicon should be affected by the Jahn-Teller effect [7].

The Jahn-Teller effect is the instability of an electronically degenerate state with respect to distortions in the crystal [8]. In the case of the indium acceptor the ground state of the acceptor is expected to have Γ_8 symmetry. Such a state is fourfold degenerate and can be split into two different twofold degenerate levels by stress or crystal distortions. According to the Jahn-Teller theorem such a state is unstable with respect to these distortions about the impurity [8].

Morgan has discussed the possibility that the dynamic Jahn-Teller effect is important for the acceptors [7]. (The difference between the dynamic Jahn-Teller effect and the normal static Jahn-Teller effect is that the dynamic Jahn-Teller effect includes the effects of the nuclear motion in the lattice, whereas the static effect only describes the effects due to static distortions of the lattice.) He finds that lattice distortions will couple to the electronic states of the acceptor and lead to a modified ground state with possible low lying excited states. The effect on the indium acceptor should be particularly pronounced since it is considerably deeper than all the group III acceptors except for thallium and the hole wavefunction is highly localized near the impurity. This leads to stronger coupling through the electron-phonon interaction and thus to a stronger Jahn-Teller effect.

Besides the evidence for the excited state presented here and in the ultrasonic absorption measurements, there is additional evidence that the Jahn-Teller effect may be active in Si:In. Morgan has pointed out that data taken in magnetic resonance experiments can be explained by the Jahn-Teller effect [7]. In these experiments it was found that the resonance linewidth of holes bound to acceptors and the g factors of holes bound to acceptors had a large stress dependence [9]. Morgan has also pointed out that the relatively small values of the deformation potential observed for the ground

state in infrared absorption experiments can be explained by the Jahn-Teller effect [10].

Although there is a great deal of evidence that indicates that the Jahn-Teller effect is active in Si:In no detailed theory has been presented at this time to account for the states which have been observed here. It appears that such a state can arise in two ways. The first of these is that the Jahn-Teller effect can give rise to a series of levels lying near the ground state as pointed out by Morgan [7]. These levels occur when the lattice distortion becomes important in changing the structure of the ground state from a purely electronic level to a mixed electronic-vibronic level. The second way a low lying state can appear is due to a suppression of the spin orbit splitting of the valence band. The spin-orbit splitting in silicon leads to the formation of two bands. The top of the valence band is fourfold degenerate; whereas, a splitoff band occurs 40 meV below the top of the valence band. In the absence of spin orbit splitting these bands would be degenerate in energy. The presence of the splitoff band leads to low lying excited states of the neutral acceptor. As Ham pointed out, the Jahn-Teller effect leads to a suppression of the spin orbit splitting and as a result it is possible that this could lead to a low lying acceptor state [11]. At this time it is not clear what the nature of the observed state is.

V. Conclusions

A line observed in the photoluminescence of silicon doped with indium has been studied as a function of temperature, doping level and pump power. The ratio of this line,which has been referred to as U1 in the literature, to the bound exciton line is found to be independent of these three parameters. As a result the splitting between this line and the bound exciton line appears to occur in the final state of the transition. The most likely explanation for the line is that an excited level of the neutral indium acceptor lies 4 meV above the ground state. It is possible that the Jahn-Teller effect may be responsible for the existence of this state.

REFERENCES

1. P. J. Dean, J. D. Cuthbert, D. G. Thomas, and R. T. Lynch, Phys. Rev. Lett. 18, 122 (1966).
2. P. J. Dean, P. Bimberg, and F. Nausfield, Phys. Rev. B15, 3906 (1977).
3. S. A. Lyon, D. L. Smith and T. C. McGill, Phys. Rev. B17, 2620 (1978).
4. M. A. Vouk and E. C. Lightowlers, J. of Luminescence 15, 357 (1977).
5. Hp. Schad and K. Lassmann, Physics Letters 56A, 409 (1976).
6. K. R. Elliott, D. L. Smith and T. C. McGill, Sol. St. Comm. 24, 461 (1977).
7. T. W. Morgan, Phys. Rev. Lett. 24, 887 (1970).
8. M. D. Sturge, Solid State Physics (Academic Press, New York, 1967) Vol. 20, pp 92.
9. G. Feher, J. C. Hensel and E. A. Gere, Phys. Rev. Lett. 5, 309 (1960).
10. A. Onton, P. Fisher, and A. K. Ramdas, Phys. Rev. 163, 686 (1967).
11. F. S. Ham, Phys. Rev. 138, A1727 (1965).

Chapter 6

SYSTEMATICS OF BOUND EXCITONS AND BOUND MULTIPLE EXCITON COMPLEXES FOR SHALLOW DONORS IN SILICON

I. Introduction

In previous chapters of this thesis the properties of excitons bound to neutral impurities have been discussed. In this chapter I report the results of some experimental investigations of systems which have more than one exciton bound to a single impurity. A state which consists of a number of excitons bound to a neutral impurity is called a bound multiple exciton complex (BMEC).

Luminescence associated with these complexes was first observed by Pokrovskii et al [1]. Pokrovskii et al observed a series of lines at lower energies than the bound exciton in the emission spectra of silicon doped with shallow imourities. The most satisfying explanation for the origin of these lines was that they were due to the radiative decay of an electron hole pair bound to a neutral impurity center at which a number of pairs was bound, bound multiple exciton complexes. Several authors have studied these complexes and have presented measurements of the pump power [1,2,3], temperature [4], and decay characteristics [2,3] of the luminescence from the series of lines observed by Pokrovskii. Such data are consistent with the model that the decay is associated with BMEC. The luminescence spectra associated with these lines obtained from silicon doped with Ga and Al also gives strong evidence for this model [5,6,7]. In these materials the excited state structure of the bound exciton has been observed. Other transitions occur in these materials which can be identified as electron

Figure 6.1. A spectrum of the low temperature photoluminescence of silicon doped with phosphorus. Transitions involving bound multiple exciton complexes give rise to two series of lines. The α series shows up in no-phonon and phonon assisted transitions. The β series only shows up in phonon assisted transitions.

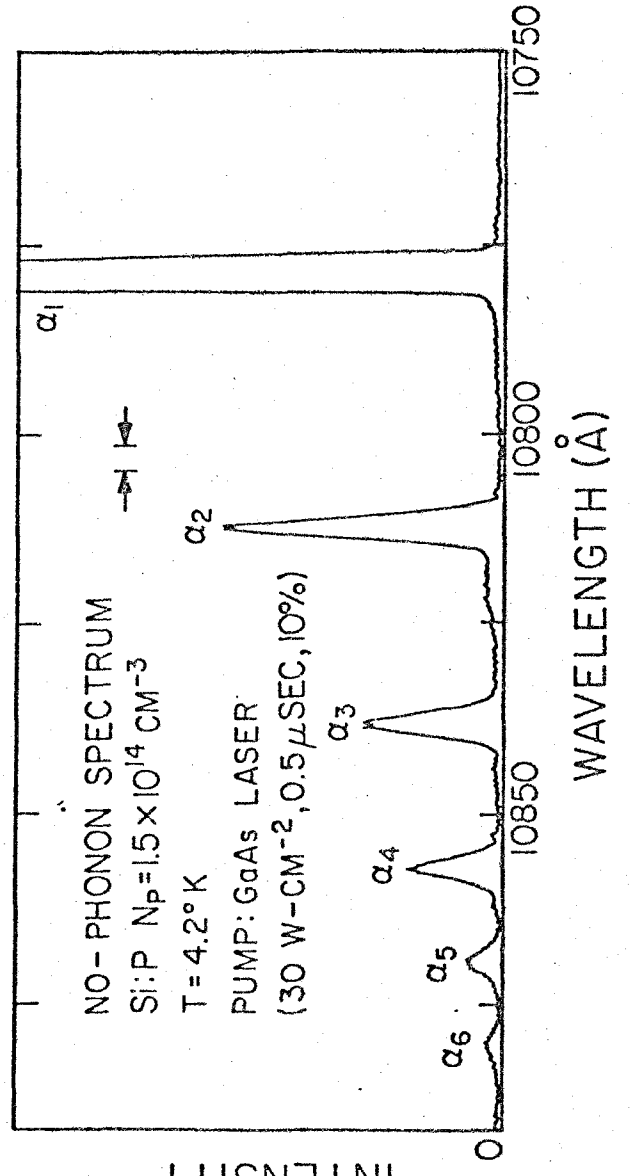
NO-PHONON SPECTRUM
Si:P N_P=1.5×10^{14} CM^{-3}
T=4.2° K
PUMP: GaAs LASER
(30 W-CM^{-2}, 0.5 μSEC, 10%)
α_1
α_2
α_3
α_4
α_5
α_6
INTENSITY
0
10850
10800
10750
WAVELENGTH (Å)

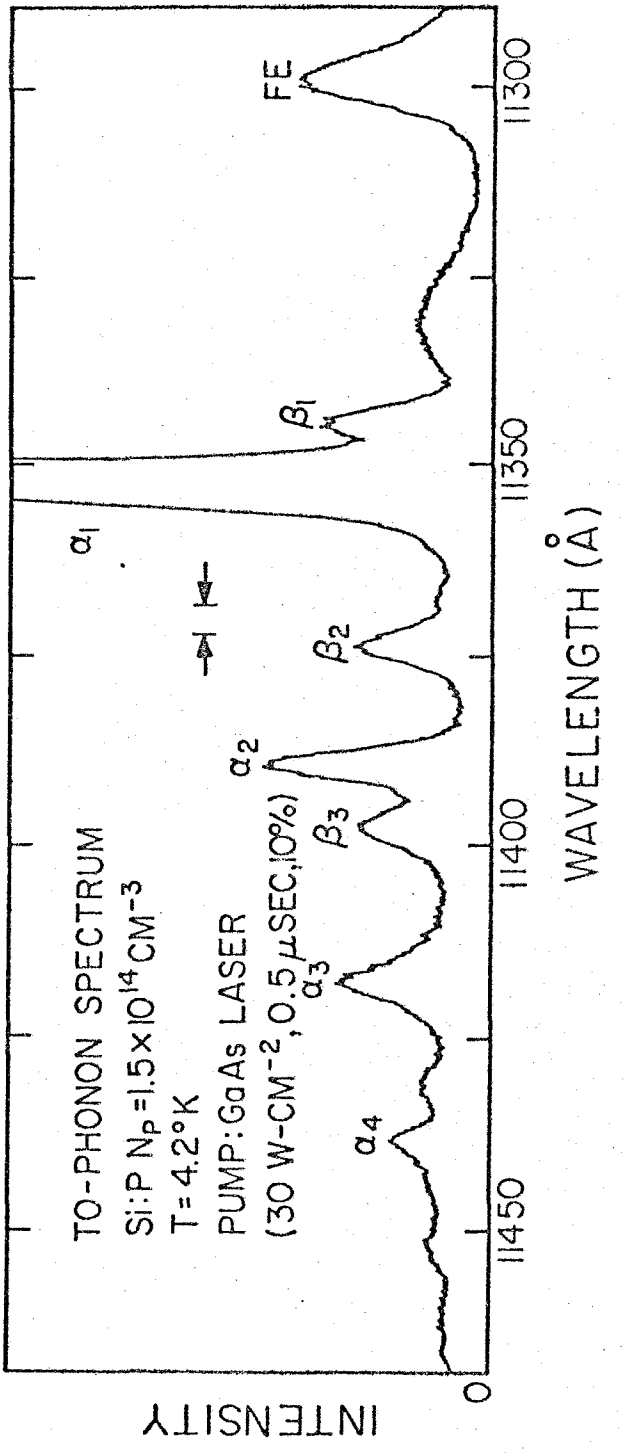
TO-PHONON SPECTRUM
Si:P N_P=1.5×10^{14} CM^{-3}
T=4.2°K
PUMP: GaAs LASER
(30 W-CM^{-2}, 0.5 μSEC, 10%)
α_1
α_2
α_3
α_4
β_1
β_2
β_3
FE
INTENSITY
0
11450
11400
11350
11300
WAVELENGTH (Å)

hole pair recombination in a cluster of two excitons bound to a single neutral acceptor which leaves a bound exciton in one of the excited states [5,6,7].

The spectrum associated with BMEC has been studied extensively in an effort to gain knowledge of the properties of these states. Fig. 6.1 shows a spectra taken in Si:P which shows the series of lines associated with BMEC recombination [8]. This spectra is seen to consist of a series of lines. Recently, Thewalt reported new features in the luminescence spectra for Si:P [9]. He noted that the lines associated with BMEC could be divided into two groups, the α series and the β series. As shown in Fig. 6.1 the α series is observed in no-phonon as well as phonon assisted transitions. The β series was only observed in phonon assisted transitions.

In addition, Thewalt [9] observed bound exciton transitions which appeared in the luminescence spectra at higher temperatures. He interpreted these transitions as being associated with excited states of the bound exciton. One of these lines which he labeled δ was identified as recombination of a bound exciton in an excited state leaving the donor in the ground state. Other lines, labeled γ_1 and γ_1' were interpreted by Thewalt [9] as being due to recombination from excited states of the BE which left the donor in one of the valley orbit states $1s(\Gamma_3)$ or $1s(\Gamma_5)$. Lightowlers *et al* [10] have reported the observation of similar transitions in Si:As, Si:Sb and Si:Bi along with Si:P.

Thewalt [9] interpreted the existence of the excited states of the bound exciton and the observed β series of the bound multiple exciton complexes as evidence supporting the shell model proposed by Kirczenow [11]. A schematic diagram which shows the essential features of this model for the observed spectra is shown in Fig. 6.2. According to the model, the states associated with bound multiple exciton complexes and bound excitons for the shallow neutral donor should show a valley orbit splitting similar to that of the neutral donor. The ground state of the bound exciton and the bound multiple exciton complexes is formed by filling shells of states which are separated in energy and which have the symmetry of the valley orbit split states for the electrons. The holes are placed in states with the Γ_8 symmetry of the valence band. For example the ground state of the bound exciton is schematically labeled $\{2\Gamma_1:\Gamma_8\}$. The ground state of a m exciton complex $\{2\Gamma_1,(m-1)\Gamma_{3,5};m\Gamma_8\}$. A single excited state is considered in which one of the electrons is promoted to the $\Gamma_{3,5}$ shell. For an m exciton complex this state is labeled $\{\Gamma_1,m\Gamma_{3,5};m\Gamma_8\}$. The observed transitions are assumed to be due to transitions between the ground state of the m^{th} complex and states of the m-1 complex. The α series is due to transitions of the type $\{2\Gamma_1,(m-1)\Gamma_{3,5};m\Gamma_8\}$ $\rightarrow\{\Gamma_1,(m-1)\Gamma_{3,5};(m-1)\Gamma_8\}$. The β series is due to transitions of the type $\{2\Gamma_1,m\Gamma_{3,5};(m+1)\Gamma_8\}\rightarrow\{2\Gamma_1,(m-1)\Gamma_{3,5};(m\Gamma_8\}$. The δ and γ_1,γ_1' lines arise from transitions associated with an excited state of the bound

exciton in this model [11].

The predictions of the current form of the shell model are in disagreement with recent measurements of the binding energy of a free exciton to a bound multiple exciton complex [4]. This binding energy can be obtained by measuring the temperature dependence of the luminescence associated with the complexes. Fig. 6.3 shows the results of these measurements. The results predicted by the shell model based on the observed spectra are represented by open triangles in the figure. The open squares are the results for the binding energy obtained from the temperature measurements. The open circles represent the results obtained from the luminescence if one assumes that the α series of lines is due to transitions from the ground state of one complex to the ground state of another. If the data agreed and the shell model was correct then the open triangles and open squares would fall on the same curve. The thermal data indicate that the binding energy of a free exciton to the complex decreases for large complexes. The shell model predicts that the binding energy increases rapidly as a function of complex number. Since the curves do not match either the shell model is incorrect or the temperature measurements are in error. To resolve this disagreement it was clear that an independent test of the shell model was necessary.

To test the predictions of the shell model and to gain insight into the structure of bound multiple excitons, the systematics of the

Figure 6.2. A schematic diagram of the spectroscopy of bound multiple exciton complexes as predicted by the shell model. For the m^{th} complex there is a ground state which can be represented schematically as $\{2\Gamma_1:(m-1)\Gamma_{3,5}:m\Gamma_8\}$ and an excited state shown as $\{\Gamma_1,m\Gamma_{3,5}:m\Gamma_8\}$. These states give rise to two distinct series of transitions, the α series and the β series.

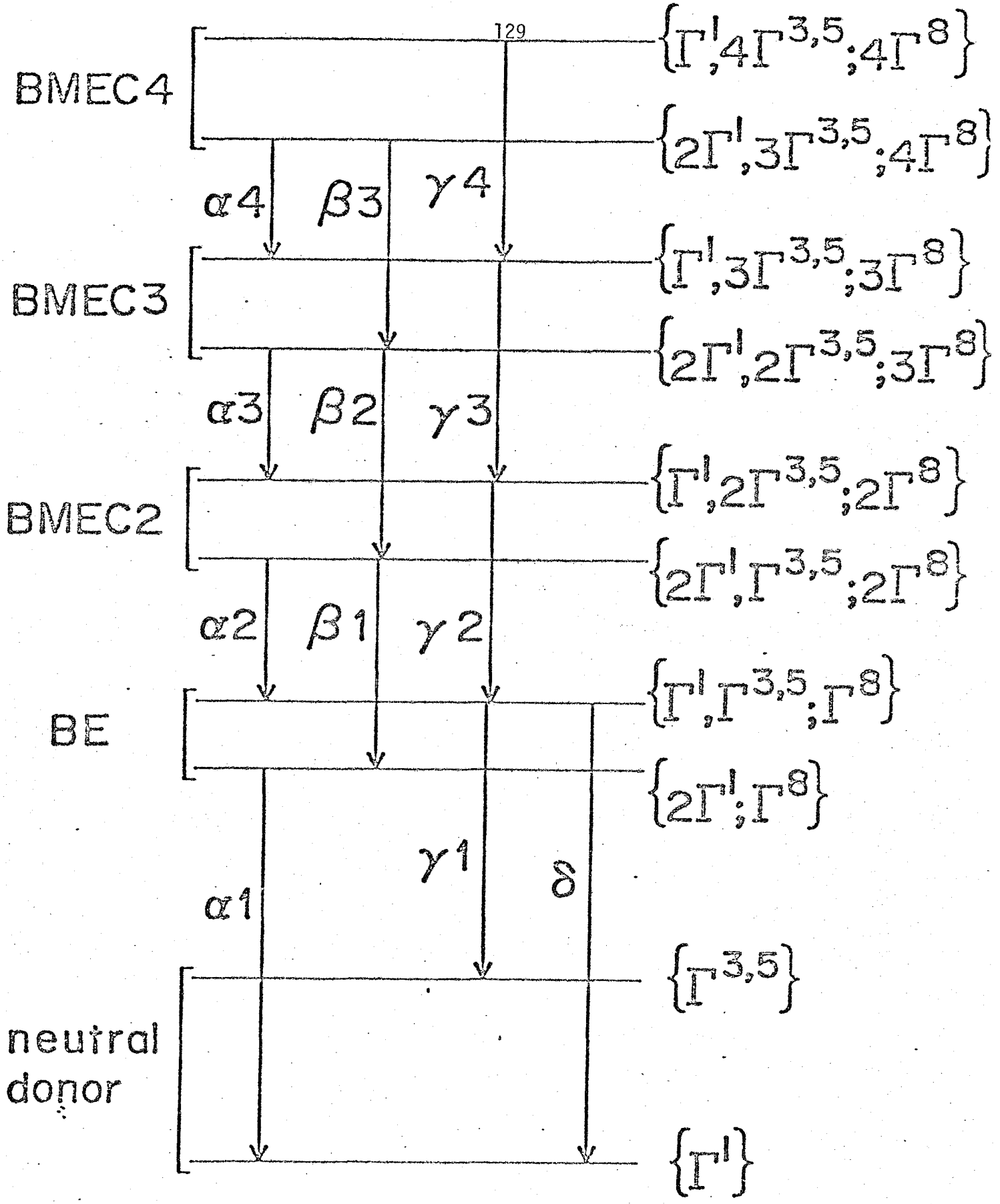
BMEC4
{Γ', 4Γ^3,5; 4Γ^8}
{2Γ', 3Γ^3,5; 4Γ^8}
α4
β3
γ4
BMEC3
{Γ', 3Γ^3,5; 3Γ^8}
{2Γ', 2Γ^3,5; 3Γ^8}
α3
β2
γ3
BMEC2
{Γ', 2Γ^3,5; 2Γ^8}
{2Γ', Γ^3,5; 2Γ^8}
α2
β1
γ2
BE
{Γ', Γ^3,5; Γ^8}
{2Γ'; Γ^8}
γ1
δ
α1
{Γ^3,5}
neutral donor
{Γ'}

spectroscopy of the other donors have been investigated. In this chapter luminescence measurements in Si:As and Si:Sb are reported. These data show transitions which correspond to bound multiple exciton recombination analogous to the β line series observed in Si:P. Using these data and previous existing data, the systematics of the line positions and splittings are discussed. While the line positions, as expected, do show some variation with the impurity, the splittings are found to be relatively independent of the impurity type. Such behavior is difficult to explain with standard explanation for the validity of the shell model.

II. Experiment

The spectra were obtained with the apparatus previously described in this thesis. Ar^+ laser excitation was used with excitation power ranging from 20 to 200 milliwatts over a 3 mm diameter spot. At higher excitation intensities and above 4.2^oK, the multiple exciton lines were obscured by a broad background. This background resembled the luminescence associated with an electron hole plasma which is observed in high purity silicon.

Samples were prepared by lapping and then etching with HNO_3:HF(7:1). The samples were grown at Hughes Research Laboratories. The impurity concentration in each sample was determined by a Hall measurement made at Hughes Laboratories. The Si:Sb sample was doped

Figure 6.3. The binding energy of a free exciton in a multiple exciton complex as a function of complex number. The circles represent the value obtained if one assumes that the α series corresponds to a ground state to ground state transition. The triangles represent the values obtained in the shell model. The squares represent data taken from measurements of the temperature dependence of the luminescence. The data are clearly not consistent.

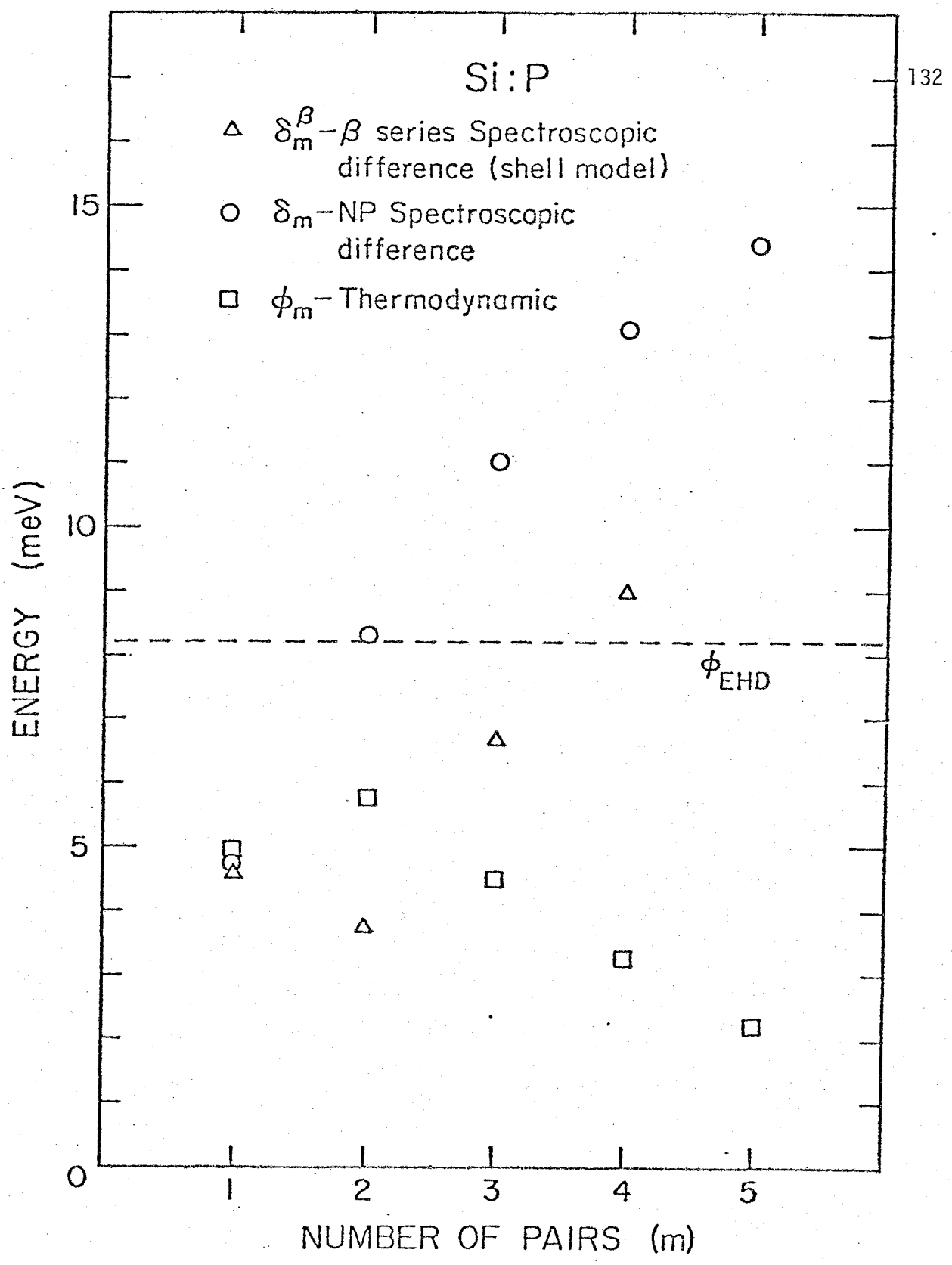
Si:P
δ_m^β – β series Spectroscopic difference (shell model)
δ_m – NP Spectroscopic difference
ϕ_m – Thermodynamic
ϕ_{EHD}
ENERGY (meV)
NUMBER OF PAIRS (m)
0
5
10
15
1
2
3
4
5

at $4x10^{16}cm^{-3}$. The Si:As sample used in these experiments was doped at $4x10^{15}cm^{-3}$.

III. Results

In Figure 6.4 spectra in Si:Sb are shown for both the no-phonon (NP) and TO-phonon assisted regions in which bound multiple excitons have been observed. In the NP region at $4.2^{o}K$ (the second panel in Fig. 6.4) a total of 5 lines are observed which are analogous to the α series observed in Si:P. In the TO-phonon assisted region (the third panel in Fig. 6.4), the replicas of the α lines seen in NP region plus the two additional lines at 1.0893 eV and 1.0870 eV, labeled β_2 and β_3, respectively, are observed. Since both the α-series and the two β lines are positioned very near in energy to corresponding lines in Si:P, they have been identified with the labels introduced by Thewalt [9].

In the top panel of Fig. 6.4 the photoluminescence spectra of Si:Sb taken at $12^{o}K$ in the no-phonon and TA-phonon assisted regions are presented. A line at 1.1407 is observed. This line appears below $15^{o}K$ in temperature. Above this temperature the line broadens and merges with the TA-phonon assisted free exciton line. The line intensity peaks at roughly $10^{o}K$ with an intensity equal to approximately half that of the no-phonon bound exciton line and disappears at temperatures below $4^{o}K$. Although the exact nature of this line is

Figure 6.4. Photoluminescence spectra of Si:Sb. The top portion shows several lines observed above 10^{o}K. The middle portion shows the α series in the no-phonon region. The bottom portion shows the α series in the TO-phonon assisted region along with the β_2 and β_3 lines.

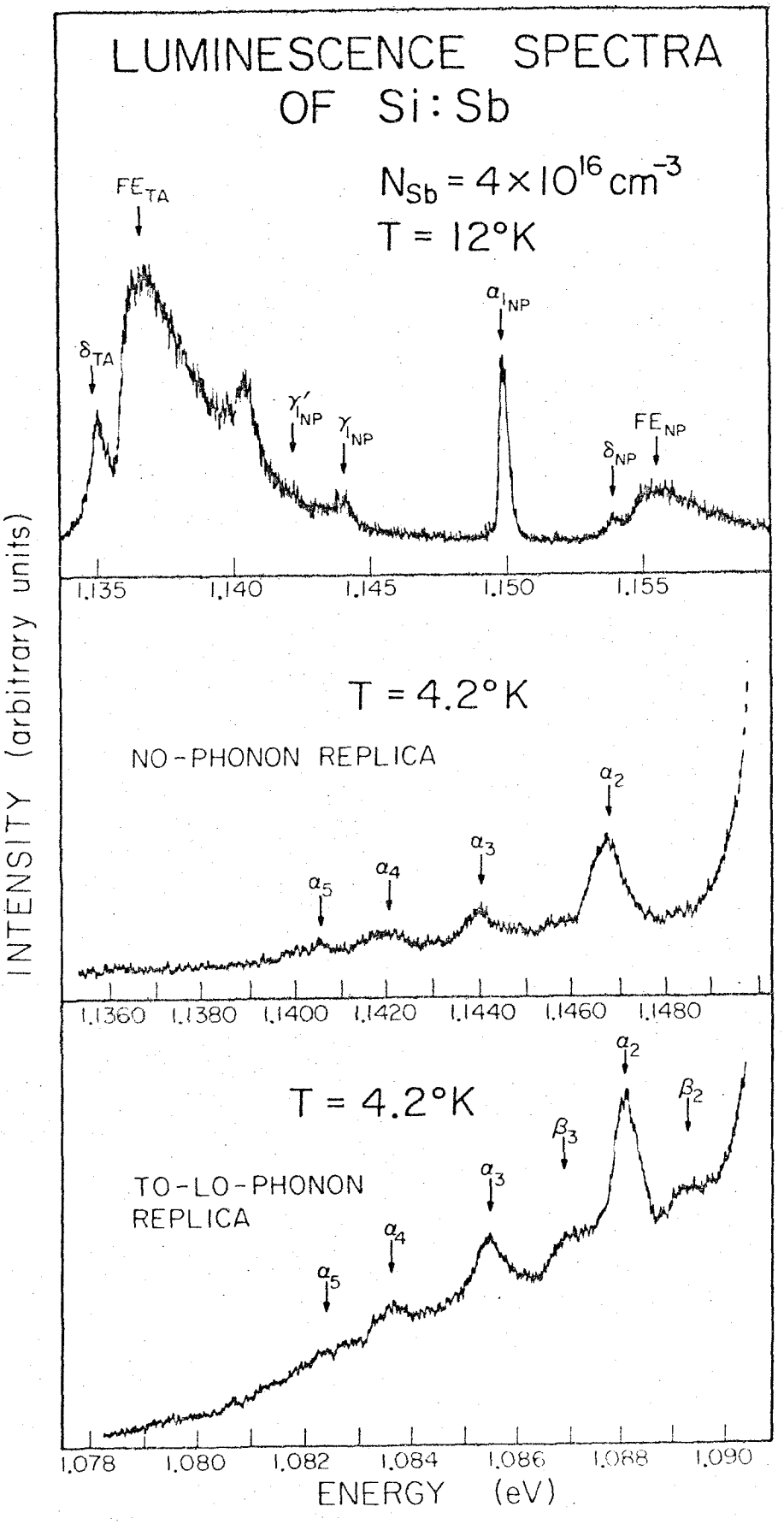
LUMINESCENCE SPECTRA
OF Si:Sb
$N_{Sb} = 4 \times 10^{16}\ cm^{-3}$
T = 12°K
FE_{TA}
δ_{TA}
γ'_{1NP}
γ_{1NP}
α_{1NP}
δ_{NP}
FE_{NP}
1.135
1.140
1.145
1.150
1.155
T = 4.2°K
NO-PHONON REPLICA
α_2
α_3
α_4
α_5
1.1360
1.1380
1.1400
1.1420
1.1440
1.1460
1.1480
T = 4.2°K
TO-LO-PHONON REPLICA
α_2
β_2
β_3
α_3
α_4
α_5
1.078
1.080
1.082
1.084
1.086
1.088
1.090
ENERGY (eV)
INTENSITY (arbitrary units)

not clear at present, it is possibly due to the radiative decay of an excited state of the bound exciton into one of the valley orbit states of the neutral donor. This line has not been observed in either the TA or TO-phonon assisted regions.

The γ_1,γ_1' and δ lines previously reported by Lightowlers, et al have also been observed. All three lines have been observed in both the no-phonon and phonon assisted regions. Thewalt [9] has interpreted these lines in terms of the shell model for the bound exciton. All three lines are assumed to originate from a single excited state of the BE. As shown in Fig. 6.2 the δ line comes from a transition leaving the neutral donor in the $1s(\Gamma_1)$ ground state. The γ_1 and γ_1' lines are assumed to result from transitions leaving the neutral donor in the $1s(\Gamma_5)$ and $1s(\Gamma_3)$ excited states, respectively. A check on this hypothesis may be made by computing the energy differences between the lines of the bound exciton and comparing the results with splittings measured in infrared (IR) absorption experiments in the neutral donor [13]. (Transitions from 1s states to 2p states occur in the infrared. Measurements of the infrared absorption spectra have been used to determine the splittings in the neutral donor.) A calculation of this splitting yields 11.7±0.1 meV for the $1s(\Gamma_1)$-$1s(\Gamma_3)$ splitting as compared to 12.14±0.1 meV in the IR absorption experiments. The value for the $1s(\Gamma_1)$-$1s(\Gamma_5)$ splitting is 10.1±0.1 meV as compared to the IR results where two lines are observed at 9.55±0.1 meV and

9.84 0.1 meV [13]. These results are in close agreement with similar measurements on the BE by Lightowlers, et al [10]. The discrepancy between the BE results and IR measurements is outside experimental error. However, as noted by Lightowlers, et al [10], one possible explanation of the discrepancy is given by assuming that the δ-line is not a single line but has a number of components.

In Figure 6.5 spectra of the luminescence of Si:As taken in the no-phonon and TO-phonon assisted regions are shown. In the middle panel of the figure, the lines analogous to the α-series in Si:P and Si:Sb are shown in the NP region. In the TO-phonon region, the bottom panel, the replicas of α-series plus two or perhaps three additional lines are observed which have been identified as β-lines. The assignment of line numbers was made on the basis of the temperature and pump power dependence data which could be obtained and by comparing line positions with those observed in Si:P [9].

In the TA-phonon assisted region two lines are observed (the lines at the far left in the middle panel of the figure) at energies higher than the bound exciton. Although the lower in energy of these lines is close to the predicted position of the boron bound exciton, the higher in energy of these does not correspond to the position of any known BE and is most likely due to a β_1 transition. No such line is observed in the no-phonon region. In the TO-phonon assisted region the line would coincide with the LO-phonon assisted BE in energy. Sauer and Weber [12] have previously reported relative positions of the

lines in the α-series in the no-phonon region. The results presented here are consistent with their results for the α-lines.

In the top panel of the figure the spectra of the γ_1' and γ_1 lines which have been resolved in the no-phonon region of Si:As are shown. The separation between these two lines agrees with the separation between the valley orbit split states (1.41 meV ± .1 meV) [13]. Again, following the interpretation of Thewalt, [9] it is possible to interpret these lines as resulting from transitions from an excited state of the bound exciton to the valley orbit split states of the neutral donor. By adding the valley orbit splitting to the energies of the γ lines and by subtracting the energy of the bound exciton ground state to ground state transition (the α_1 line), the energy of the excited state of the bound exciton relative to the ground state of the bound exciton can be obtained. This excited state lies 5.8 ± .1 meV above the ground state of the BE which is very close to the FE threshold which lies at 5.5 ± .1 meV [10] above the ground state. The position of this excited state does not coincide with the position of the initial state of δ transition which lies at 4.4 ± .1 meV.

In Table 6.1 the line positions for all lines reported in this study are summarized. Data previously reported for Si:P by Thewalt [9] have also been included.

Figure 6.5. Photoluminescence spectra of Si:As. The top portion shows the no-phonon replicas of the γ lines. The middle portion shows the α series in the no-phonon region and two lines on the far left associated with recombination in the TA-phonon assisted region. The bottom portion shows the α and β series in the TO-phonon assisted region.

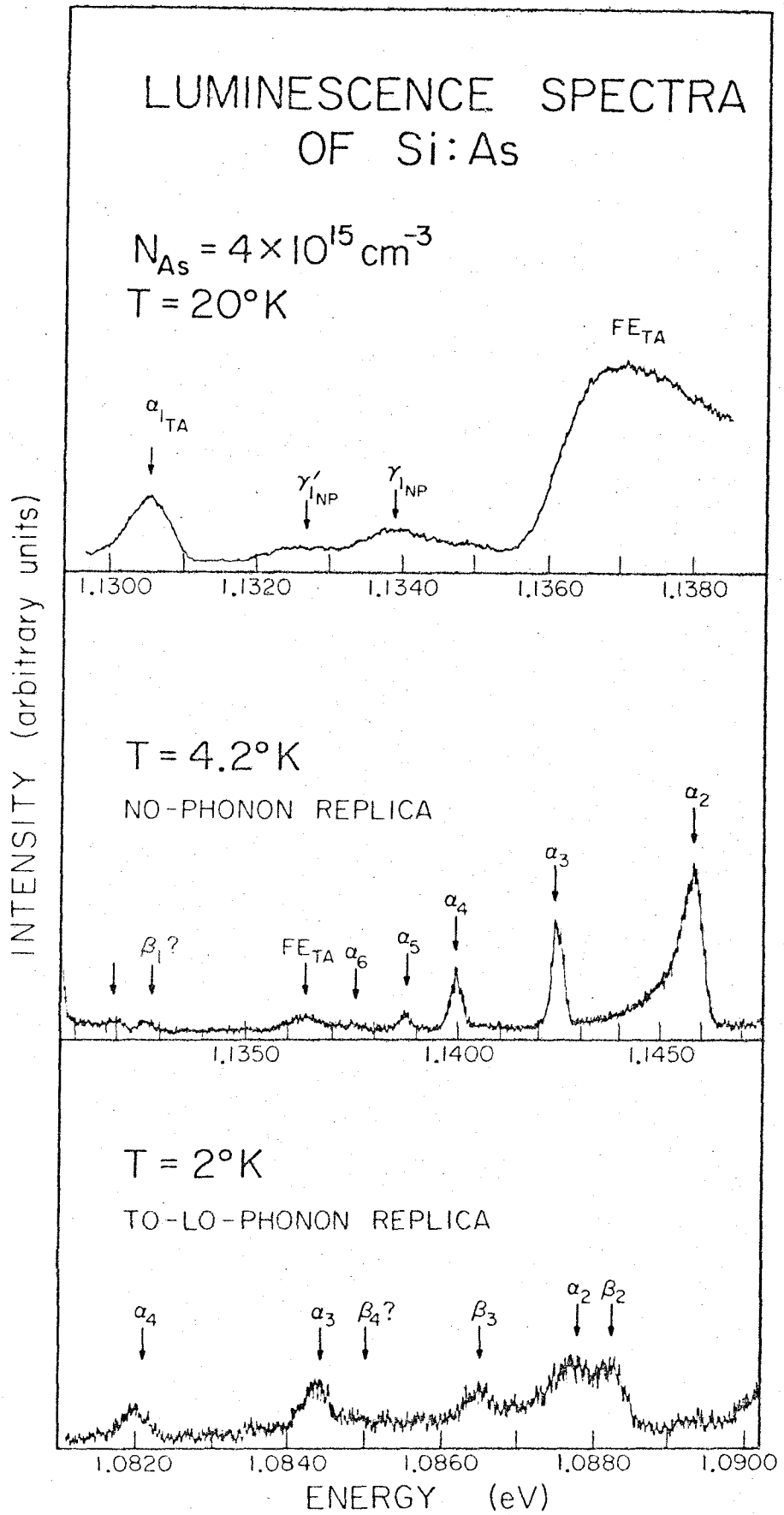
LUMINESCENCE SPECTRA
OF Si:As
$N_{As} = 4 \times 10^{15}\ cm^{-3}$
T = 20°K
FE_{TA}
$\alpha_{1_{TA}}$
$\gamma'_{1_{NP}}$
$\gamma_{1_{NP}}$
1.1300
1.1320
1.1340
1.1360
1.1380
T = 4.2°K
NO-PHONON REPLICA
α_2
α_3
α_4
β_1?
FE_{TA}
α_6
α_5
1.1350
1.1400
1.1450
T = 2°K
TO-LO-PHONON REPLICA
α_4
α_3
β_4?
β_3
α_2
β_2
1.0820
1.0840
1.0860
1.0880
1.0900
INTENSITY (arbitrary units)
ENERGY (eV)

IV. Discussion

The theoretical problem for the bound exciton and bound multiple exciton complexes is a difficult one since one may need to deal realistically with the many valleyed nature of the conduction band; the degeneracy of the valence band; the electron and hole interaction with the impurity potential; and the electron-electron, electron-hole, and hole-hole interactions. Since no one has been able to perform a realistic calculation of the bound multiple exciton structure, it is worthwhile to examine the data for systematic trends as a function of impurity and number of excitons.

As noted above the bound exciton exhibits at least one excited state in the spectroscopy. The δ line is assumed to be due to a transition from the excited state of the bound exciton to the ground state of the neutral donor. The γ_1 and γ_1' are assumed to be transitions from the same excited state of the bound exciton to the excited states of the donor. Hence, the position of the δ, γ_1, and γ_1' lines relative to the α_1 line (which is due to a transition between the ground state of the bound exciton to the ground state of the neutral donor) gives a splitting between the ground state and excited state. In Fig. 6.6 this splitting has been plotted as a function of the valley orbit splitting of the neutral donor. The data in this plot for Si:P were taken from Ref. 9 and the data for Si:As, Si:Sb, and Si:Bi were taken from Ref. 10. Points are given

both for the Γ_1-Γ_3 and Γ_1-Γ_5 splittings in the neutral donor. The values computed for the δ and γ' lines are given for Si:As where there is a rather large discrepancy. The data suggest that the excited state splitting approaches a finite value of $\sim$3 meV as the valley orbit splitting approaches zero. For the shallow donors, this splitting between the ground state and the excited state is a substantial fraction of the valley orbit splitting in the neutral donor. For example, in Si:P this splitting is about one-third the valley orbit splitting. The observed splitting changes by at most 50% when the valley orbit splitting changes by slightly more than a factor of 4. The relative independence of this splitting on the valley orbit splitting in the neutral donor suggests that the electron-electron interaction may play an important role in determining this splitting. Recent theoretical work suggests that one might want to minimize electron-electron repulsion by assigning the electrons to orthogonal valleys in the bound exciton [14]. These results further suggest that a model based totally on the assignment of electrons to single particle states ordered as the valley orbit split states in the neutral donor [11] may be an inadequate description [15].

The shell model [11] gives a description of the origin of the α and β series of lines. The ordering of states predicted by the shell model and the expected transition scheme was discussed in the introduction to the chapter and is shown in Fig. 6.2. The splitting between the α and β lines should give the energy difference between

Table 6.1. Line positions of no-phonon replicas of bound excitons and bound multiple exciton complexes for Si:P, Si:As and Si:Sb. When a no-phonon replica was not observed, the energy was obtained from the TA or TO replicas of the transitions using $h\omega_{TO}$ = 58.1 meV or $h\omega_{TA}$=18.7 meV [10]. All line positions are given in eV.

	Si:P[a]	Si:As[b]	Si:Sb[b]
α_1	1.15001	1.1492	1.1501
α_2	1.14647	1.1457	1.1467
α_3	1.14371	1.1425	1.1440
α_4	1.14172	1.1400	1.1420
α_5	1.14046	1.1388	1.1405
α_6	1.13931	1.1375	------
β_1	1.15078	1.1514[c]	------
β_2	1.14790	1.1463[d]	1.1474[d]
β_3	1.14560	1.1446[d]	1.1451[d]
β_4	-------	1.1429[d]	------
γ_1	1.14252	1.1339	1.1441[d]
γ_1'	1.14135	1.1325	1.1423[d]
δ	1.15432	1.1535[d]	1.1540
δ'	1.15373	------	------
other	-------	------	1.1407

a) Reference 9. All values ± .05 meV.
b) All values ±.06 meV.
c) The TA-phonon assisted replica was used to obtain this energy.
d) The TO-phonon assisted replicas were used to obtain this energy.

Figure 6.6. The splitting between the ground state and excited state of the bound exciton versus the valley orbit splitting P, Sb, As, and Bi in Si. The symbol As_{δ} refers to the data point associated with the δ transition, and the symbol As_{γ} refers to the point associated with the γ transition.

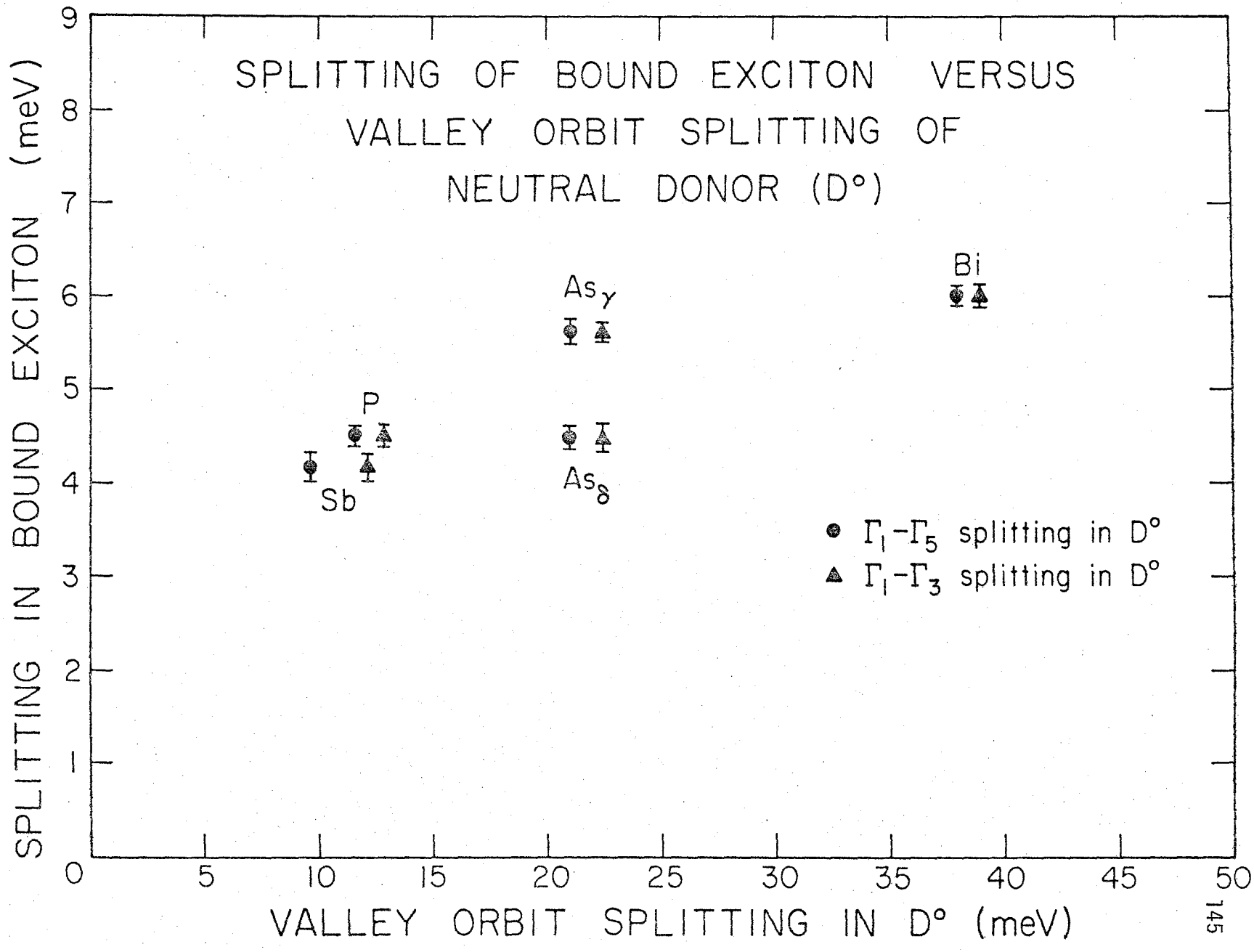
SPLITTING OF BOUND EXCITON VERSUS
VALLEY ORBIT SPLITTING OF
NEUTRAL DONOR (D°)
SPLITTING IN BOUND EXCITON (meV)
VALLEY ORBIT SPLITTING IN D° (meV)
0
1
2
3
4
5
6
7
8
9
5
10
15
20
25
30
35
40
45
50
Bi
As$_\gamma$
P
Sb
As$_\delta$
Γ_1-Γ_5 splitting in D°
Γ_1-Γ_3 splitting in D°

the $\{2\Gamma_1,(m-1)\Gamma_{3,5};\ m\Gamma_8\}$ and $\{\Gamma_1,m\Gamma_{3,5};m\Gamma_8\}$ configurations. In Fig. 6.7 this splitting has been plotted as a function of m for Si:P, Si:As and Si:Sb. The data for Si:P were taken from Ref. 9. For comparison the neutral donor splittings have been plotted for m=0. The results in this figure show that the splittings for the higher exciton complexes become almost independent of the line number and the valley orbit splitting. For these shallower donors this splitting is a significant fraction of the valley orbit splitting in the neutral donor. The insensitivity of the splitting to dopant and exciton number suggests that the electron-electron interaction which should be rather insensitive to the strength of the central cell connection may be playing a rather large role in determining this splitting.

V. Conclusions

The observation of several new lines in the luminescence associated with the bound exciton and bound multiple exciton complexes in Si:As and Si:Sb has been reported. The systematics of splittings between the ground state and the observed excited states of the bound exciton are found to be relatively independent of the impurity type. In addition the spectroscopy of bound multiple exciton complexes has been found to show certain set regularities. The splittings observed for the final states of transitions involving bound multiple excitons are observed to be relatively independent of both the impurity type and the number of excitons bound to the impurity. These

Figure 6.7. The splitting between the β_m and the α_{m+1} line positions versus the number of excitons bound to a valley orbit splittings are plotted at m=0 for each of the impurities.

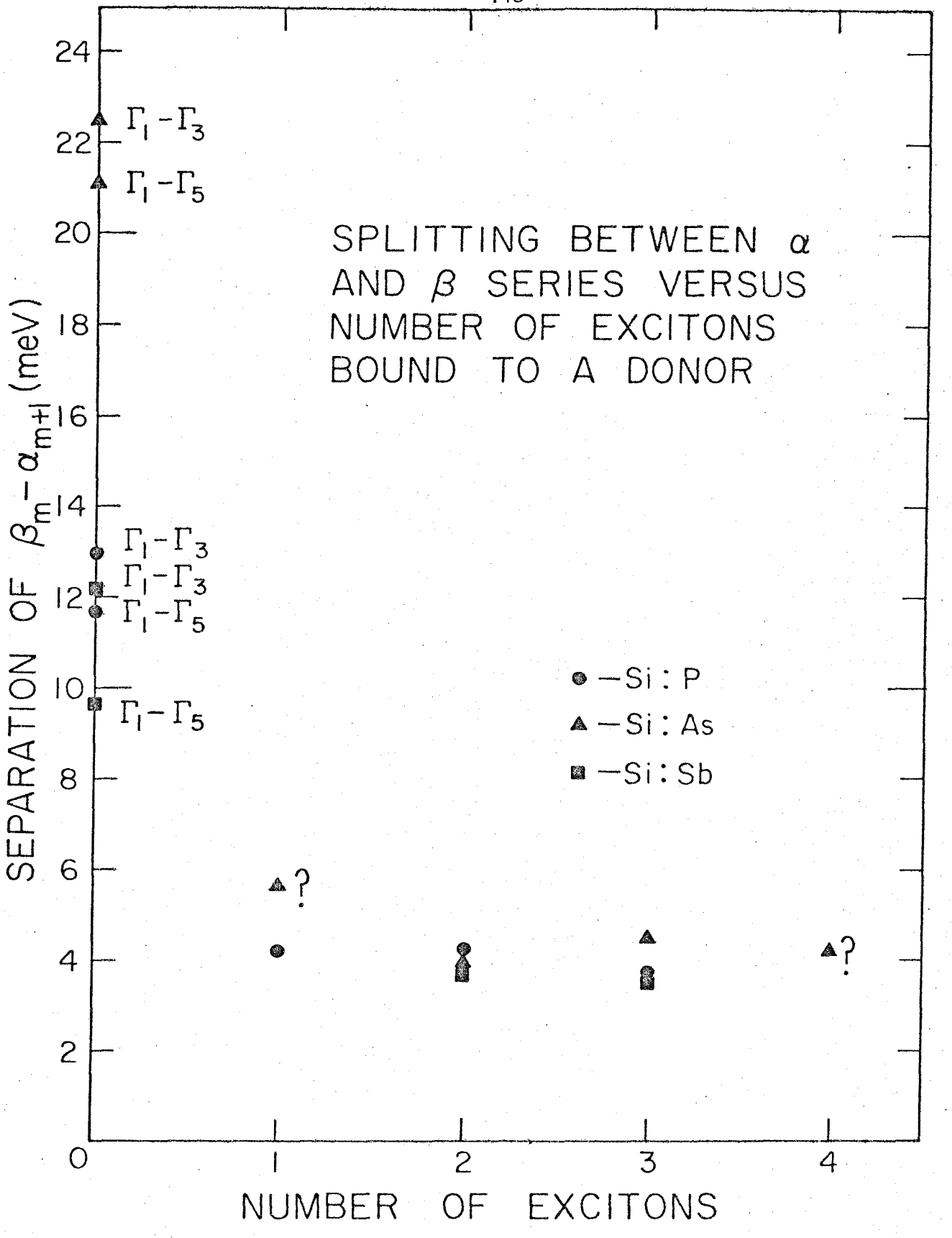
SPLITTING BETWEEN α AND β SERIES VERSUS NUMBER OF EXCITONS BOUND TO A DONOR
SEPARATION OF $\beta_m - \alpha_{m+1}$ (meV)
NUMBER OF EXCITONS
0
2
4
6
8
10
12
14
16
18
20
22
24
1
2
3
4
$\Gamma_1 - \Gamma_3$
$\Gamma_1 - \Gamma_5$
$\Gamma_1 - \Gamma_3$
$\Gamma_1 - \Gamma_3$
$\Gamma_1 - \Gamma_5$
$\Gamma_1 - \Gamma_5$
● — Si : P
▲ — Si : As
■ — Si : Sb
▲?
▲?

results indicate that the electron-electron interaction may be playing a large role in determining the splitting. This behavior is not explained by the shell model which is the only existing model for the decay of the bound multiple exciton complexes.

REFERENCES

1. A. S. Kaminskii and Ya. E. Pokrovskii, JETP Lett. 11, 255 (1970).
2. R. Sauer, Phys. Rev. Lett. 31, 376 (1973).
3. K. Kosai and M. Gershenzon, Phys. Rev. B9, 723 (1974).
4. S. A. Lyon, D. L. Smith, T. C. McGill, Phys. Rev. Lett. 41,56 (1978).
5. M.L.W. Thewalt, Phys. Rev. Lett. 38, 521 (1977).
6. E. C. Lightowlers and M. O. Henry, J. Phys. C10, L247 (1977).
7. S. A. Lyon, D. L. Smith, and T. C. McGill, Phys. Rev. B17, 2620 (1978).
8. A. Hunter, private communication.
9. M.L.W. Thewalt, Solid St. Commun. 21, 937 (1977); Can. J. Phys. 55, 1463 (1977).
10. E. C. Lightowlers, M. O. Henry, and M. A. Vouk, J. Phys. C10, L713 (1977).
11. G. Kirczenow, Solid State Commun. 21, 713 (1977).
12. R. Sauer and J. Weber, Phys. Rev. Lett. 39, 770 (1977).
13. For Si:P, Si:As, and Si:Sb see, R. L. Aggarwal and A. K. Ramdas, Phys. Rev. 140A, 1246 (1965). For Si:Bi see, H. J. Zerger, W. L. Krag and L. M. Roth, MIT Lincoln Laboratory, Quarterly Report, Solid State Research, 1961 (unpublished). As quoted in N. R. Butler, P. Fisher, and A. K. Ramdas, Phys. Rev. B12, 3200 (1975).
14. P. D. Altakov, K. N. El'tsov, G. E. Pikus, and A. A. Rogachev, JETP Letters 26, 338 (1977).

15. From purely dimensional considerations one would expect the electron electron interaction to vary approximately as $\frac{e^2}{a_o}$ where a_o is the characteristic size of the orbit. However, the valley orbit splitting is much more sensitive to orbit size since it depends on the amplitude of the wavefunction in the central cell and the large fourier components of the wavefunction. For example, see F. Bassani, G. Iadonisi, and B. Prez iosi, Rep. Prog. Phys. 37, 1099 (1974).

Chapter 7

CAPTURE CROSS-SECTION OF EXCITONS ON NEUTRAL INDIUM IMPURITIES IN SILICON

I. Introduction

Semiconductor luminescence is a valuable tool which can be used to characterize the impurity content in semiconductor materials. In a normal measurement of semiconductor luminescence, a sample is excited with an external light source or electron beam. This excitation creates electron hole pairs in the semiconductor. At low temperatures these electron hole pairs bind together forming free excitons. The free excitons can bind to impurity centers as bound excitons and the bound exciton luminescence spectra can be measured to detect the impurity centers. Using luminescence to detect impurities has the advantage that both donor and acceptor impurities can be detected simultaneously in the same material. [1]

To use semiconductor luminescence measurements as a quantitative tool to determine the impurity content of a semiconductor, it is necessary to know the details of the process by which the free excitons are captured by the impurity site. This capture process has not been previously studied. In this chapter the results of a study of the capture of free excitons on neutral indium acceptors is presented. This study is the only known study of such a capture process in any semiconductor system.

This measurement is made possible by the fact that the decay of excitons in indium doped silicon is limited by the capture process for temperatures between $10^{o}K$ and $30^{o}K$ at doping levels less than

$10^{16}cm^{-3}$. By measuring the bound exciton decay, it is possible to obtain a measure of the capture rate. It is found that the capture process can be characterized by a temperature dependent capture cross-section, σ_c. The capture cross-section for the indium bound exciton is found to be a strong function of temperature. The experimental results show that the capture cross-section decreases rapidly with increasing temperature. The value changes from approximately $10^{-13}cm^2$ at 10^oK to about $2x10^{-15}cm^2$ at 30^oK.

II. Experiment

Measurements were made on four separate silicon samples doped with indium. The impurity content was determined in each of these with a Hall measurement performed at Hughes Research Laboratories and were determined to be $2x10^{14}cm^{-3}$, $3.2x10^{15}cm^{-3}$, $5.5x10^{15}cm^{-3}$ and $2x10^{17}cm^{-3}$. The ratio of residual electrically active impurities to indium in each sample was less than .1 in the $2x10^{14}cm^{-3}$ sample and less than .01 in the remaining samples.

Optical excitation was provided by a commercial GaAs laser diode placed near the sample in a variable temperature dewar. The incident pump power on the sample was approximately one watt in a 1 mm^2 area for a duration of 100 to 200 nanoseconds. The lifetime in each sample was measured at several different temperatures.

The zero phonon bound exciton emission, which occurs at 1.1410 eV, is the most prominent spectral feature in the photo-

luminescence of Si:In and was used for all measurements. The photoluminescence was selected with a grating spectrometer and the decay was monitored with a cooled S-1 photomultiplier in conjunction with a gated photon counting system. The system response was tested by monitoring the output of the excitation and was found to be approximately 5 nanoseconds.

III. Results and Discussion

The decay of an exciton bound to a neutral indium is dominated by an Auger process. Such a process can be represented schematically as

$$A_x^0 \rightarrow A^- + h \quad , \qquad (1)$$

where A_x^0 represents a bound exciton, A^- represents a negatively charged acceptor and h is a free hole. In such a process an electron hole pair in the bound exciton recombine with the recombination energy being transferred to the second hole in the bound exciton.

This Auger decay is rapid for the Si:In bound exciton. In a heavily doped sample with $N_{In} = 2x10^{17}cm^{-3}$ the decay was measured to be less than 5 nanoseconds in this study [2]. More recent measurements of the bound exciton lifetime indicate a lifetime of 3 nanoseconds [3]. Recent calculations by Osbourn and Smith yield a decay time which agrees with this measurement [4].

In Figure 7.1 the results of measurements of the decay time are

Figure 7.1. The observed decay time of the 1.1410 eV luminescence of the Si:In bound exciton at different temperatures and doping levels. The free exciton lifetime is about 2.6 μsec (Ref. (5)); whereas, the Auger decay time for the bound exciton is approximately 3 nanoseconds.

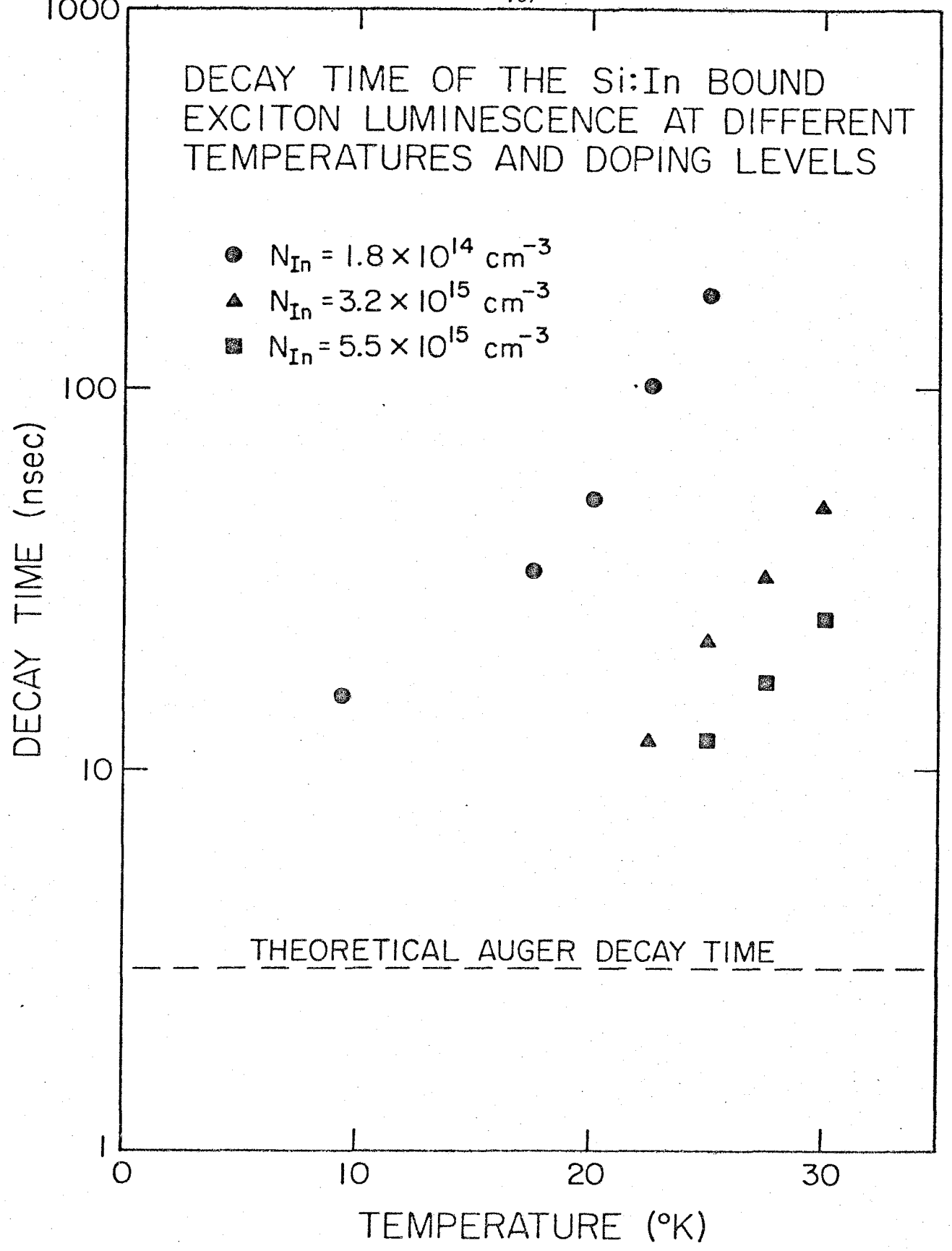
DECAY TIME OF THE Si:In BOUND EXCITON LUMINESCENCE AT DIFFERENT TEMPERATURES AND DOPING LEVELS
$N_{In} = 1.8 \times 10^{14}$ cm^{-3}
$N_{In} = 3.2 \times 10^{15}$ cm^{-3}
$N_{In} = 5.5 \times 10^{15}$ cm^{-3}
THEORETICAL AUGER DECAY TIME
DECAY TIME (nsec)
1000
100
10
1
0
10
20
30
TEMPERATURE (°K)

shown as a function of temperature and doping level. These results show that at In concentrations less than $10^{16}cm^{-3}$ the decay time has a strong dependence on both the doping level and the temperature of the sample. These decay times are also much longer than the Auger decay time. Since these decay times are longer than the Auger time, it can be concluded that the Auger process is not the rate limiting step in the decay process. A reasonable explanation of the observed lifetimes is that the decay is limited by the process in which a free exciton becomes bound to the neutral indium site.

There are several reasons why the capture process has not been previously observed. First of all, the residual impurity content in all semiconductors except for Ge and Si is typically too high to allow such a measurement. The capture time on a site is expected to be inversely proportional to impurity concentration and capture times are normally too short to observe at impurity levels greater than $10^{16}cm^{-3}$. Secondly, it is not possible to measure the direct capture process for most impurities in Si and Ge. At high temperatures thermal excitation rates of the exciton off the impurity site are too large compared to the bound exciton decay rate. At low temperatures the capture rate is too large compared to the bound exciton decay rate.

A simple model of the capture process is one in which only one type of impurity is taken to be present in the semiconductor. An optical excitation pulse is assumed to produce a free exciton gas with

density n_{ex} in steady state equilibrium with excitons bound to neutral impurities. Following such a pulse the following rate equations describe the decay for this simple case.

$$\frac{dn_{ex}}{dt} = - n_{ex} N_I \sigma_C v_T \quad , \tag{2}$$

and

$$\frac{dn_{BE}}{dt} = - \frac{n_{BE}}{\tau_{BE}} + N_I \sigma_i v_T n_{ex} \quad , \tag{3}$$

where N_I is the concentration of neutral cents, σ_c is defined as the capture cross-section, v_T is the thermal velocity, n_{EX} and n_{BE} are the respective free and bound exciton densities, and τ_{BE} is the bound exciton lifetime. Following a long optical pulse at the generation rate g, these equations have the following solutions.

$$n_{EX} = g \tau_c \exp -(t/\tau_c) \quad , \tag{4}$$

where

$$\frac{1}{\tau_c} = N_I \sigma_c v_T \tag{5}$$

and

$$n_{BE} = g\tau_{BE} \left(\frac{\tau_c \exp \frac{-t}{\tau_c} - \tau_{BE} \exp \frac{-t}{\tau_{BE}}}{\tau_c - \tau_{BE}} \right) \tag{6}$$

For

$\tau_c >> \tau_{BE}$, we have

$$n_{BE} = g\,\tau_{BE}\exp -(t/\tau_c) \quad . \qquad (7)$$

The effects of the free exciton decay have been neglected in these equations since the decay rate of the free exciton is at least an order of magnitude lower than the decay rates which have been measured in this experiment [5]. Also the effects of free electrons and holes have been ignored since most of the electron hole pairs are bound into the exciton state at these temperatures and densities. (Estimates of the number of electron hole pairs bound into excitons based on mass action for 10^{15} pairs/cm^3 yield that greater than 70% are bound in free excitons at 30^{o}K. At lower temperatures a much larger percentage of the pairs are bound as excitons.)

For the simple model to be valid, it is also necessary that most of the indium sites remain neutral. If the recapture of the free hole created during the Auger decay was not fast, a significant fraction of indium centers would be ionized. In such a case a pump power dependent decay would be expected. The results of measurements of the pump power dependence of the decay time indicate that the decay time is independent of pump power. This observation is consistent with an estimate of the fraction of ionized indium centers based on published values of the capture rate of free holes on ionized indium centers [6]. Such an estimate indicates that in the

worst case 10% of the centers are ionized. It can be concluded that most of the indium centers remain neutral during the decay under the conditions used in this experiment.

Finally, the release of an exciton from the indium site must be slow compared to the Auger rate. The release rate has been estimated making use of detailed balance, the measured value of the binding energy, and the capture cross-section, σ_c, measured here. These estimates indicate that the Auger rate is several orders of magnitude greater than the release rate for temperatures less than $30^{o}K$. It should be noted that this condition is not met for the shallower acceptors B, Al, and Ga which have smaller exciton binding energies[7] and larger bound exciton decay times [2,3,4].

Roughly the same values for σ_c are obtained at a given temperature between different samples in spite of the fact that the doping level varies by a factor of 20. Thus the capture time, τ_c, scales as expected. This substantiates the use of the simple model to describe the decay. Fig. 7.2 shows the measured values of the capture cross-section, σ_c, as a function of temperature. The cross-section was calculated from the measured decay time using Eq. 5 with v_T computed from

$$v_T = \sqrt{\frac{8k_BT}{\pi m_{ex}}} \qquad (8a)$$

Figure 7.2. The measured temperature dependence of the capture cross-section of free excitons on neutral indium impurities in silicon. The data are given for different doping levels ranging from $1.8 \times 10^{14} cm^{-3}$ to $5.5 \times 10^{15} cm^{-3}$.

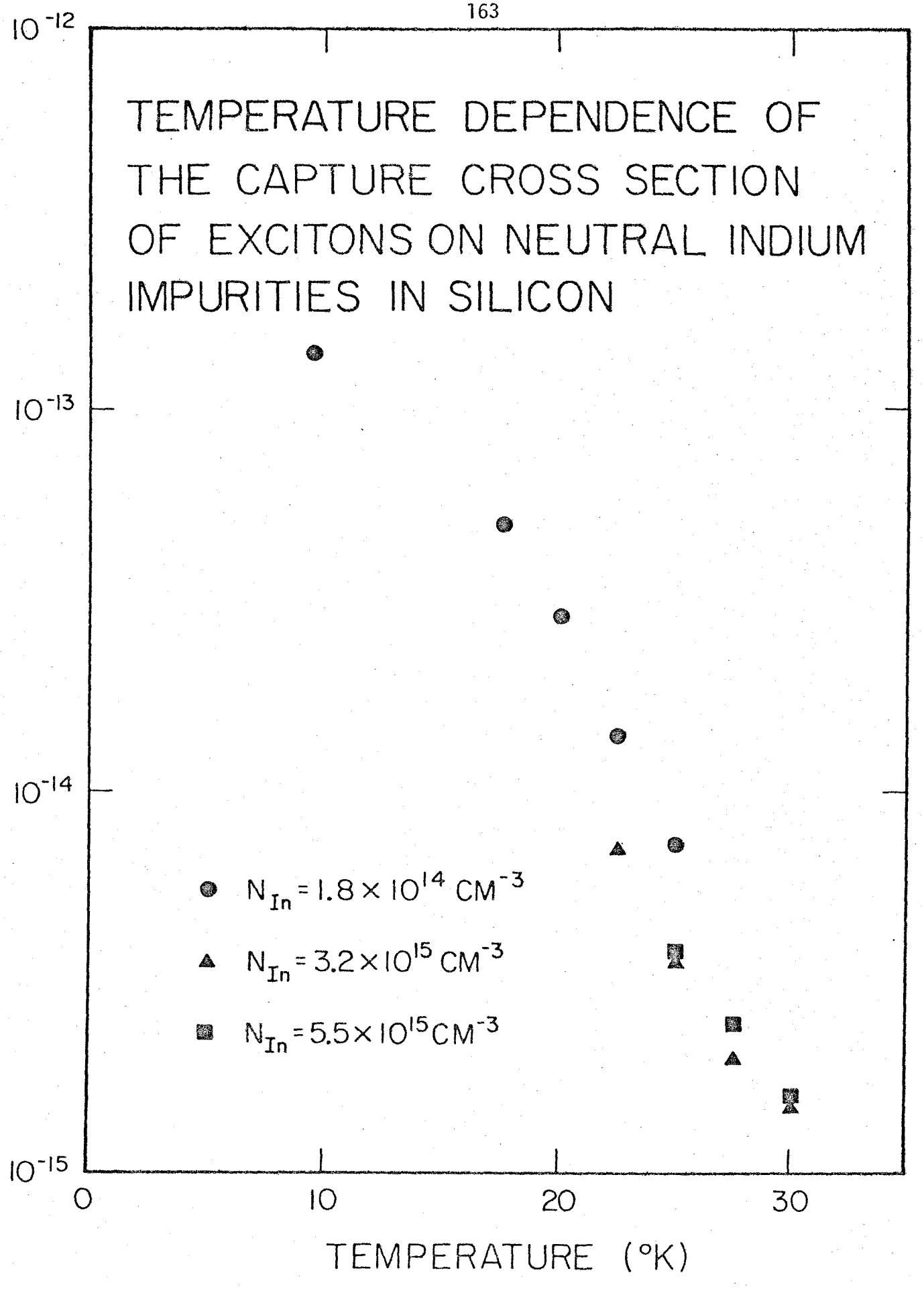
TEMPERATURE DEPENDENCE OF THE CAPTURE CROSS SECTION OF EXCITONS ON NEUTRAL INDIUM IMPURITIES IN SILICON
10^{-12}
10^{-13}
10^{-14}
10^{-15}
$N_{In} = 1.8 \times 10^{14}\ CM^{-3}$
$N_{In} = 3.2 \times 10^{15}\ CM^{-3}$
$N_{In} = 5.5 \times 10^{15} CM^{-3}$
0
10
20
30
TEMPERATURE (°K)

with

$$m_{ex} = 0.60\ m_o \qquad (8b)$$

where m_o is the free electron mass [8].

The data indicate that σ_c increases rapidly with decreasing temperature. A similar increase in the capture cross-section is observed for the capture of free carriers on ionized impurities. An explanation for such carrier capture by ionized impurities was first proposed by Lax [9,10,11]. In this model capture of the free carriers into the excited states of the impurity is followed by the subsequent decay into the ground state via a cascade process through the lower excited states. The effective capture cross-section is highly temperature dependent because thermal emission from the higher energy excited states competes with the decay of the free carrier to the lower energy states of the impurity as the temperature is lowered. A similar model might be appropriate in the case of exciton capture. The exciton would initially be captured in an excited state and rapidly decay to the ground state via lower excited states and with phonon emission. The "sticking probability" of the exciton in the excited states would provide a rapid temperature dependence.

A knowledge of the excited state structure of the bound exciton is necessary for a test of this model. Data concerning the excited

states presented in earlier chapters indicate that a calculation of the capture cross-section for the bound exciton may be in some respects simpler than a similar calculation for the neutral impurity. The calculation for the neutral impurity is complicated by the fact that a coulombic potential has an infinite number of bound states through which capture can occur. The experimental results presented earlier in this thesis, particularly those of Chapter 4, show no indication that a large number of weakly bound states exist for excitons on impurity sites. The evidence suggests that there may be in fact only a finite number of bound states in these systems. For Si:In one would expect the basic structure of the bound exciton to be that of a pseudodonor. In such a case one expects the excited states to be either excitations of the electron or hole. The excitations of the electrons are donor-like with only a few excited states below the free exciton continuum. The excitations of the hole resemble those of the A^+ state (the A^+ consists of two holes bound to a negatively charged acceptor site). In analogy with the atomic H^- ion only a finite number of excited states is expected for the A^+. Thus only a finite number of excited states is expected for the bound exciton.

IV. Conclusions

The first measurement of the capture cross-section of a free

exciton on a neutral impurity has been reported. By measuring the decay of the bound exciton luminescence it has been possible to measure the capture rate of free excitons on neutral indium centers in silicon. The capture rate scales as expected with the indium concentration, and it is possible to define a temperature dependent capture cross-section to describe the decay. The measured capture cross-section is a strong function of temperature varying two orders of magnitude over the range $10^{o}K$ to $30^{o}K$. The cross-section reaches a value greater than $10^{-13}cm^{2}$ at the lower temperature. The large temperature dependence of the capture cross-section is most likely due to the capture into excited states of the bound exciton followed by the subsequent decay into the ground state via phonon emission.

REFERENCES

1. See, for example, J. I. Pankove, Optical Processes in Semiconductors, Prentice-Hall, Inc., Englewood Cliffs, New Jersey (1971); and the references contained therein.
2. S. A. Lyon, G. C. Osbourn, D. L. Smith, and T. C. McGill, Solid State Commun. (in press).
3. W. Schmid, Phys. Stat. Solidi b84, 529 (1977).
4. G. C. Osbourn and D. L. Smith, submitted to Phys. Rev.
5. J. D. Cuthbert, Phys. Rev. B1, 1552 (1970). We have measured a lifetime of 1.7 μs in lightly doped ($\sim 10^{12} cm^{-3}$) silicon.
6. G. K. Wertheim, Phys. Rev. 109, 1086 (1958).
7. M. A. Vouk and E. C. Lightowlers, in Proceedings of the Thirteenth International Conference on the Physics of Semiconductors, Rome (edited by F. G. Fumi), p. 1098, Tipografia Marver, Rome (1976).
8. We estimate the exciton mass using the "single band variational" approach discussed by S. Zwerdling, B. Lax, L. M. Roth, and K. J. Button, Phys. Rev. 114, 80 (1959).
9. See, for example, A. G. Milnes, Deep Impurities in Semiconductors (John Wiley & Sons, New York, 1973); and the references contained therein.
10. M. Lax, Phys. Rev. 119, 1502 (1960).
11. G. Ascarelli and S. Rodriquez, Phys. Rev. 124, 1321 (1961).